Pharmacological studies of bioactive compounds from medicinal mushrooms in Northeast of Thailand

A thesis presented by

Kanidta Niwasabutra

in fulfilment of the requirement for the degree of

Doctor of Philosophy

2020

Strathclyde Institute of Pharmacy and Biomedical Sciences

University of Strathclyde

Declaration of Author's Rights

This thesis is the result of the author's original research. It has been composed by the author and has not been previously submitted for examination which has led to the award of a degree.

The copyright of this thesis belongs to the author under the terms of the United Kingdom Copyright Acts as qualified by University of Strathclyde Regulation 3.50. Due acknowledgement must always be made of the use of any material contained in, or derived from, this thesis.

Signed:

Date:

Acknowledgements

PUBLICATIONS

Woods, N., Igoli, J., Altwaijry, N.A., Tuslimire, J., Niwasabutra, K., Acevedo, R., Gray, A. I., Watson, D.G., Ferro, V.A. Natural vaccine adjuvants and immunopotentiators derived from plants, fungi, marine organisms and insects. Immunopotentiators in Modern Vaccines. Elsevier, 2016.

Niwasabutra, K., Igoli, J., Young, L., Gray, A.I., Ferro, V.A. Effect of crude extracts from mushrooms on different cancer cell lines. Planta Med. 2016, Dec; 81(S 01): S1-S381.

Obeid, M.A., Al Qaraghuli, M.M., Alsaadi, M., Alzahrani, A.R., Niwasabutra, K. and Ferro, V.A. Delivering natural products and biotherapeutics to improve drug efficacy. Therapeutic Delivery, 2017, 8(11), pp.947-956.

Al Qaraghuli, M.M., Alzahrani, A.R., Niwasabutra, K., Obeid, M.A. and Ferro, V.A. Where traditional drug discovery meets modern technology in the quest for new drugs. Annals of Pharmacology and Pharmaceutics, 2017, 2(11), pp.1-5.

Alqarni, A. M., Niwasabutra, K., Muhamad S., , Fearnley, H., Fearnley J., Ferro, V. A. and. Watson, D. G. Propolis Exerts an Anti-Inflammatory Effect on PMA-Differentiated THP-1 Cells via Inhibition of Purine Nucleoside Phosphorylase. Metabolites, 2019, 9(4), 75.

Obeid, M.A., Teeravatcharoenchai, T., Connell, D., Niwasabutra, K., Hussain, M., Carter, K., Ferro, V.A. Examination of the effect of niosome preparation methods in encapsulating model antigens on the vesicle characteristics and their ability to induce immune responses. Journal of Liposome Research, 2020, May 28: 1-8

Abstract

In north-eastern Thailand, there are many varieties of mushrooms that the local people consume in high quantities annually; some of which are used for medicinal purposes. The local people use them for treatment by boiling with water and drinking the liquor, while some people finely grate the mushrooms, mould them into a bolus and eat it like a tablet as an anti-cancer and anti-diabetic treatment. In the present study, the compounds from three mushrooms *P. everhartii*, *P. laevigatus* and *F. cajanderi* were extracted with ethanol and biological evaluation such as anti-cancer, anti-Alzheimers, anti-microbial and anti-inflammatory activity carried out.

An ethanol crude extract of *F. cajanderi* showed cytotoxicity against ovarian carcinoma (A2780), prostate carcinoma (LNCap) and breast carcinoma (ZR75-1) with IC50 of 149.70 μg/ml, 125.60 μg/ml and more than 150 μg/ml, respectively. While EtOH crude extracts of *P. everhartii* and *P. laevigatus* showed cytotoxicity against LNCap at IC50 80.46 μg/ml and 125.90 μg/ml, respectively and against ZR75-1 at IC50 of more than 150 µg/ml. An ethanol crude extract of *F. cajanderi* showed antimicrobial activity against three gram-positive bacteria (*Bacillus subtillis*, *Staphylococcus aureus*, *and Listeria monocytogenes*) and one gram-negative strain (*Pseudomonas aeruginosa*) at a concentration of 1 mg/ml. Three ethanol crude extracts of mushroom *F. cajanderi*, *P. everhartii* and *P. laevigatus* showed anti-inflammatory activity in THP-1 cells stimulated with lipopolysaccharide at concentrations of 31.25μg/ml, 7.81μg/ml and 1.76μg/ml, respectively.

In terms of compound elucidation, 7-methoxyindole-3-carboxylic acid methyl ester, an alkaloid compound, was isolated for the first time from *P. everhartii* and an ester of malonic acid of a lanostanoid type triterpene was isolated for the first time from *F. cajanderi*. The pure compound 7-methoxyindole-3-carboxylic acid methyl ester purchased (P) from a commercial source and extracted (E) of *P. everhartii* showed significant anti-inflammatory activity at concentrations of 20 μg/ml and 30 μg/ml in THP-1 cells and at a concentration of 30 μg/ml in NCTC cells. The highest percentage of acetylcholinesterase inhibitory activity was 70% at 150 μg/ml for P and E.

All six genes (*Ccl2*, *Cxcl10*, *Cxcl13*, *Tnfsf10*, *Il6*, *and Tnf-α*) showed down-regulation in all samples. RNA-Seq of P and E showed the cytokine-cytokine receptor interaction pathway was affected in almost all treatment samples. RT-qPCR showed that *TNFα*, *IL6* and *CCL2* were up-regulated in three samples (sample E 10 μg/ml, sample E 30 μg/ml and sample P 30 μg/ml) with a 1-2 fold increase and *CXCL13*, *CXCL10* and *TNFS10* showed down-regulation with a 1-2 fold change.

These findings suggest that 7-methoxyindole-3-carboxylic acid methyl ester from *P. everhartii* could be developed as a potential anti-inflammatory therapy in the future according to the *in vitro* results. The ethanol crude extract from *F. cajanderi* could be considered for further anti-cancer and anti-microbial study.

Contents

List of Figures

List of Tables

List of Abbreviations and Symbols

Acetone-d6	Deuterated acetone
ATCC	American Type Cell Culture
BSA	Bovine Serum Albumin
CC	Column Chromatography
$CDCl_3$	Deuterated Chloroform
cDNA	Complementary Deoxyribonucleic Acid
COSY	^{1}H-^{1}H COrrelation SpectroscopY
DMSO	Dimethyl sulphoxide
DNA	Deoxyribonucleic acid
EtoAc	Ethyl acetate
EtOH	Ethanol
FBS	Fetal Bovine Serum
Hex	Hexane
HMBC	Heteronuclear Multiple Bond Coherence
HMQC	Heteronuclear Multiple Quantum Coherence
kD	Kilodaltons
LC-MS	Liquid Chromatography-Mass Spectroscopy
MeOH	Methanol
MIC	Minimum Inhibitory Concentration

mRNA	Messenger Ribonucleic Acid
NMR	Nuclear Magnetic Resonance
PBS	Phosphate Buffered Saline
PPIB	Peptidylprolyl Isomerase B
PCR	Polymerase Chain Reaction
RPMI	Roswell Park Memorial Institute
qRT-PCR	Quantitative Real Time Polymerase Chain Reaction
RNA	Ribonucleic Acid
TLC	Thin Layer Chromatography
VLC	Vacuum Liquid Chromatography

Chapter 1 Introduction

1.1 Research Background

The background to the research carried out in the present project, relates to work previously carried out at the Thailand Institute of Scientific and Technological Research (TISTR), Thailand. TISTR is devoted to collection, preservation and distribution of microorganisms in Thailand. One project was carried out between Mahasarakam University (MSU) and TISTR. MSU set up the Natural Medicinal Mushroom Museum which houses a collection of information about medicinal mushrooms in order for the data to be used to develop new medicines for curing diseases. From the collaboration between MSU and TISTR many projects have been established in order to collect, identify and study the properties of medicinal mushrooms. In the current project, medicinal mushrooms were collected from the North-East of Thailand (Figures 1.1 and 1.2).
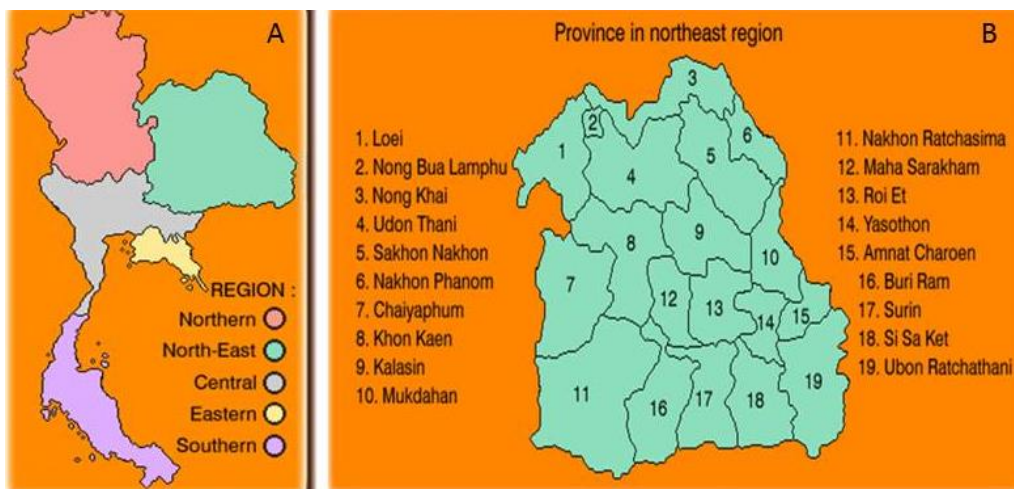
Figure 1.1(A) The map of all regions in Thailand, comprising five regions (Northern, North-East, Central, Eastern and Southern). (B) There are 19 provinces in the North-East region.

Collection and study of mushroom specimens was made from mixed dipterocarp forests and deciduous forests in Nakhon Ratchasima, Maha Sarakham, Mukdahan, Sakon Nakhon, Yasothon, Roi Et, Chaiyaphum, Khon Kaen and Amnat Charoen. All samples (791) were collected 10 times by TISTR staff, hunters and Mr.Winai Klinhom (a lecturer at MSU with expertise in classifying mushroom species by their physical characteristics). By looking at the appearance of the mushrooms and classifying all species of mushroom specimens they found that the mushrooms in the genus *Phellinus* and *Russula* were the most common groups in the mixed dipterocarp and deciduous forests, and *Amanita*, *Boletus* and *Ganoderma* were the second group; *Fomitopsis* was found in smaller quantities together with 97 other genus of mushrooms.

Figure 1.2 A hunter collecting mushrooms from a mixed dipterocarp forest. Taken with permission (April 2013).

Figure 1.3 Mr. Winai Klinhom explaining how to classify mushroom species from their physical characteristics. Taken with permission (April 2013).

1.2 General Information of Mushrooms

Mushrooms have been used for food and in supplements or medical treatments for a millennium. In the last 30 years, the scientific study of mushrooms has increased and revealed compounds with antitumor, immunomodulatory, antioxidant, antihypercholesterolemia, antidiabetic, antibacterial and antiviral effects (Zhang *et al*., 2016).

About 140,000 different species of mushroom exist in the world, but only 10% are known and about 700 species have established pharmacological properties (Lull *et al*., 2005). In North-East Thailand, there are many varieties of mushrooms that the local people consume in high quantities and some of these are used for medicinal purposes; however, there are no scientific reports of studies on these. Both *Phellinus* species and *F. cajanderi* have been used in traditional medicine for anti-cancer, antivirus and anti-diabetic and the local people in North-East of Thailand believed that it can also be used to improve health and prevent disease. The local people in North-East of Thailand use the mushrooms for treatment by boiling and drinking the water and some finely grate and mould the material into a bolus and eat it like a tablet. From interviews with the local people who used the mushroom for medical treatment in 2014, it can be summarised that they used the mushrooms, especially brown mushroom (*Phellinus*), for treatment when they feel unwell - after boiling in water or soaking in rice whiskey. They said it makes them recover but no scientific data exists to confirm it. In the previous study by TISTR, they found that mushrooms in the genus *Phellinus* had good biological properties such as anti-microbial and the genus *Fomitopsis* in its filamentous form

can be stored in 15% glycerol at -80ºC and still be alive after 2 years. The information of interviews from the local people that used mushrooms was shown in Appendix A. Bioactive compounds have been extracted from *Phellinu*s and *Fomitopsis* mushrooms and used for medicinal uses as described in Tables 1.2 and 1.3. According to the information of interviews and biological activities of bioactive compounds from *Phellinu*s and *Fomitopsis* as reviewed in table 1.2 and 1.3, two species of *Phellinu*s and one of *Fomitopsis* that can cultivated filamentous in the laboratory were chosen to study. In the present study, the compounds from three mushrooms *P. everhartii*, *P. laevigatus* and *F. cajanderi* (Figure 1.4) were extracted, compound elucidation carried out and biological activity evaluated.

Figure 1.4 Images of freshly picked mushrooms, A: *Phellinus everhartii*, B: *P. laevigatus*, C: *Fomitopsis cajanderi*

Table1.1 Biological activities of *Phellinus* mushrooms.

Mushroom species	Bioactive components	Biological properties	Reference
P. nigricans	Proteoglycans	Anti-tumor against mice transplanted with Sarcoma 180 and immunomodulating activities by stimulating lymphocyte proliferation and increasing production of nitric oxide (NO) and Tumour Necrosis Factor *alpha* (TNF-α) in macrophages *in vitro*.	Li *et al*., 2008
P. igniarius	EtOH crude extract	Cytotoxicity effect against HepG2, AGS, SGC-7901 and Hela human cancer cell lines	Wang *et al*., 2018
P. igniarius	MeOH extracts from dried mycelia	Antioxidant properties at EC_{50} less than 10 mg/ml	Lung *et al*., 2010

Table 1.2 Biological activities of *Phellinus* mushrooms (continued).

Mushroom species	Bioactive components	Biological properties	Reference
P. igniarius (L.) Quel	Polyphenol extract	Prevents acrolein toxicity at 2 and 5 μM in a mouse neuroblastoma (Neuro-2a) cell line at 0.5 and 2 μg/ml	Suabjakyong *et al*., 2015
P. baumii	Ethyl acetate extract	Anti-inflammatory effects by suppressing inducible nitric oxide synthase (iNOS) and cyclooxygenase-2 (COX-2) and reducing the level of mRNA expression of proinflammatory cytokines interleukin (IL-)1β, IL-6 and granulocyte macrophage colony stimulating factor (GM-CSF)	Yayeh *et al*., 2012

Table 1.2 Biological activities of *Phellinus* mushrooms (continued).

Mushroom species	Bioactive components	Biological properties	Reference
P. baumii	EtOH crude extraxt	Anti-inflammatory activity by inhibiting NO production in Lipopolysaccharides (LPS) activated RAW 264.7 macrophages	Lee *et al*., 2017
P. linteus	Polysaccharides	Immunosuppressive effects by decreasing IFN-γ titres from 135.2 pg/ml to 32.6 pg/ml after 48 h incubation	Kozarski *et al.*, 2011
P. linteus	Crude extract	Attenuating tumor growth and inducing apoptosis of prostate cancer PC3 or Du145 cells in nude mice injected with extract every two days for 12 days	Tsuji *et al*., 2010

Table 1.2 Biological activities of *Phellinus* mushrooms (continued).

Mushroom species	Bioactive components	Biological properties	Reference
Phellinus sp.	Crude extract	Antioxidant activity by exhibiting radical scavenging activity with an IC50 ranging from 7.3 to 19.80 μg/ml	Seephonkai *et al.*, 2011
P. pini	Polysaccharides	Antioxidant activity by scavenging 2,2-diphenyl-1-picrylhydrazyl (DPPH) radicals and hydroxyl radicals, chelate ferrous ion and reduces ferric ions	Jiang *et al.*, 2015
P. merrillii	Crude extract, n-butyl alcohol (n-BuOH) and ethyl acetate (EtOAc) fractions	Antioxidant and free radical scavenging activities	Chang *et al.*, 2007

Table 1.2 Biological activities of *Phellinus* mushrooms (continued).

Mushroom species	Bioactive components	Biological properties	Reference
P. gilvus	Aqueous extract	Inhibitory effect against gram negative bacteria *Escherichia coli* ATCC 25922 and *Klebsiella pneumonia* ATCC 10031 at MIC 360 mgL^{-1} and 90 mgL^{-1}	Sittiwet & Puangpronpitag, 2008

Table 1.2 Biological activities of *Fomitopsis* mushrooms.

Mushroom species	Bioactive components	Biological properties	Reference
F. pinicola	Crude extract	Treatment of atherosclerosis by drecreasing serum glucose and lipids in the blood of diabetic rats	Cha *et al*., 2009
F. pinicola	Chloroform extract	Suppression of proliferation on tumour cell line S180 and inhibition of the growth of S180 solid tumor and prolongs the survival time of tumour-bearing mice	Gao *et al*., 2018
F. rosea	Triterpenes	Antibacterial activity against *Staphylococcus aureus*	Popova *et al*., 2009

Table 1.3 Biological activities of *Fomitopsis* mushrooms (continued)

Mushroom species	Bioactive components	Biological properties	Reference
F. pinicola	Crude extract	Antioxidant from 60 to 120 µg/ml, the DPPH scavenging rate increased from 50.3 to 88.2% and the superoxide anion radical scavenging rate increased from 35.5 to 90.5% from 500 to 700 µg/ml. Anti-tumour activities were shown by decreasing cell viability of cancer cell lines when the concentration of the extracts increased especially HeLa and Hep3B (cell viability rate 20-25% with MeOH extract concentration 1000 µg/ml	DuBok Choi *et al.*, 2007

1.2.1 *Phellinus laevigatus* **(Fr.)**

P. laevigatus (Fr.) is a dark brown mushroom, with a perennial fruit body. It is woody, hard, widely and firmly attached to tree substrates, is totally effused, when growing on vertical surfaces, especially on broken ends of fallen logs, with a crusty tipper surface, up to 1 cm wide or more, but also in these cases flat, not projecting much from the surface. Fruit bodies when young are small, round, separate, later fusing together to form bodies measuring about 10-20 x 5-10 cm, or, in favourable conditions, under whole logs, reaching a length of several metres. The thickness of fruit bodies is 0.1-0.5 cm, and in old specimens up to 2.7 cm. The hymenial layer in the fruit body grows in a horizontal or oblique position even in fruit bodies growing on vertical surfaces they form low steps with sloping margins and the outermost tubes open at the side. The actively growing hymenial surface is not very dark brown, with bronze or olive tints and a silky glitter in the side view; when old they turn deep brown, sepia to chocolate colour. Non-growing pore surfaces, for instance in specimens collected in late winter or early spring, are light grey to brownish grey and with no glitter. Pores are regular, (5 -) 6-8 (- 12) per mm; in the surface view they are round, oval or slightly angular, while in transverse section they are round or ellipsoid, (0.01-) 0.08-0.12 (- 0.15) mm in diameter, dissepiments ca. 0.03-0.06 mm thick.

The fruit body contracts rather strongly when drying, which results in loosening of margins, especially on bark substrates, and either inrolling or cracking of the tube layer. Spores (3.7-) 3.8-5.0 (-5.4) x (2.8-) 3.0-3.9 (- 4.2) cm, single, ellipsoid, seldom slightly ovate, obtuse-based, with applanated supra-apicular region. The wall is thin, ca. 0.3-0.4 µm, smooth and colourless (Niemelä,1972).

1.2.2 *Phellinus everhartii*

P. everhartii is a yellowish brown mushroom. The basidiocarps are sessile, ungulate, up to 6 x 13 x 8 cm; the upper surface is yellowish brown to blackish, sometimes very finely tomentose, becoming glabrous and encrusted with age, usually sulcate, rimose; margin concolorous, rounded; the pore surface glancing with a golden luster, dark yellowish to reddish brown (ochraceous-tawny, buckthorn brown or cinnamon brown). The pores are circular to angular, 5-6 per mm, with thick, entire dissepiments; context reddish brown, woody, faintly zonate, up to 5 cm thick; tube layers are concolorous with the context, rather distinctly stratified, each layer up to 6 mm thick; context with masses of hard granular tissue that appear under a 30x lens as dark, solid or resinous areas in a matrix of paler brown interwoven mycelium; hyphae of dark masses agglutinated and hard to separate, tissue breaking out in small chunks (Núñez & Ryvarden, 2000).

Both mushrooms are found growing in hardwood forests of North America, mainly in the East, in East Asia known from Far East Russia including in Thailand.

1.2.3 *Fomitopsis cajanderi*

Fomitopsis is another genus of mushroom that has been found to have good biological properties; however, the scientific data is sparse at present. *F. cajanderi* is a pink mushroom. The basidiocarp is perennial, sessile to effused-reflexed or occasionally resupinate, solitary or imbricate, up to 20x7x10 cm; the upper surface is light brown to pale pinkish in young specimens, darkening to pinkish brown or grey to blackish with age, tomentose to fibrillose or glabrous; the pore surface is rose coloured. The pores are circular to angular, with thick, entire dissepiments, 4-5 per mm; the context is corky, light pinkish brown, azonate, up to 1 cm thick, tube layers stratified, paler than the context, up to 2 cm thick. The hyphal system is dimitic; contextual generative hyphae thin-walled, with clamps, hyaline, 2-4 µm in diameter; contextual skeletal hyphae are pale brown in KOH, rarely branched, non-septate, thick-walled, 2.5-6 µm in diameter (Ryvarden & Gilbertson, 1993).

1.2.4 Bioactive compounds from mushrooms

There are diverse bioactive compounds in mushrooms that are beneficial in medical therapies. Examples of secondary metabolites extracted from different species of mushroom and their biological properties are summarised in Table 1.1.

Patel & Goyal (2012) described the range of bioactive compounds in mushrooms including lentinan, theanine, hispolon, psilocybin, grifolin, ganoderic acid and polysaccharides; potential substances with anti-tumor properties.
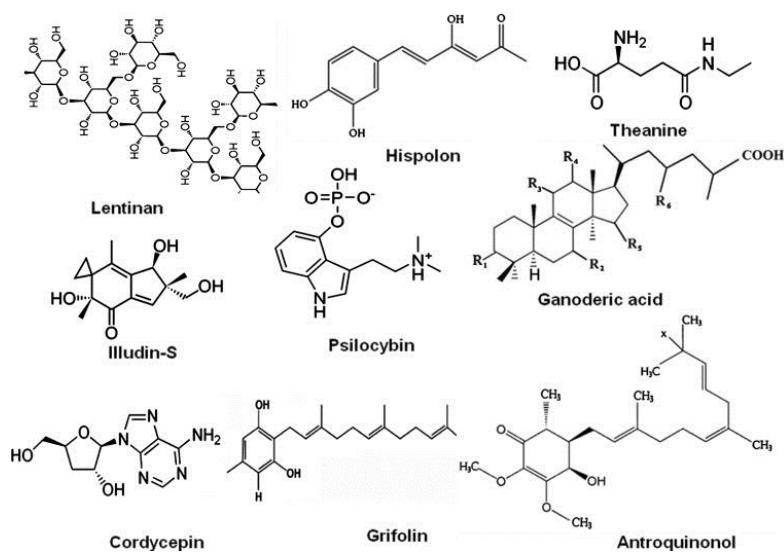
Figure 1.5 Structure of bioactive compounds isolated form mushrooms

Table1.3 Secondary metabolites and biological properties of mushrooms

Compound name	Species	Biological activity
Triterpenoids		
Acids		
1. Eburicoric acid	LS, LO	Anti-cancer
2. Sulfurenic acid	LS, LO	Anti-leukaemia
3. Versisponic acid D	LO	Anti-thrombin
4. 3-O-Acetyleburioic acid	LS	Anti-leukaemia
5. 16α-Hydroxyeburiconic acid	FP	Antibacterial
6. Fomefficinic acid D	LS, LO	Anti-leukaemia
7. Versisponic acid C	LS	Anti-leukaemia
8. 15α-Hydroxytrametenolic acid	LS	Anti-leukaemia
9. (3β)-3-(acetyloxy)-Lanosta-8,24-dien-21-oic acid	LS	Anti-leukaemia
10. Tsugaric acid A	FP	Antibacterial
11. Pinicolic acid A	FP	Antibacterial
12. Fomitopsic acid	FP	Antimicrobial
13. 24-Methyl-3-oxo-Lanosta-8,25-dien-21-oic acid	FP	Antibacterial
14. Fomitopinic acid A	FP	Anti-inflammatory
15. Fomitopinic acid B	FP	Anti-inflammatory
16. Polyporenic acid A	PB	Anti-inflammatory
17. (3α,12α,25S)-3-(acetyloxy)-12-hydroxy-24-methylene-	PB	Anti-inflammatory, inhibition of bacterial

Lanost-8-en-26-oic acid		Hyaluronidase
18. (3α,12α,25S)-3-[(carboxyacetyl)oxy]-12-hydroxy-24-methylene-Lanost-8-en-26-oic acid	PB	Anti-inflammatory
19. (3α,12α,25S)-12-hydroxy-3-(3-methoxy-1,3-dioxopropoxy-24-methylene-Lanost-8-en-26-oic acid	PB	Anti-inflammatory, inhibition of bacterial hyaluronidase
20. (3α,12α,25S)-3-[(3S)-4-carboxy-3-hydroxy-3-methyl-1-oxobutoxyl]-12-hydroxy-24-methylene-Lanost-8-en-26-oic acid	PB	Anti-inflammatory
21. (3α,12α,25S)-12-hydroxy-3-[[(3S)-3-hydroxy-5-methoxy-3-methyl-1,5-dioxopentyl]oxy]-24-methylene- Lanost-8-en-26-oic acid	PB	Anti-inflammatory, inhibition of bacterial hyaluronidase
22. (+)12α,28-Dihydroxy-3 α-(3'-methylglutaryloxy)-24-methyllanosta-8,24(31)-dien-26-oic acid	PB	Anti-inflammatory

23. Polyporenic acid C	PB,FP	Anti-inflammatory, inhibition of bacterial hyaluronidase, antibacterial
	PB,FP	Antibacterial
24. (16α)-16-(acetyloxy)24-methlene-3-oxo-Lanosta-7,9(11)-dien-21-oic acid		
	FF	Antitumor
Esters and lactones		
25. Betulin 28-O-acetate	LS, FF	Antitumor
	FP	Antibacterial
Alcohols	FF	Antitumor
26. Δ7-Ergostenol		
27. Ergosterol D		
28. (+)-Betulin	FF	Antitumor
	LS, PB, FF	Cytotoxic, antitumor
Ethers and peroxides		
29. (5α)-3,3-dimethoxy-Ergosta-7,22-diene	FF	Antitumor
30. Ergosterol peroxide		
	FP	Anti-inflammatory
	FP	Anti-inflammatory

Aldehydes and ketones	FP	Anti-inflammatory
31. (22E)-Ergosta-7,22-dien-3-one	FP	Anti-inflammatory
	FP	Anti-inflammatory
Glycosidic triterpenes	FP	Anti-inflammatory
32. Fomitoside A	FP	Anti-inflammatory
33. Fomitoside B	FP	Anti-inflammatory
34. Fomitoside C	FP	Anti-inflammatory
35. Fomitoside D	FP	Anti-inflammatory
36. Fomitoside E	FP	Anti-inflammatory
37. Fomitoside F		
38. Fomitoside G		
39. Fomitoside G	FP, LS, PB	Antioxidant
40. Fomitoside H		
41. Fomitoside I	FP, LS, PB	Antioxidant
42. Fomitoside J		
Miscellaneous triterpenes	FP, LS, PB	Antioxidant
Organic acids and related compounds	LS	Antioxidant
43. p-Hydroxybenzoic acid	LS	Antioxidant
	LS	Antioxidant
44. Protocatechuic acid	PB	Matrix metallo-proteinase inhibitor
	LS	Antioxidant

45. Vanillic acid		
	LS	Cytostatic
46. Gallic acid		
47. p-Coumaric acid	LS	Antioxidant
48. Caffeic acid	LS	Antioxidant
49. 2-[(2E)-4-hydroxy-3-methyl-2-buten-1-yl]-1,4-Benzenediol	LS	Antioxidant
50. Chlorogenic acid	FF	Antitumor
	LO	Antimicrobial
Benzofurans		
51. (±)-Laetirobin	LO	Antimicrobial
Flavonoids and related compounds		
52. Kaempferol	PB	Antibiotic
53. Quercetin		
54. (2R,3S)-(+)-Catechin		
Coumarins		
55. Daphnetin		
56. 2H-6-chloro-2-oxo-4-phyl-1-Benzopyran-3-carboxylic acid ethyl ester		
57. 6-Chloro-4-phenyl-coumarin		

N-containing compounds		
58. Piptamine		

Source: Grienke *et al*., 2014

LS: *Laetiporus sulphureus*, FF: *Fomes fomentarius*, PB: *Piptoporus betulinus*,

LO: *Laricifomes officinalis*, FP: *Fomitopsis pinicola*

1.3 Properties of mushrooms

Mushrooms have been used not only for food, but also for medical treatments. Historically, mushrooms have been used in traditional medicine, but because of the limited scientific data with respect to clinical trials, their use in the pharmaceutical industry remains low. So far, there have been many reports on the health benefits of mushrooms to humans in treatment of various diseases from countries such as China, India, Korea and Japan (De Silva *et al.*, 2012).

1.3.1 Medicinal properties of mushrooms

1.3.1.1 Anti-cancer properties

There is scientific data to demonstrate that some species of mushroom contain bioactive compounds for inhibiting or destroying cancer cells.

Patel & Goyal (2012) reported that some species in the genus *Agaricus*, *Agrocybe, Garnoderma*, *Pleurotus*, *Trametes, Inonotus, Amauroderma , Innotus, Phillanus* and *Antrodia* have anti-cancer activity. For example, *Trametes versicolar*, commonly known as turkey tail mushroom or cloud mushroom can inhibit the proliferation of hepatoma cancer cell lines *in vitro* and *in vivo*. Jiao *et al*. (2013) found that the water extract of *Amauroderma rude* had the highest activity in killing three human breast

carcinoma cell lines, MDA-MB231, MDA-MB468 and MT-1 and the size of tumors that formed by injecting with 4T1 cells in Balb/c mice were decreased. Lee *et al*. (2009) revealed that a water extract of *Innotus obliquus* inhibited growth of HT-29 human colon cancer cells, while Roupas *et al*. (2012) demonstrated that triterpenoids, hyper-branched, beta-glucan extracted from *Garnoderma lucidum*, *Pleurotus tuberregium*, *Cordyceps sinensis* and *Innotus obliquus* showed anti-cancer activity by inhibiting proliferation of HepG2 (human hepatocellular carcinomas), exhibiting tumor-selective and cytotoxic (*in vivo*) mechanisms. Zhao *et al.* (2003) described an antitumor lectin isolated from *Agrocybe aegerita* that strongly inhibited growth of human tumor cell lines HeLa, SW480, SGC-7901, MGC80-3, BGC-823, HL-60 and mouse sarcoma S-180.

1.3.1.2 Anti-viral properties

Generally, viral diseases are a major problem that are difficult to treat because of high genetic variability (Ohta *et al*., 2007). Vaccines and anti-viral agents are used to control and prevent viruses. However, there are other ways such as stimulation of the innate immune response to protect against infectious diseases. An acidic polysaccharide (APS) extract from *Cordyceps militaris* has shown therapeutic effects on influenza virus infection by increasing TNF-α and IFN-γ levels in mice (Ohta *et al*., 2007). Aqueous and ethanol extracts and polysaccharides from *Lentinula edodes* have been shown to inhibit the initial process of poliovirus type 1 and bovine herpes virus type 1 (Rincao *et al*., 2012).

1.3.1.3 Anti-microbial properties

Smolskaitė *et al*. (2015) found that *Inonotus hispidus* had antimicrobial activity against gram-positive bacteria (*Bacillus cereus*), gram negative bacteria (*Pseudomonas aeroginosa*) and fungi (*Candida albicans*). Roupas *et al*. (2012) reported that *A. blazei* Murill extract was active against *Streptococcus pneumonia* 6B infection in mice.

1.3.1.4 Antioxidant properties

Palacios *et al.* (2011) assessed eight types of mushrooms (*Agaricus bisporus*, *Boletus edulis*, *Calocybe gambosa*, *Cantharellus cibarius*, *Carterellus cornucopioides*, *Hygrophorus marzuolus*, *Lactarious deliciosus*, *Pleurotus ostreatus*) for antioxidant activity. *Cantharellus cibarius* showed the highest activity and *Agaricus bisporus* the lowest. Reis *et al.* (2012) compared the antioxidant properties between fresh cultivated mushrooms and mycelium. The highest antioxidant activity was found for *A. bisporus* with no correlation between fresh mushrooms and mycelium.

1.3.1.5 Anti-inflammatory properties

Polysaccharides extracted from *A. bisporus* and *A. brasiliensis* stimulate the production of pro-inflammatory cytokines Tumor Necrosis Factor alpha (TNF-α), Interleukin-1 beta (IL-1β) and the enzyme Cyclooxygenase-2 (COX-2) from THP-1 cells. Fangkrathok *et al*. (2013) demonstrated that an extract of *Lentinus polychrous* had anti-inflammatory effects *in vitro* by decreasing the expression of inducible Nitric Oxide Synthase (iNOS), IL-1β) IL-6, TNF-α and COX-2. TNF-α production was decreased significantly in Lipopolysaccharides-activated macrophages

Wen *et al*. (2011) found that a mycelium extract of *Antrodia cinnamomea* had anti-inflammatory activity both *in vitro* and *in vivo*. *In vitro*, an extract of *Antrodia cinnamomea* inhibited the production of pro-inflammatory cytokines (TNF-α and IL-6) and mediators (Nitric Oxide (NO) and Prostaglandin E_2 (PGE2) in LPS-stimulated RAW264.7 cells and human Peripheral Blood Mononuclear Cells (PBMCs) and decreased iNOS and COX-2 levels in LPS-stimulated RAW264.7 cells. According to *in vivo* assessment, the extract showed significant anti-inflammatory activity by decreasing oedema in a carrageenan-induced paw oedema mouse model.

1.3.1.6 Other therapeutic activities

Roupas *et al*. (2012) reported that an extract of *P. ostreatus* prevented selenite-induced cataractogenesis in 75% of rats. Furthermore, *A. blazei* showed anti-hyperglycemic, anti-arteriosclerotic and anti-diabetic activity in rats. Krediet *et al*., 2020 reviewed that psilocybin has been studied for the treatment of depression, tobacco and alcohol addiction, obsessive-compulsive disorder, and depression and anxiety in patients with life-threatening diagnoses and recently received breakthrough designations from the FDA for use in depression.

1.3.2 Medical mushroom use in clinical trials

There are many clinical trials reported for polysaccharides of mushrooms namely lentinan (*L. edodes*), schizophyllan (*S. commune*), PSK and PSP (*T. versicolor*), and Grifron-D (*G. frondosa*) used to treat cancer patients (Sullivan *et al*., 2006). A clinical trial of schizophyllan showed that the survival rate of neck and head cancer patients was increased and in some cases this substance increased overall survival of stage II cancer patients when combined with radiotherapy (Sullivan *et al*., 2006).

Another successful clinical trial used a combination chemotherapy of mitomycin C, 5-fluorouracil and PSK (from mushrooms). The result was the survival rate of patients increased two-times compared with only using chemotherapy treatment without PSK (Sullivan *et al*., 2006).

In addition, a clinical trial in Japan has shown that patient survival can be significantly extended in stomach, colon-rectum, esophagus, nasopharynx, and lung (non-small cell types) cancers and in a HLA B40-positive breast cancer subset after treatment with PSK from *Coriolus versicolor* (Kidd, 2000). In China, clinical trials (Phase II and Phase III) of PSP from *C. versicolor* has revealed that PSP significantly extended five-year survival in esophageal cancer, improved quality of life and enhanced immune status in 70-97 percent of patients with cancers of the stomach, esophagus, lung, ovary, and cervix (Kidd, 2000).

At present there is a product from mushrooms that is used as an adjuvant therapy in conjunction with radiotherapy and chemotherapy launched under different brands such as Ganodex, Immuna, Lentinex, Immunglukan, Bene-X and Zymucan (El Enshasy & Hatti-Kaul, 2013).

1.4 Project aims

According to the previous study carried out at TISTR, many crude extracts from mushrooms in the genus *Phellinus* had shown good biological activity and from interviewing the local people that used these mushrooms for medical purpose, two species of *Phellinus* mushrooms were chosen for further study. In addition, *F. cajanderi* was chosen as it can be cultivated in the laboratory and could be useful for commercial development in the future.

The aims were:

- To collect, extract and identify bioactive compounds from mushrooms *P. everhartii*, *P. laevigatus* and *F. cajanderi* (Chapter 2).
- To investigate biological activity including anti-inflammatory, cytotoxicity, anticholinesterase and antimicrobial of crude extracts and pure compound 7-methoxyindole-3-carboxylic acid methyl ester (Chapter 3).
- To examine the effect of pure compound 7-methoxyindole-3-carboxylic acid methyl ester on gene expression in THP-1 cells using RNA-Seq and qRT-PCR (Chapter 4).

Chapter 2 Phytochemistry

2.1 Introduction

Several extraction methods have been used to explore natural materials. Most of the conventional techniques such as Soxhlet extraction, maceration and hydro-distillation are based on the extracting ability of different solvents and the application or absence of heat and stirring (Azmir *et al*., 2013). The Soxhlet extractor was designed for lipid extraction by the German chemist Franz Ritter Von Soxhlet in 1879. In this technique, the ground sample is placed in a thimble chamber and then moved into a thimble-holder which is filled with extraction solvent and heated in the lower flask. After reaching an overflow level, the solution of the thimble-holder is aspirated by a siphon and the siphon unloads the solution back into the distillation flask (Azmir *et al*., 2013). This solution carries extracted solutes into the bulk liquid and solute remains in the distillation flask and the solvent passes back to the solid bed of plant material. The process runs repeatedly until the extraction is completed. Presently it is used for the extraction of compounds from different materials.

Maceration is commonly used in wine making with a variety of solvents and has been developed and widely used in medicinal plant research (Nn, 2015). This method is used in a closed container system by soaking material at room temperature for at least three days and then filtrated and evaporated (Majekodunmi, 2015). This technique is simple, cheap and easy, but there is a large amount of solvent waste to manage (Nn, 2015).

Hydro-distillation can be achieved using water, water and steam or steam only (Azmir *et al*., 2013).

The efficiency of these traditional methods depends on the solvents and polarity of the targeted compounds. There are three types of solvents; polar, medium-polar and non-polar. The polar solvents extract non-polar and polar compounds, but non-polar solvents extract only non-polar compounds (Majekodunmi, 2015). Some classes of compounds extracted using different solvents are given in Table 2.1.

Table 2.1Examples of some compound classes extracted by different solvents

Solvents	Bioactive compounds
Water	Anthocyanins, Tannins, Saponins, Terpenoids
Ethanol	Tannins, Polyphenols, Flavonols, Terpenoids, Alkaloids
Methanol	Anthocyanin, Terpenoids, Saponins, Tannins, Flavones, Polyphenols
Chloroform	Terpenoids, Flavonoids
Dichloromethane	Terpenoids
Ether	Alkaloids, Terpenoids
Acetone	Flavonoids

Now, there are new techniques which have been introduced to increase efficiency and decrease extraction time. Some of these include ultrasound assisted extraction, enzyme-assisted extraction, microwave-assisted extraction, pulsed electric field assisted extraction, supercritical fluid extraction and pressurised liquid extraction (Azmir *et al*., 2013). Some plant products may need unique extraction processes and no single extraction method can be termed as best. Sample preparation methods such as drying, grinding could affect the efficiency of extraction and selected methods also depend on the study objectives, nature and size of sample and the target compounds (Nn, 2015).

Yan *et al*., 2017 mentioned that the method of extraction for polysaccharides from mushroom material was 80% (v/v) ethanol followed by three successive extractions

with water (100ºC, 3 h), 2% (w/v) ammonium oxalate (100ºC, 3 h) and 5% (w/v) sodium hydroxide (80ºC, 3 h).

Polysaccharide from fruiting bodies of sanghuang mushroom (*P. baumii* Pilat) was extracted using hot water extraction three times for 2 h each after exhaustive reflux extraction with ethanol for 12 h to remove lipids (Ge *et al*., 2013).

Laovachirasuwan *et al*. (2016) studied *Phellinus* spp. extracted using a water, ethanol and alkaloid extraction procedure. The mushroom water extract was extracted with 1,500 ml of distilled water using the decoction method at 90ºC for 4 h. The ethanol extract was macerated with 1,500 ml of 95% ethanol at room temperature for 7 days. The procedure for alkaloid extraction was swirled around with 500 mL of 10% (v/v) ammonia solution for 5 min. Then, the extracted part was diluted with 2,500 mL of methanol and heated at 60°C for 30 min. The *Phellinus* mushroom extracts were filtered through Whatman No.1 and concentrated using a rotary evaporator. Each *Phellinus* mushroom extract was dried by freeze dryer.

In this study *Phellinus* and *Fomitopsis* mushrooms were collected and ground to powder form and were extracted by maceration and Soxhlet. The crude extracts were fractionated using column chromatography and sephadex and isolated compounds analysed by NMR.

2.2 Materials

n-Hexane HPLC grade (VWR chemicals , UK)

Dimethyl sulphoxide (Sigma-Aldrich, UK)

Ethyl acetate HPLC grade (VWR chemicals, UK)

Methanol HPLC grade (VWR chemicals, UK)

Ethanol HPLC grade (VWR chemicals, UK)

Deuterated (99.9%) solvents: Chloroform-d, DMSO-d6, and Acetone-d6

(Sigma-Aldrich, UK)

p-anisaldehyde (Sigma-Aldrich, UK)

Column grade silica gel (Silica gel 60, mesh size 20-200 μm) (Merck, Germany)

TLC grade silica gel 60H (Merck, Germany)

TLC pre-coated aluminium sheets (20 x 20 cm). Silica gel PF254

(Merck,Germany)

2.3 Methods

2.3.1 Sample collection

The mushrooms, *F. cajanderi* (Kar.:Kolt & Pouzar), *P. everhartii*, *P. laevigatus* were collected from Phu Pha Kham Tumbon Phuwong Nhnogsoung City, Mukdaharn Province in the North-East of Thailand in April 2014 and identified by Mr Winai Klinhom of the Mahasalakam University.

2.3.2 Extraction

The mushrooms were air-dried and cut into small pieces and ground using a blender. The ground mushrooms (50 g or 200 g) were extracted successively by maceration with Hex, EtOAc, EtOH and then EtOH: water (50:50) for two days each. The extracts were evaporated using a rotary evaporator. Alternatively, a Soxhlet apparatus was used to extract 200 g of material using EtOH for seven days.

2.3.3 Fractionation of crude extracts

2.3.3.1 Thin Layer Chromatography (TLC)

Thin layer chromatography (TLC) is used to separate compounds from extracts and fractions. The samples were dissolved in an appropriate solvent (determined by trial and error) and spotted onto silica gel 60H silica aluminum plates, 1 cm from the bottom edge using a capillary tube. A mobile phase (solvent mixture depending on the polarity of the extract or fraction) was added to a TLC tank (4-5 mm depth) and left until the environment was saturated. The spotted TLC plate was placed in the chamber until the solvent reached the top of the plate. The plate was removed, air-dried and observed under UV light at 254 nm (short wavelength) and 366 nm (long wavelength). Any visible bands were marked by pencil before the plate was sprayed with anisaldehyde-H_2SO_4 spray (5 ml sulphuric acid, 85ml methanol, 10 ml glacial acetic acid and 0.5 ml anisaldehyde) and heated at 110°C for a minute. Fractions (from column chromatography (CC) – see section 2.3.3.2) shown to have similar compound profiles were pooled together.

2.3.3.2 Column Chromatography (CC)

CC was used to separate mixtures of compounds in the extracts. A glass column 45×3 cm with a tap was packed with a wet slurry of silica gel 60. The extracts were pre-adsorbed with a small amount of silica gel 60 and dried before placing the dry slurry on top of the column. The mobile phase (250-300 ml) was added and the column was eluted gradient wise (Table 2.2). Fractions were collected (10 ml per glass vial) and examined by TLC. Fractions with similar band profiles were combined together.

Table 2.2 Sequence of CC solvent systems

	Solvent (%)		
	Hexane	**Ethyl acetate**	**Methanol**
1	100	0	0
2	90	10	0
3	80	20	0
4	70	30	0
5	60	40	0
6	50	50	0
7	40	60	0
8	30	70	0
9	20	80	0
10	10	90	0
11	0	100	0
12	0	90	10

2.3.3.3 Gel filtration using Sephadex

A gel filtration column using Sephadex was used for separation of compounds based on their molecular size. A wet slurry of Sephadex LH-20 was packed in a glass column with a tap approximately 45x2.5 cm. The extracts were dissolved in MeOH and added onto the column. MeOH was also used to elute the column and fractions (5 ml) were collected in glass vials.

2.3.3.4 Vacuum Liquid Chromatography (VLC)

Silica gel 60H was dry-packed in a suction filtration glass funnel (diameter 9.5 cm) under vacuum. The EtOH extract and EtOH:water extract were loaded on the VLC column and eluted gradient wise using 400 ml of each different solvent system as in Table 2.3. TLC was used to examine the fractions.

Table 2.3 Sequence of VLC solvent systems

	Solvent (%)		
	Hexane	**Ethyl acetate**	**Methanol**
1	90	10	0
2	70	30	0
3	50	50	0
4	30	70	0
5	0	100	0
6	0	90	10
7	0	70	30
8	0	50	50

2.3.4 Nuclear Magnetic Resonance (NMR)

Samples were dissolved in deuterated chloroform ($CDCl_3$) or dimethyl sulphoxide (DMSO-d_6) depending on their solubility and transferred to NMR tubes (5mm x 178mm). One-Dimensional NMR (1D) was used for preliminary investigation of the fractions and compounds from their proton or carbon spectra. Two-Dimensional NMR (2D) and COrrelation SpectroscopY (COSY) was used to determine ^{1}H-^{1}H proton-proton correlations; Heteronuclear Multiple Quantum Correlation (HMQC) was used to identify the correlation between protons and carbons via ^1J couplings. Heteronuclear Multiple Bond Correlation (HMBC) provided the long range correlation between the protons and carbons through ^2J and ^3J and even ^4J couplings (H-X-C-C correlations). The NMR spectra were obtained on a JEOL Eclipse 400 spectrophotometer operating at 100 MHz for ^{13}C and 400 MHz for ^{1}H and a Bruker Avance DRX-500 (500 MHz) spectrometer for HMQC and HMBC.

2.3.5 Mass spectrometry

Liquid chromatography mass spectrometry (LC-MS) was used to confirm the molecular weights and molecular formulae of pure compounds. Samples were prepared in 1 mg/ml of methanol and 10 µl of solution was injected into an Agilent Zorbax Eclipse (C18 column (4.6x150mm, 5µM). The LC-MS analysis was carried out in the Department of Pure and Applied Chemistry, Strathclyde University.

2.3 Results

2.3.1 Fractionation of crude extracts and identification of compounds

Following extraction using a Soxhlet apparatus, the crude extracts were examined by NMR. The EtOH extract of *F. cajanderi* (Kar) Kolt& Pouzar from VLC was a white powder and identified as a mixture of two triterpenes. The EtOH extract of *P. laevigatus* was a brown crystalline solid. No single compound was isolated from both these crude extracts. Fraction 30-33 of EtOH crude extract of *P. everhartii* from Sephadex gel filtration chromatography was a brown-yellowish crystalline solid identified as a pure compound.

The major compound class from *F. cajanderi* (Kar) Kolt& Pouzar and *P. laevigatus* appeared to be triterpenes, an indole alkaloid was the major compound obtained from *P. everhartii.* The structure of the triterpene from *F. cajanderi* extract is given in Figure 2.1 and the structure of the alkaloid from *P. everhartii* extract is given in Figure 2.2. The structure of the triterpene from *P. laevigatus* is yet to be fully determined.

2.3.2 Fractionation of *F. cajanderi* (Kar) Kolt& Pouzar crude extract

CC, gel filtration and VLC were applied to fractionate *F. cajanderi* ethanol crude extract. The fractions were collected and the profiles examined using TLC and NMR. The major compound was an ester of malonic acid of a lanostanoid type triterpene as called compound FVC (Figure 2.6).

The NMR spectra for the fractions are shown in Figures 2.1-2.5. The proton spectrum (Figure 2.1) was typical of a triterpene as there were a number of proton signals between 0.5 and 3.0 ppm. There was a pair of deshielded (ethylenic) protons at 6.20 and 5.94 ppm. These could come from an exomethylene group in the compound. There were three signals from protons attached to oxygen bearing carbons at 4.77(t), 4.16(m) and 3.45(s).

Figure 2.1 The ^{1}H NMR spectrum of VLC EtOH 5 fraction of *F. cajanderi* in CDCl₃
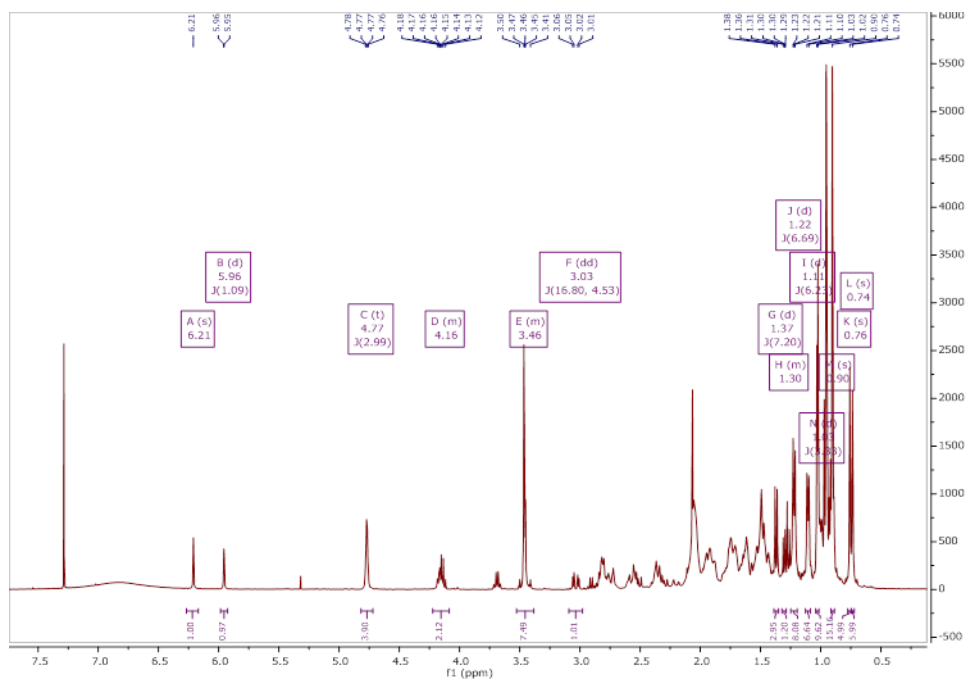
Figure 2.1 The ^{1}H NMR spectrum of VLC EtOH 5 fraction of *F. cajanderi* in CDCl$_3$

The carbon spectrum (Figure 2.2) gave signals for oxygen bearing carbons between 160 to 215 ppm and two unsaturated carbon signals between 120 and 150 ppm. The ^{13}C spectrum also showed an oxygen bearing methine carbon at 80.2 ppm, an oxygen bearing methylene around 60 ppm and a lot of CH, CH$_2$ and CH$_3$ carbons between 10.0 and 50.0 ppm.
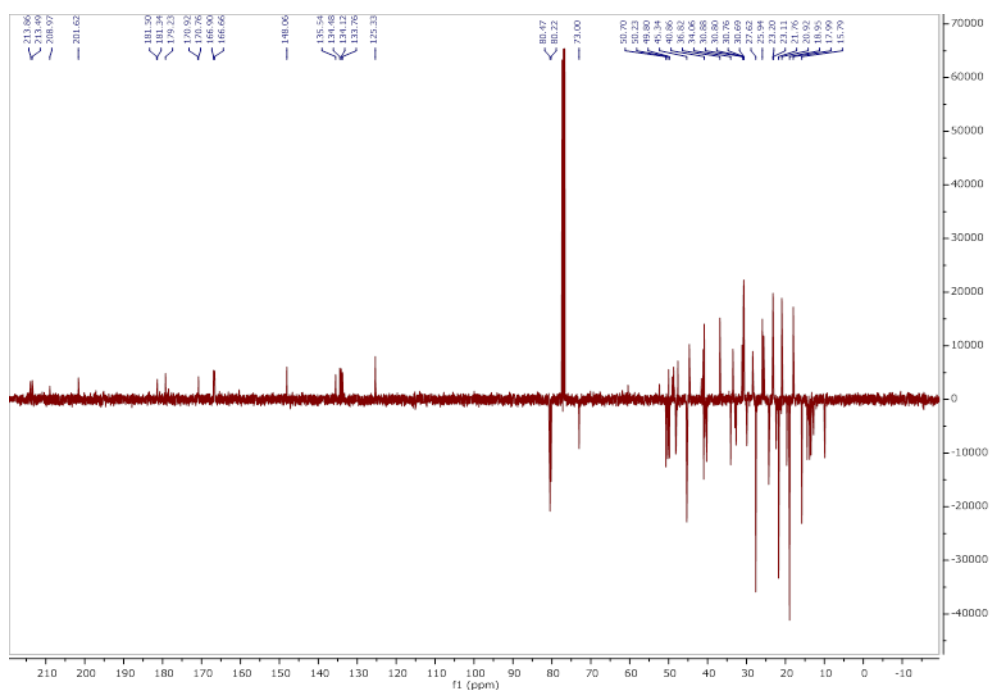
Figure 2.2 The[13]C NMR spectrum of VLC EtOH 5 fraction *F. cajanderi* in CDCl$_3$

From the correlations in the 2D spectrum for the compound (Figure 2.3), it was identified as follows: the ^{1}H-^{1}H COSY spectrum (Figure 2.3) identified the methyl doublets and the methine proton to which they are coupled.
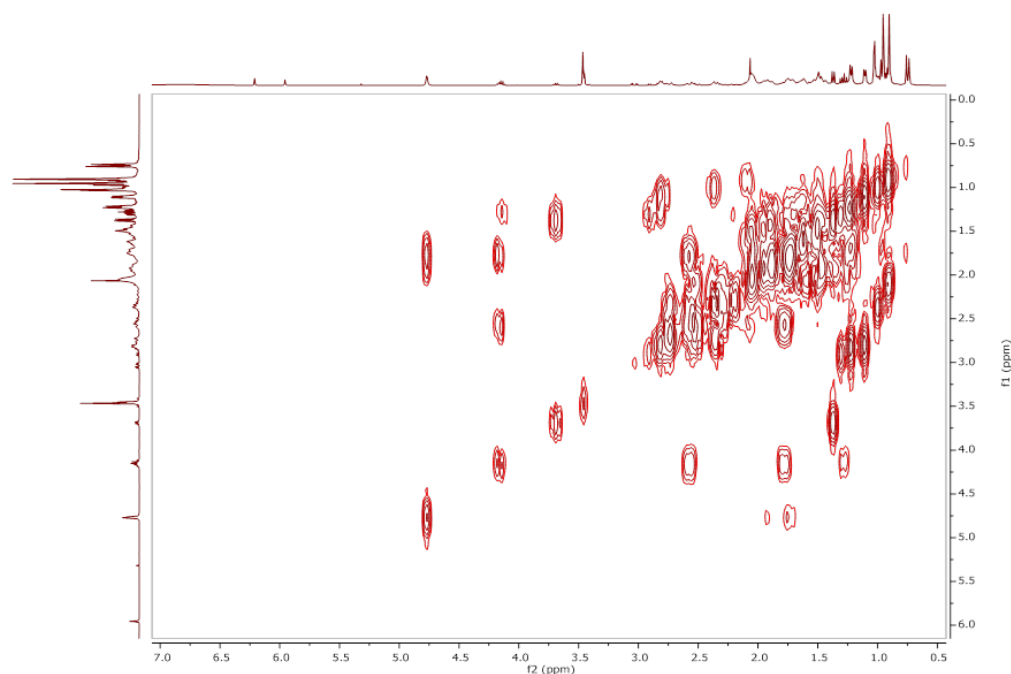
Figure 2.3 The COSY spectrum of VLC EtOH 5 fraction *F. cajanderi* in CDCl$_3$

From the HSQC (^{1}H-^{13}C) correlations (^1J) or direct coupling, the protons attached to the various carbons were identified (Figure 2.4). In the HMBC (^{1}H-^{13}C, $^{2,3}J$) (Figure 2.5) or long range correlations were observed. The exomethylene protons gave correlations to a saturated ketone carbon at 201.5 ppm hence the exomethylene group must be next to the ketone. The proton quartet at 3.70 ppm gave correlations to carbonyl at 179.0 (COOH), the ketone at 201.5 and the exomethylene carbons at 147.8 (C) and 125.0 (CH$_2$). Another proton quartet at 2.10 also showed correlations to the ketone, therefore the ketone must be in the middle of a side chain attached to the steroid. Correlations from the methylene group at 3.37 to carbonyl carbons at 171.3 and 167.3 as well as the methine carbon at 80.5 indicated a malonyl ester attached to the position C-3 of the steroid. This is confirmed by correlations from two geminal methyl groups to the C-3. The presence of a double bond between C-8 and C-9 was confirmed by correlation from H-19 and H-28 to the carbon at 134.7 and 133.9, respectively. Therefore, the structure was identified to be an ester of a malonic acid of a lanostanoid type triterpene as called Compound1 earlier reported by Chairul *et al.* (1990) (Figure 2.6). The assignment of the proton and carbon chemical shifts for the compound which were compared with literature reports is given in Table 2.4.
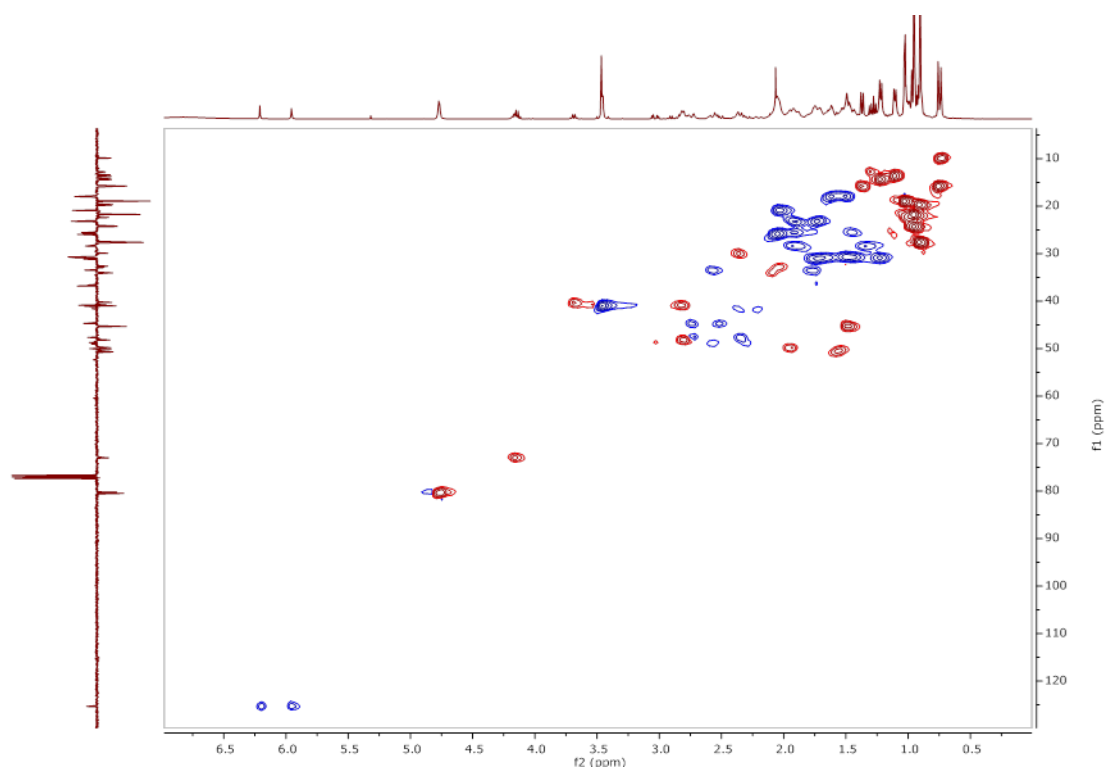
Figure 2.4 The HSQC spectrum of VLC EtOH 5 fraction *F. cajanderi* in CDCl₃
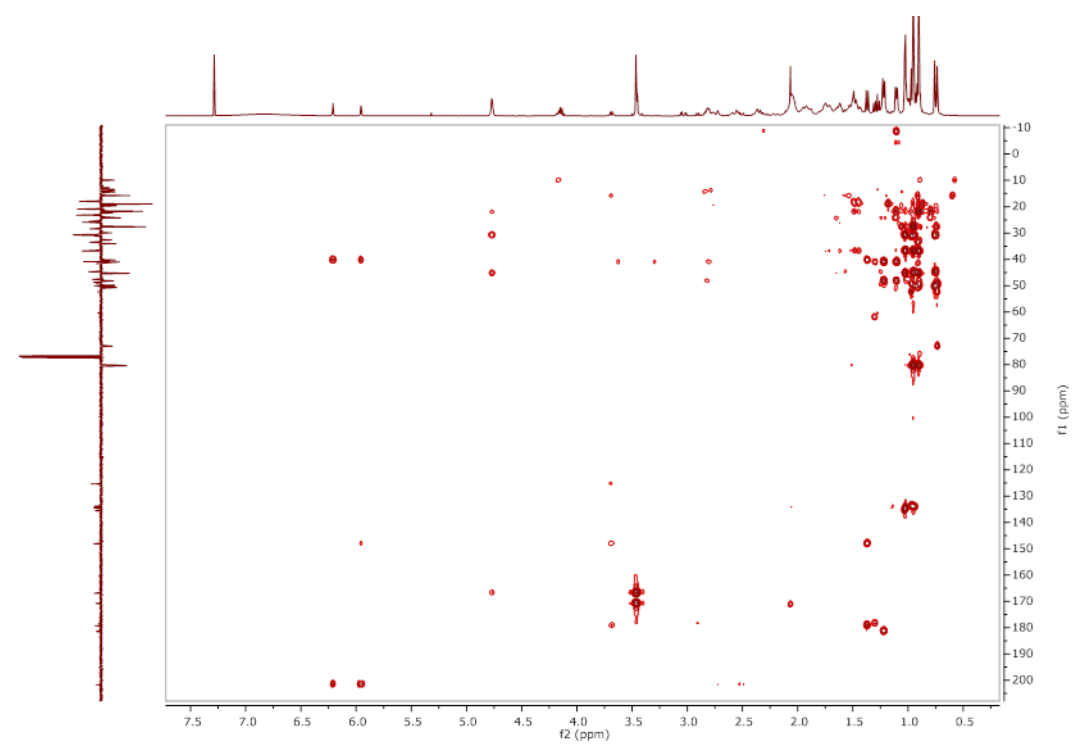
Figure 2.5 The HMBC spectrum of VLC EtOH 5 fraction *F. cajanderi* in CDCl₃

Table 2.4 Chemical shift assignments for compound 1 from VLC5.

Position	Experimental (CDCl₃)		Literature* (CDCl₃)	
	Proton δ ppm (mult, *J*Hz)	Carbon δ ppm (mult, *J*Hz)	Proton δ ppm (mult, *J*Hz)	Carbon δ ppm (mult, *J*Hz)
1	1.52,1.42	30.3		30.9
2	1.74, 1.93	20.8		23.4
3	4.78	80.8		80.6
4	-	36.8		37
5	1.49	45.7		45.6
6	-	18.0		18.2
7	-	26.0		26.2
8	-	133.7		134.4
9	-	134.5		134.8
10	-	36.8		37.0
11	-	21.0		21.1
12	-	30.9		31.0
13	-	44.7		44.9
14	-	50.0		50.2
15	-	31.2		31.1
16		28.5		28.6

17		50.1		50.5
18	0.75	15.8		16.0
19	0.76	19.0		19.1
20	2.09	34.0		34.2
21	0.92	19.7		19.8
22	2.75, 2.52	44.5		44.9
23	-	201.5		201.8
24	-	147.8		148.4
25	2.83	40.3		40.4
26		179.0		178.7
27	1.22	14.2		16.1
28	0.95	24.3		24.5
29	0.9	27.3		27.8
30	0.96	21.8		21.9
31	6.21, 5.96	125.2		125.2
1'	-	166.4		167.3
2'	3.47	40.4		41.1
3'		170.7		199.1

*Data from (Chairul *et al*., 1990)
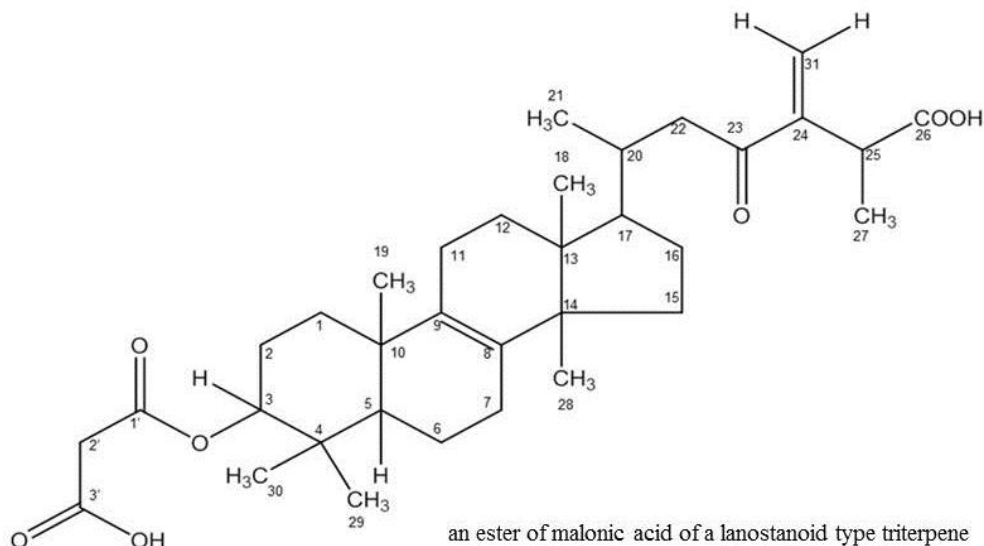
Figure 2.6 The structure of compound 1 from *F. cajanderi* ethanol extract.

2.3.3 Fractionation of *P. everhartii* crude extract

The crude EtOH extract of *P. everhartii* (1 g) was subjected to Sephadex gel filtration chromatography eluted with methanol. Over 70 fractions (5 ml each) were collected and examined by TLC and NMR to determine similar fractions which were then combined (Figure 2.7). The fractions from vials 26 to 29 and vials 30 to 33 were pooled after checking their TLC and proton NMR profiles. The compound from vials 30 to 33 was identified as 7-methoxyindole-3-carboxylic acid methyl ester as called compound E (Figure 2.13). The NMR spectra (Figure 2.8-2.12) showed four aromatic proton signals at δ_H 6.69 (d, $J = 7.8$), 7.05 (t, $J = 7.9$), 7.60 (d, $J = 8.0$) and 7.90 (d, $J = 3.1$) ppm, one methoxy at δ_H 3.89 (-OCH$_3$), one carbomethoxy group at 3.78 (-COOCH$_3$) and one exchangeable proton signal at 11.30 ppm (-NH). The ^{13}C NMR spectrum along with the HSQC (^{1}H-^{13}C ^1J correlations) showed eleven carbon signals made up of four aromatic methine carbons at δ_C 103.5, 122.8, 114.2 and 132.0, one oxy-quaternary at 147.6 and three aromatic quaternary signals at 127.8, 128.4 and 108.7. It also showed one carbomethoxy at δ_C 51.0 (COO$\underline{C}$H$_3$), a methoxy at 55.7 (-O$\underline{C}$H$_3$), one oxygenated aromatic quaternary at 147.3 and an ester carbonyl at 166.3 ($\underline{C}$OOCH) ppm. Using the correlations from its 2D NMR spectra, the

structure was confirmed as follows: the COSY spectrum indicated an ABC coupling between the three aromatic protons hence the aromatic ring must be trisubstituted. The long range (^{1}H-^{13}C ^3J) correlations from the aromatic proton triplet at δ_H 7.05 ppm and the methoxy protons at 3.89 to the oxygenated aromatic carbon at δ_C 147.3 indicate the carbon to be methoxy bearing and it must be C-7. The presence of an indole moiety was indicated by the exchangeable proton signal at δ_H 11.30 ppm which must be from an −NH group and this proton is coupled in the COSY to the proton at δ_H 7.90 ppm (H-2) which showed long range correlations to C-4a and C-7a. A long range correlation from the carbomethoxy group at 3.78 to the carbonyl carbon at 166.3 indicates a methyl ester and this ester group must be substituted at C-3. Other long range correlations from the rest of the protons confirmed the structure and the assignment of the proton and carbon chemical shifts (Table 2.5) for the compound which were in agreement with literature reports in Figure 2.13 (Samchai *et al.*, 2011).

Table 2.5 Chemical shift assignments for the compound E isolated from fractions 30-33.

Position	Experimental (in acetone-d)		Literature* (in CDCl$_3$)	
	Proton δ ppm (mult, J Hz)	Carbon δ ppm (multiplicity)	Proton δ ppm (mult, J Hz)	Carbon δ ppm (multiplicity)
1	11.3	-	8.83	
2	7.90	132.2	7.88	130.2
3	-	108.7	-	109.3
4	7.61	114.2	7.75	114.0
4a	-	128.3	-	126.7
5	7.06	122.8	7.19	122.6
6	6.70	103.7	6.71	103.0
7	-	147.6	-	146.1
7a	-	127.7	-	127.2
3-C=O	-	166.8	-	165.7
COOCH$_3$	3.78	51.3	3.92	51.0
7-OCH$_3$	3.88	55.9	3.96	55.4

*Data from (Samchai *et al*., 2011)
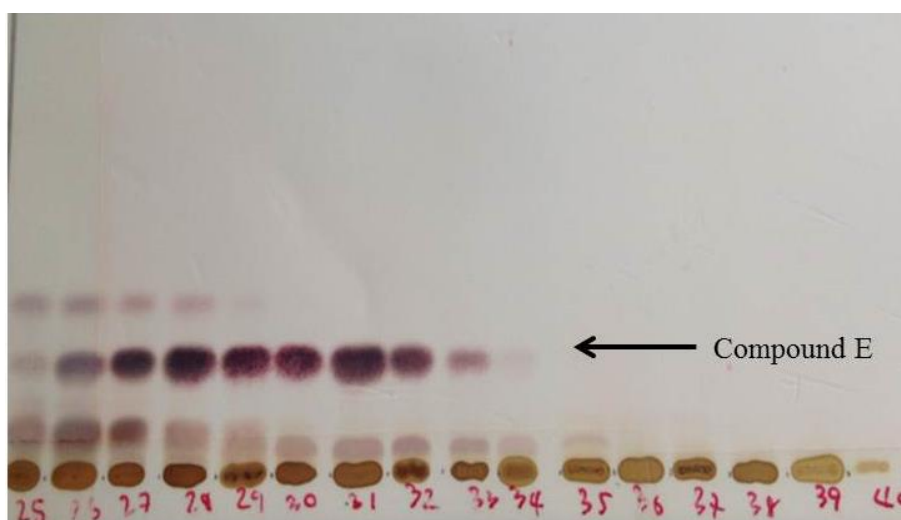
Figure 2.7 TLC plate of *P. everhartii* crude extract in mobile phase Hex: EtOAC (70:30) (Lane 1-16, fractions 25-40)
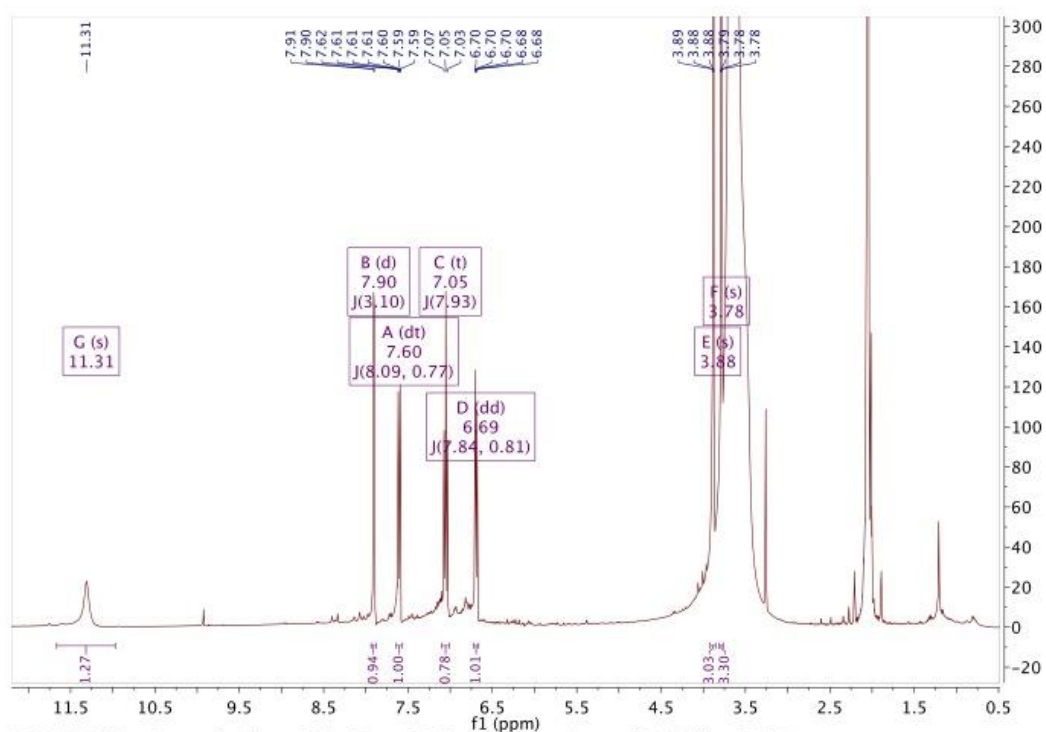
Figure 2.8 The ^{1}H NMR spectrum of PE EtOH, fractions 30-33 in acetone-d
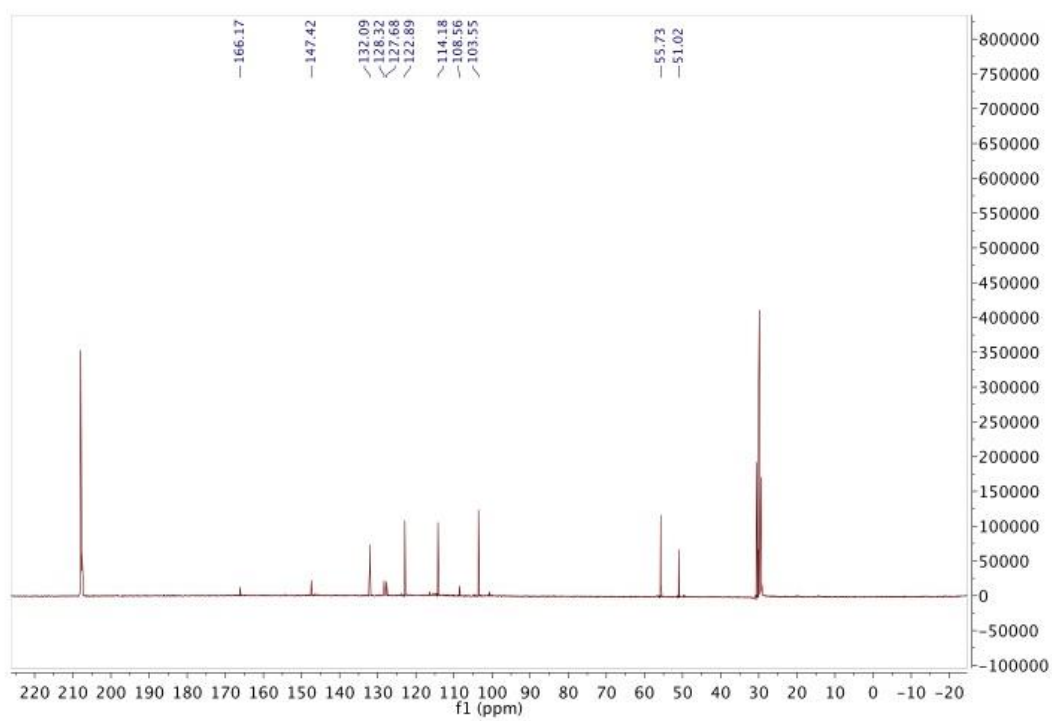
Figure 2.9 The ¹³C NMR spectrum of PE EtOH, fractions 30-33 in acetone-d
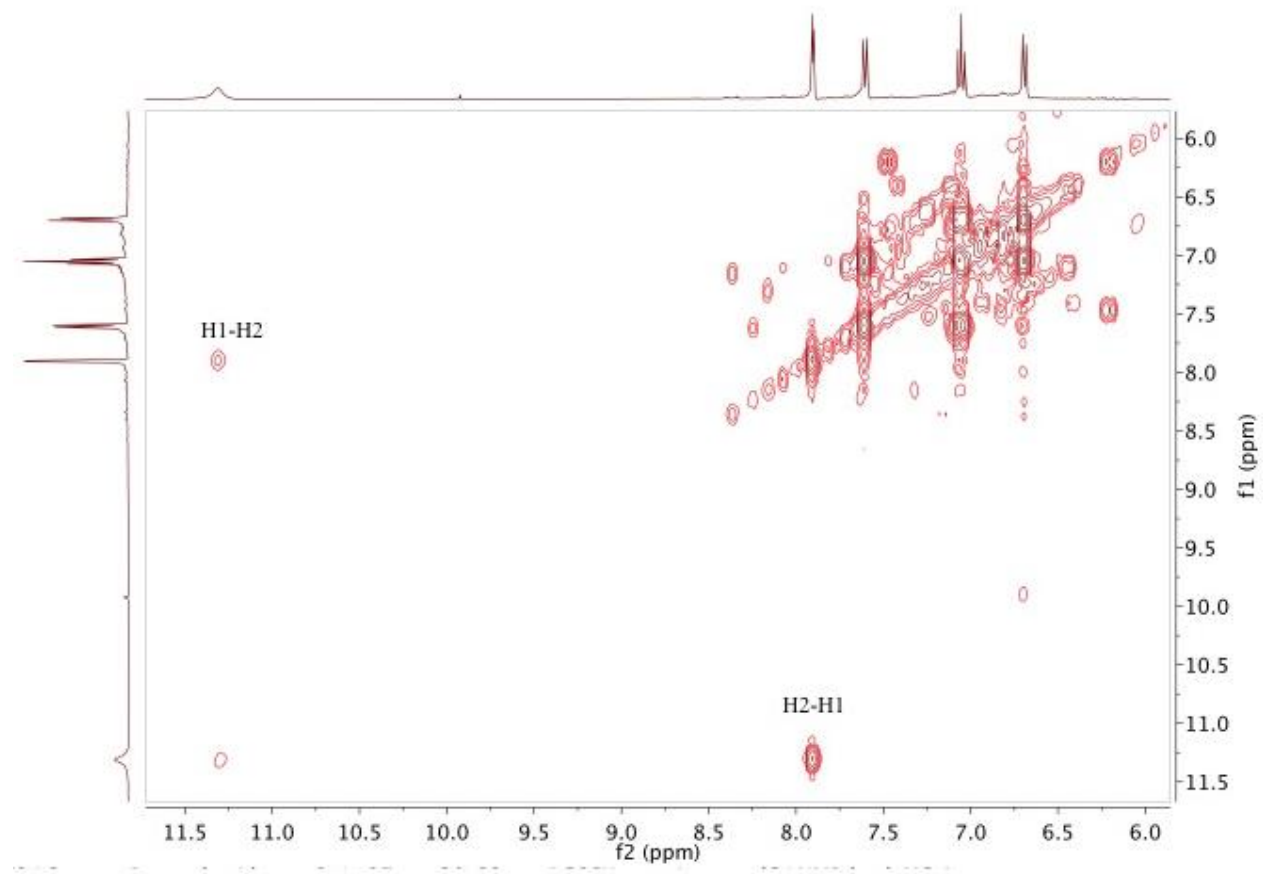
Figure 2.10 The COSY spectrum of PE EtOH, fractions 30-33 in acetone-d
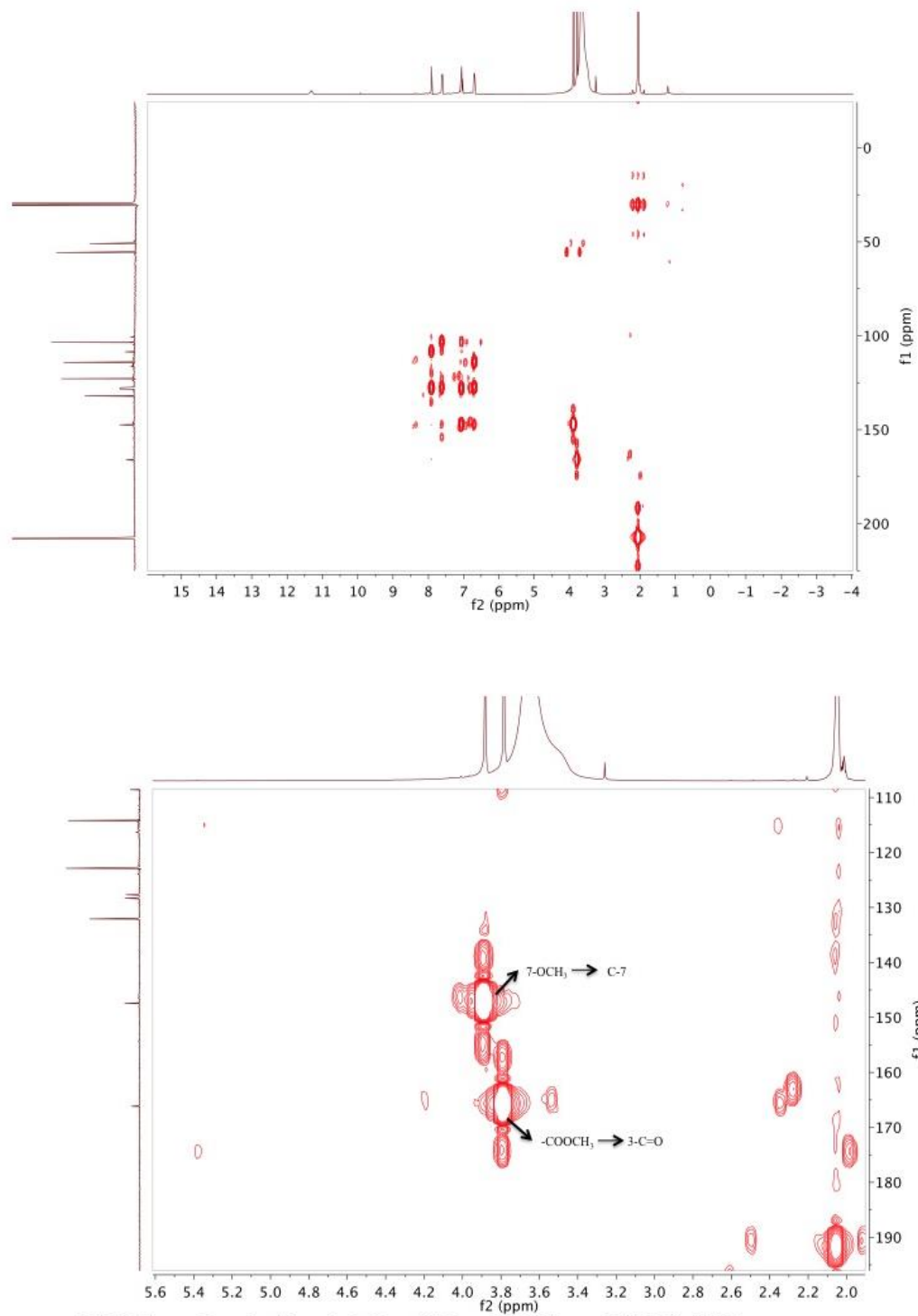
Figure 2.11 The HMBC spectrum of PE EtOH, fractions 30-33 in acetone-d
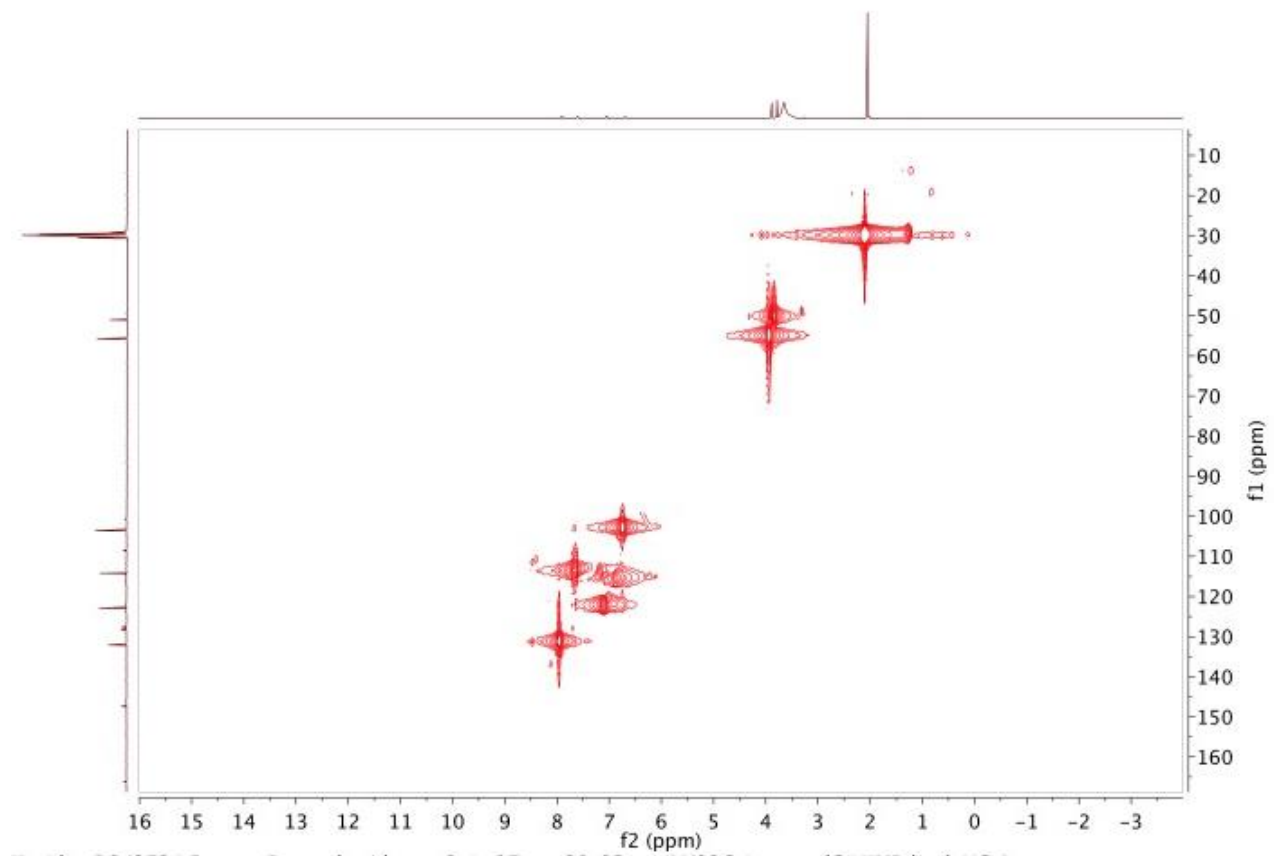
Figure 2.12 The HSQC spectrum of PE EtOH, fractions 30-33 in acetone-d

7-methoxydole-3-carboxylic acid methyl ester
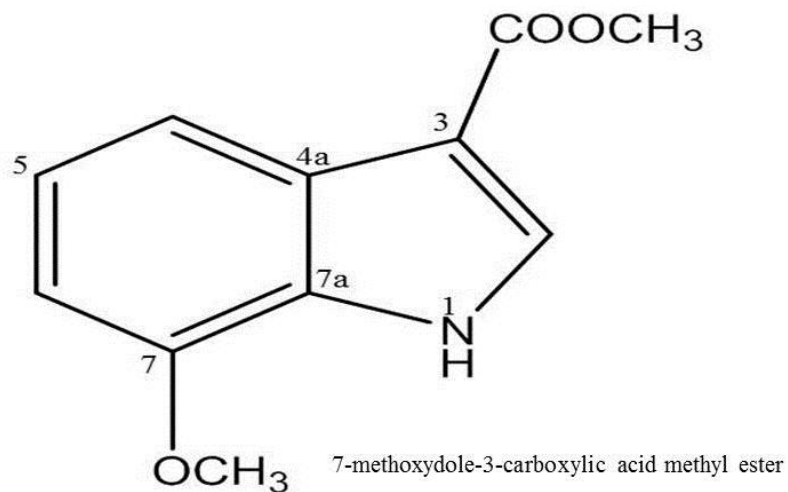
Figure 2.13 The structure of compound E from PE EtOH.

Based on the identification by NMR and compared with literature reports, a purchased sample of 7-methoxydole-3-carboxylic acid methyl ester was purchased (P) and used to confirm the isolated compound by NMR and LC-MS. The result of LC-MS is given in Figure 2.14. The LC-MS result for the P and E showed identical results.
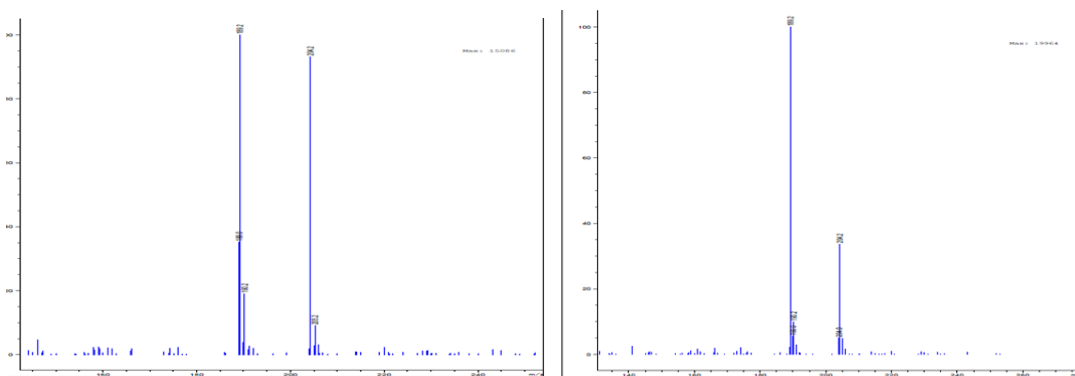
Figure 2.14 LC-MS chromatogram of P and E

Summary of the phytochemical process carried out on *P. everhartii*, *P. laevigatus* and *F. cajanderi*
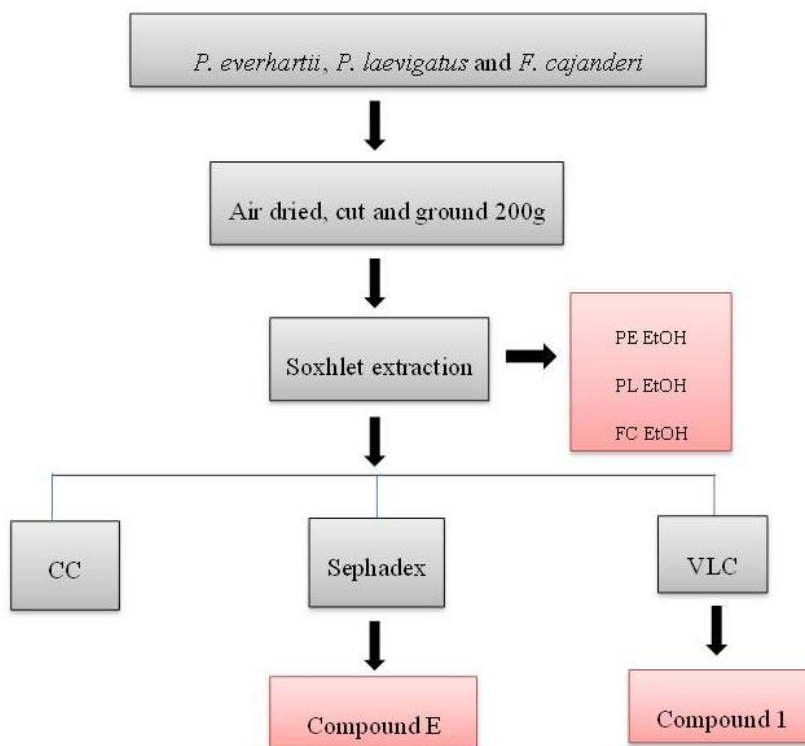
PE EtOH: *P. everhartii* extract from EtOH

PL EtOH: *P. laevigatus* extract from EtOH

FC EtOH: *F. cajanderi* extract from EtOH

Compound E: Purified extract of *P. everhartii* from Sephadex

Compound 1: Purified extract of *F. cajanderi* from VLC

Figure 2.15 Schematic diagram showing the extraction and isolation processes carried out on three mushrooms.

2.4 Discussion and conclusion

Medicinal mushrooms are a potential source of therapeutic compounds which can be used for medical treatment. Most mushroom studies have focused on the extraction of polysaccharides, polysaccharide-protein complex, protein-glucan complex or using crude extracts to examine the biological activity (Sliva, 2010). In this study, the fruiting body of the mushroom *P. everhartii* was extracted by Soxhlet using EtOH solvent and purified by Sephadex gel filtration chromatography eluting with MeOH. A brown-yellowish crystal was identified as a pure compound 7-methoxyindole-3-carboxylic acid methyl ester (E) that was isolated and purified by Sephadex chromatography. Samchai *et al.* (2011) studied this compound isolated from *P. linteus* that was extracted with MeOH and then partitioned with CH_2Cl_2 and purified on a silica gel column (200-300 mesh) and then Sephadex LH-20.The spectra for the compound isolated in this study agreed with literature data (Samchai *et al.*, 2011) and also gave an identical spectrum to a purchased sample (P). There are no previous reports demonstrating any biological activity for this compound.

Some papers have studied alkaloids isolated from plants such as Jerantinine B; one of seven novel *Aspidosperma* indole alkaloids isolated from the leaf extract of *Tabernaemontana corymbosa* which targets tumorigenesis and cancer cell survival (Qazzaz *et al*., 2016). Phan *et al*. (2018) recently reviewed alkaloids as nitrogen-containing heterocyclic compounds. The best known mushroom alkaloids are the hallucinogenic indole derivatives which encompass psilocin and psilocybin. Psilocin is an indole alkaloid found in the genus Psilocybe and is considered a natural monophenol which exhibits various properties including toxicity, antioxidant and therapeutic action. As mentioned above no biological studies have been reported on the alkaloid 7-methoxyindole-3-carboxylic acid methyl ester from *P. everhartii*, but there are many biological activity reports in genus *Phellinus* such as that by Kozarski *et al*. (2011) who extracted *P. linteus* with hot water followed by ethanol precipitation and partially purified the polysaccharides which showed immunosuppressive effects on human PBMCs.

The fruiting body of *F. cajanderi* was extracted by Soxhlet using EtOH solvent and then purified using chromatographic techniques such as CC, gel filtration and VLC. The white powder was a major compound that was identified by NMR as an ester of malonic acid of a lanostanoid type triterpene (compound 1) and was confirmed by comparison with literature reports. The isolation of a similar triterpene has been reported from a mushroom of the *Garnoderma spp*., but there have been no previous reports of this compound in *F. cajanderi*. The fruiting body of *Garnoderma spp* was extracted with chloroform and separated by HPLC with a reverse phase silica gel column and gave three pure crystalline compounds including an ester of malonic acid of a lanostanoid type triterpene (Chairul *et al*., 1990). There are no previous biological activity reports for this compound, but there are reports of triterpene compounds in different plants and mushrooms. The crude hydroalcoholic extract from leaves of *Sphagneticola trilobata* (Asteraceae) which contains terpenes and flavonoids among its major secondary metabolites, indicated antimicrobial activity against bacterial cultures isolated from human and dog skin (Greice *et al*., 2019). The triterpenes and steroids of Chaga mushroom showed activity against various cancer cell lines *in vitro* and *in vivo* (Krohn *et al*., 2011).

Generally phytochemical profiles are determined by several methods such as NMR, LC-MS, GC-MS and chemical tests or reagents. Llauradó *et al*. (2013) detected phytochemical profiles using different reagents such as Dragendorff's and Wagner reagents to detect alkaloids, Lieberman-Burchard and Solkowski assays were used to identify terpenoids and Fehlings and Benedict reagents were used for reducing sugars (Llauradó *et al*., 2013). In this study NMR, LC-MS and reagents such as anisaldehyde-H_2SO_4 spray were used to identify the compounds.

The crude extracts from *P. everhartii*, *P. laevigatus* and *F. cajanderi*, fractions, semi-purified compounds from *F. cajanderi* and pure compounds P and E from *P. everhartii* were then evaluated for their biological activities in Chapter 3.

Chapter 3 Biological activity

3.1 Introduction

Medicinal mushrooms have been demonstrated to have bioactivities, including anti-cancer, anti-Alzheimer, anti-microbial and anti-inflammatory effects. Various methods have been used to screen biological activity. This chapter aims to evaluate the biological activity of crude extracts from the mushrooms and isolated compounds described in Chapter 2.

3.1.1 Cytotoxicity

In vitro cytotoxicity assays are used to determine toxicity of extracts or compounds in cell culture by measuring the number of viable cells remaining after a defined incubation period (Riss *et al.*, 2011). The AlamarBlue™ assay is commonly used to evaluate metabolic function, manitoring cellular health and assesses cell viability and cytotoxicity (Rampersad, 2012). AlarmarBlue™ is water-soluble, stable in culture medium, non-toxic, permeable through cell membranes and contains fully oxidised resazurin which is blue and non-fluorescent (Pace & Burg, 2013). Reduction of resazurin to resorufin in a redox reaction results in a colour change that is pink and fluorescent. This reaction can measure the intracellular process and metabolic activity in terms of a quantitative colormetric and/or fluometric reading or qualitative as a visible change in colour (Rampersad, 2012). Cytotoxicity assay is widely used by the pharmaceutical industry to evaluate the potentioal antitumoral effect of chemotherapheutic drugs (A. M. Silva *et al*., 2019). Therefore in this study, cytotoxicity was used as measure to screen for anti-cancer activity.

3.1.2 Anti-Alzheimer activity

Oxidative stress has been detected in a number neurodegenerative diseases and it has been reported that H_2O_2 induced apoptosis in neuron of the central nervous system. H_2O_2 is a major Reactive Oxygen Species (ROS) so inhibition of ROS production is able to prevent from damage or death that lead to neurodegenerative diseases (Park *et. al*., 2015.

At present, cholinesterase inhibition is the main treatment for Alzheimer's disease (AD). An acetylcholinesterase (AChE) inhibitor inhibits cholinesterase from breaking down acetylcholine (Ach) that is associated with loss of cholinergic neurons in the brain and a decreased level of Ach (Krsti *et al*., 2013). There are several AChE inhibitors that have been approved by the Food and Drug Administration in United States such as tacrine, donezepil, rivastigmine and galantamine (Filho *et al*., 2006). However, the previous AChE inhibitors which mentioned above showed many side effects such as nausea, vomiting, headaches, diarrhoea, and dizziness (Mehta *et al*., 2012). Amplex Red (10-acetyl 3,7 dihydroxyphenoxazine) is fluorogenic probe has been used to detect and quantify hydrogen peroxide in cell-free systems and in cellular systems where the probe is used for determination of extracellularly released H_2O_2 (Debski *et al*., 2016). It is promising tools used to measure AchE activity. The methods includes a series of coupled enzyme reaction involving Ach, choline oxidase, HRP and Amplex Red, which ultimately produce fluorescent resorufin (Santillo & Liu, 2015). AChE hydrolyzes acetylcholine (ACh) into choline, which will be transformed to the fluorescent resorufin in a series of reactions that include generation and use of H_2O_2, choline oxidase, horseradish peroxidase, and Amplex Red (10-acetyl-3,7-dihydroxyphenoxazine) (Figure 3.1).
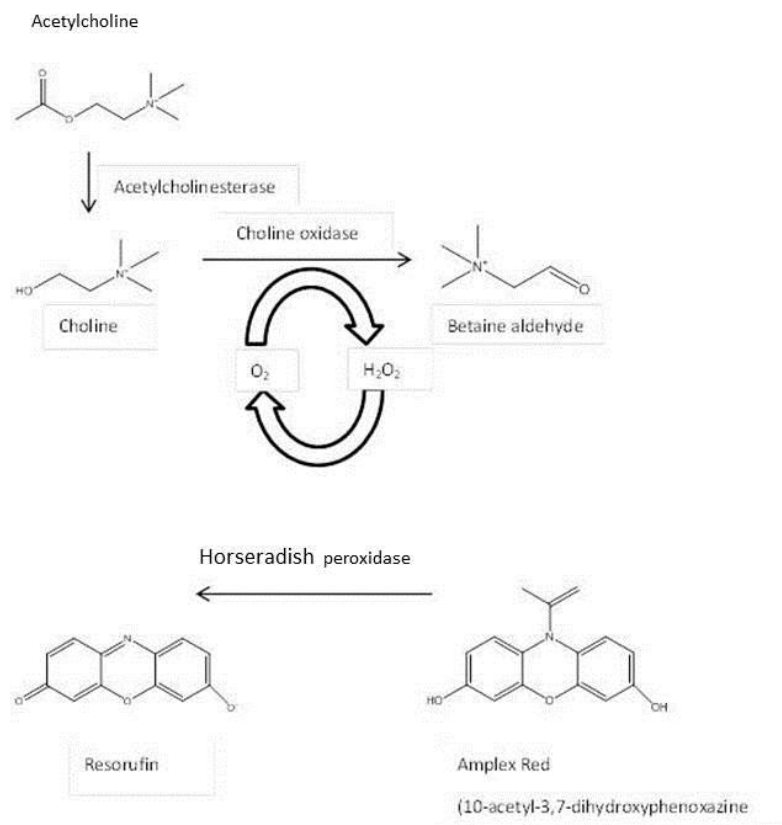
Figure 3.1 Amplex Red assay scheme for measuring AchE activity, in which a series of three coupled enzyme assays ultimately produce resorufin, a fluorescent species.

3.1.3 Antimicrobial activity

Currently there are many screening methods for determining antimicrobial activity such as bioautography, diffusion and dilution methods (Valgas *et al*., 2007). In this project, agar well diffusion was used for preliminary screening. It is widely used and a simple test for antimicrobial activity (Balouiri *et al*., 2016). The agar diffusion is conventionally used and it is inoculated with a standardised bacterial suspension. The test sample, containing the potential active compound as deposited in a well created in a cylinder (plug) is placed on the inoculated agar plate (Munir *et al*., 2020). The test sample diffuses in the agar medium that has a microbial inoculum spread on the surface and inhibits the growth of the microbial strain. This growth inhibition

diameter is dependent on the antimicrobial susceptibility of an organism, the diffusion potential of testing antimicrobial agents in agar medium, and the efficacy of the active compounds (Munir *et al*., 2020).

3.1.4 Anti-inflammatory activity

TNF-α is a member of the cytokine family being considered a proinflammatory substance produced by macrophage and other cells belonging to the innate immunity (A. M. Silva *et al*., 2019). TNF-α is a key mediator of inflammatory response (Ismail *et al*., 2006). TNF-α is well characterized as a pathogenic mediator in diverse inflammatory diseases, including Alzheimer's disease (AD), Parkinson's disease (PD), stroke, psoriasis, arthritis, septic shock, and pulmonary disorders.

NFκB is a central mediator of pro-inflammatory gene induction and functions in both innate and adaptive immune cells and regulates a large array of genes involved in different processes of the immune and inflammatory response (Liu *et al*., 2017). NFκB targets therapeutics in inflammatory diseases by blocking NFκB activity.

THP-1 cell line was isolated from the peripheral blood of a 1-year old male patient suffering from acute monocytic leukemia (Chanput *et al*., 2014). This cell line has been widely used to study immune responses. THP-1 monocytes can be fully differentiated into macrophages using phorbol-12-myristate-13-acetate (PMA) after at least 48 h of incubation at a minimal concentration of 100 ng/ml PMA (162 nM) (Chanput *et al*., 2014). THP-1 cells were used to investigate the anti-inflammatory properties of the extracts and compounds in this project, by measuring cytokine release stimulated with LPS.

Mushrooms have been used for their medicinal properties for centuries and have been a significant therapeutic raw material in folk medicines (Muszyńska *et al*., 2018) Anti-inflammatory compounds from mushrooms are summarized in Table 3.1.

Table 3.1 Example of anti-inflammatory compounds in mushrooms.

Bioactive compound	Mushroom species	Assay model	Results/mechanism of action	References
Polysaccharides	*Agaricus blazei*	Mouse bone marrow-derived mast cells (BMMCs) stimulated with PMA+A23187	Inhibition of IL-6 production, down regulation of phosphorylation of Akt, inhibition of β-hexosaminidase degranulation, inhibition of prostaglandin D(2), and leukotriene C(4) production.	Song *et. al.*, 2012
Polysaccharides	*Pleurotus pulmonarius*	(i) Male Swiss mice (acetic acidinduced inflammation)	(i) Dose-dependent anti-inflammatory response, inhibition of leukocyte migration(82%), IC50of 1.19 (0.74–1.92) mg/kg, 3 mg/kg i.p. glucan injection reduced 85% of writhes	Smiderle *et al.*, 2013
		(ii) Mice (3.5% dextran sulfate	(ii) Fruiting body and mycelia extracts	Lavi *et al.*,

		sodium,DSS in drinking water for 14 days, with20 mg fruiting body or mycelia extract/mouse/day)	suppressed inflammatory reactions in vivo in DSS induced colonic inflammation by down regulating TNF-α secretion and inhibiting NF-κB activation	2012 Lavi *et al.*, 2010
		(iii) Acetic acid induced colitis in rats(2% pleuran, or 0.44% hydrogel for 4weeks)	(iii) Reduction in macroscopic damage score by 51 and 67% for pleuran diet and hydrogel,respectively; reduction in the activity of myeloperoxidase and neutrophil infiltration	Bobek *et al.*, 2001
		(iv) Murine macrophage RAW264.7cells, female Balb/C mice	(iv) Suppression of LPS-induced dependentactivation of TNF-α, IL-6, and IL-12, inhibitionof LPS-induced production of PGE2 and NO. Suppression of LPS-induced production ofTNF-αin mice and concanavalin A-stimulated proliferation and secretion of INF-γ,IL-2,andIL-6 in mouse splenocytes	Jedinak *et al.*, 2011

Polysaccharides	*Caripia montagnei*	(i)MaleSwissmicetreatedwith10, 30,and 50 mg/kg with mushroom glucan	(i) 50 mg/kg glucan reduced inflammatory infiltrate produced by thioglycolate-induced peritonitis by 75.5%, reduced NO level, IL-1ra,IL-10, and IFN-γ	Queiroz *et al*., 2010
Polysaccharides	*Lactarius rufus*	(i) Swiss mice, formalin-induced nociception, 30 mg/kg i.p. of fruiting body extract (soluble, insoluble, andmodified)	(i) Inhibition of neurogenic pain by 36, 47, and58% for soluble, insoluble, and modified glucans, respectively	Andrea Caroline Ruthes *et al*., 2013
Polysaccharides	*A. bisporus*	(i) Male Swiss mice, formalin-induced licking	(i) Inhibition of neurogenic and inflammatory phases, antinociceptive effect with IC50of 36.0(25.8–50.3 mg/kg)(ii) Decreased iNOS and COX2	Andrea C. Ruthes et al., 2013
Polysaccharides	*Lentinus edodes*	i) Male Swiss mice, acetic acid induced inflammation, 3–100	(i) Inhibition of induced nociception with IC50of 13.8 (7.8–23.5) mg/kg, 97% inhibition	Carbonero *et*

		mg/kg i.p. fruiting body concentrate	at100 mg/kg (ii) Inhibition of peritoneal capillary permeability and leukocyte infiltration (76%inhibition), IC5013.9, 8.2–23.7, and 100%inhibition, IC506.5, 1.5–28.2 mg/kg, respectively	*al*., 2008
Polysaccharides	*L. polychrous*	(i) Carrageenan-induced paw edemain male Sprague-Dawley rats, murine macrophage RAW 264.7 cells	(i) Dose-dependent inhibition of NO, intracellular O2−production(ii) Decreased expression of iNOS, IL-1β,IL-6,TNF-α,andCOX-2	Fangkrathok *et al*., 2013
Polysaccharides	*Termitomyces albuminosus*	(i) Acetic acid induced writhing in male ICR mice, formalin test, xylene, and carrageenan induced ear edema	(i) Inhibition of ear swelling by 61.8, 79.0, and81.6% for treatment with dry matter of the culture broth (1000 mg/kg), crude saponin extract (200 mg/kg), or crude polysaccharide extract (200 mg/kg), respectively	Lu *et al*., 2008

Polysaccharides	*Phellinus linteus*	(i) Croton oil induced ear edema and acetic acid induced writhing in male ICR mice	(i) Extract treatment with 1 mg/ear gave 45 and 41.5% inhibition in ear plug weight and thickness, respectively; oral administration of extract (100–400 mg/kg) inhibited writhing number (35.9–68.9%)	Kim *et al*., 2004
Polysaccharides	*Pholiota nameko*	(i) Xylene induced ear edema, adult Swiss mice and Sprague-Dawley rats, formaldehyde, egg albumin, and carrageenan induced paw edema in rats and mice	(i) Extract (5 mg/ear) inhibited ear edema, suppression of egg albumin, carrageenan and formaldehyde-induced paw edema at100–400 mg/kg i.p., 10.96–43.75% inhibition of granuloma tissue growth, no production of gastric lesions in rats	Li *et al*., 2008
Polysaccharides	*Flammulina velutipes*	(i) Male Wistar rats, fed100–300 mg/kg mushroom for 30 days	(i) Decreased levels of CD4+CD8+,MPO,andICAM-1, with increased level in IL-10 in serum	Wu *et al*., 2010
Terpenoids	*Cyathus africanus*	(i) Mouse monocyte-	(i) Cyathins D-H 3 and 5, neosarcodonin,	J. Han *et al*.,

		macrophage RAW 264.7 cells, NO assay	and11-O-acetylcyatha-triol inhibited NOproduction with an IC50value of 2.75, 1.47, 12.0,and 10.73μM, respectively	2013
Terpenoids	*C. hookeri*	(i) Mouse monocyte-macrophageRAW 264.7 cells, NO assay	(i)InhibitionofNOproductionwithanIC50of15.5, 52.3, and 16.8μM, respectively.	Xu *et al*., 2013
Terpenoids	*Ganoderma lucidum*	(i) LPS-stimulated murine macrophageRAW 264.7 cells, NO assay	(i)InhibitionofTNF-α, IL-6, NO, and PGE2,downregulation of iNOS and COX-2,inhibition of NF-κB, decreased NF-κB-DNAbinding activity, and suppression of p65phosphorylation	Dudhgaonka r *et al*., 2009
		(ii) Acetic acid induced ear edema infemale ICR and SENCAR mice	(ii) Significant inhibition of inflammation(1μg/ear) in mice with IC50values between0.07 and 0.39 mg/ear, with inhibition ratiorangingfrom58to97%	Akihisa *et al*., 2007

Terpenoids	*Inonotus obliquus*	(i) Murine macrophage RAW 164.7cells	(i) Reduced nitrate levels by an average of 50%,dose-dependent inhibition of IL-1β,IL-6,andTNFα	Van *et al*., 2009
			(ii) Trametenolic acid, ergosterol peroxide,3β-hydroxy-8,24-dien-21-al, ergosterol and inotodiol inhibited NO production, and NF-κB luciferase activity, with an inhibition percentage of 50.04, 36.88, 20.36, 6.00, and3.13%, respectively	Ma *et al*., 2013
			(iii) Methanolic extract inhibited production of NO, prostaglandin E2,andTNF-α, inhibition of mRNA expression of iNOS and COX-2	Park *et al*., 2005
Peptides	*Cordyceps sinensis*	(i) Acetic acid induced inflammation in mice	(i) Decreased level of TNF-α,IL-1β,dose-dependent inhibition of abdominal constrictions	Qian *et al*., 2012

Phenolics	*Lactarius deliciosus*	i) LPS-stimulated RAW 364.7macrophage cells, nitrite, and cytokine assays	(i) 0.5 mg/mL mushroom extract inhibited NOproduction and expression of iNOS, IL-1β,andIL6 mRNAs	Moro *et al.*, 2012
Phenolics	*Daldinia childiae*	(i) LPS-stimulated RAW 264.7macrophage cells	(i) Daldinals suppressed NO production withIC50values ranging between 4.6 and 15.2μM and inhibited iNOS mRNA synthesis	Wu *et al.*, 2010
Phenolics	*Albatrellus caeruleoporus*	(i) LPS-stimulated mouse macrophage RAW 264.7 cells	(i) Grifolins inhibited NO production with IC50 values ranging between 22.9 and 29μM	Quang *et al.*, 2006
Syringaldehyde and syringic acid	*Elaphomyces granulates*	(i) Mouse macrophage RAW 264.7cells	(i) Crude ethanolic extract (50μg/mL)inhibited COX-2 activity by 68%, purified syringaldehyde, and syringic acid inhibitedCOX-2 activity in a dose-dependent manner, with an IC50of 3.5 and 0.4μg/mL, respectively	Stanikunaite *et al.*, 2009

Agaricoglycerides	*Grifola frondosa*	(i) Acetic acid- and formalin-induced inflammation in Wister rats, treatment with orally fed extracts(100–500 mg/kg/day)	(i) 500 mg/kg/day inhibited induced up regulation of NF-κB and the production ofIL-1β,TNF-α, ICAM-1, COX-2, and iNOS, suppressed acetic acid induced abdominal constrictions and formalin-induced spontaneous nociceptive behavior	C. Han & Cui, 2012

Source: (Elsayed *et al*., 2014)

In this study three different methods were used to investigate anti-inflammatory property. Firstly TNF-α production from differentiated THP-1 cells stimulated with LPS was used to measure ability of crude extract and purified compound to decrease proinflammatory cytokines. A second assay was carried out using L929 cells to confirm the ability of the extracts to protect against TNF-α induced cytotoxicity. The analysis of TNF-α cytotoxicity in the standard L929 bioassay was simple and rapid bioassay with characteristics of high sensitivity and good reproducibility. The literature reviewed that the standard error of the sample mean (SEM) in the standard L929 assay for TNF-quantitation was reported to range from 5-15% and L929 bioassay system was rather consistent so it would be of benefit to the analysis or quantitation of TNF-α cytotoxicity. In the last assay NCTC cells were used to study the ability to inhibit or decrease NF-ƙB expression. The transcription factor NF-κB is a critical regulator of immune and inflammatory responses. NCTC cells can be transfected with a NF-ƙB luciferase reporter vector. Once NF-ƙB is activated, this vector is bound to the NF-ƙB and luciferase will be detected by luminescence at 961nm wavelength. Therefore, anti-inflammatory agents show low luminescence readings while inflammatory agents show high luminescence readings.

3.2 Materials and Methods

3.2.1 Materials

3.2.1.1 Cell lines

- A2780 ovarian carcinoma (ECACC 93112519)
- A375 malignant melanoma (ECACC 88113005)
- LNCaP prostate carcinoma (ECACC 89110211)
- PNT2 normal prostate (ECACC 95012613)
- ZR75-1breast carcinoma (ECACC 87012601)
- L929 (ECACC 85011425)
- NCTC 2544 stably expressing PAR-2
- SHSY5Y (ECACC 94030304)
- THP-1 (ATCC TIB 202)

3.2.1.2 Microoganism strains

- *Bacillus subtillis* ATCC 6633
- *Staphylococcus aureus* ATCC 25923
- *Listeria monocytogenes* DMST31802
- *Pseudomonas aeruginosa* ATCC 9027
- *Escherichia coli* ATCC8739
- *Salmonella* Typhimurium ATCC11331
- *Salmonella* Enteritidis DMST15676

3.2.1.3 Reagents and chemicals

- 3,3′,5,5′-tetramethylbenzidine (TMB) (Sigma Aldrich, UK)
- Actinomycin D (Sigma Aldrich, UK)
- Amplex Red (Sigma Aldrich, UK)
- AlamarBlue^{TM} Cell Viability Assay (Invitrogen, UK)
- Bright-Glo (Promega, USA)
- CellTiter-Glo® Reagent (Promega, USA)
- Dulbecco's Modified Eagle's Medium (DMEM) (Gibco, UK)
- Foetal calf serum (FCS) (Invitrogen, UK)

- L-glutamine (Invitrogen, UK)
- Lipopolysaccharide (LPS) (Sigma Aldrich, UK)
- MG132 (Sigma Aldrich, UK)
- Nutrient agar (Merck, USA)
- Nutrient broth (Merck, USA)
- Penicillin/Streptomycin (Invitrogen, UK)
- Phorbol 12-myristate 13-acetate (PMA) (P8139) (Sigma Aldrich, UK)
- RPMI 1640 (Lonza, Belgium)
- Resazurin sodium salt (Sigma-Aldrich, USA)
- Sodium acetate (Sigma Aldrich, UK)
- Sodium chloride (Sigma Aldrich, UK)
- Sodium phosphate dibasic heptahydrate (Sigma Aldrich, UK)
- Sodium phosphate monobasic (Sigma Aldrich, UK)
- Sodium pyruvate (Sigma Aldrich, UK)
- TNFα Ready-Set-Go Kit (eBioscience, USA)
- Tris-HCl (Sigma Aldrich, UK)

3.2.2 Methods

3.2.2.1 Cytotoxicity assay for anti-cancer activity

A cytotoxicity assay was carried out with reasazurin sodium salt in solution to measure the metabolic activity of crude extract and to detect the effect of crude extracts on cell viability. Cells were seeded in a 96 well plate at a density of $1x10^5$cells/ml in 100 μl per well and incubated at 37^0C in 5% CO_2 and 100% humidity for 24 h. The crude extracts (1 mg) were dissolved in 1ml DMSO and serially diluted 1:2 starting with a final concentration of 125 μg/ml to 1.76 μg/ml; these were added to the cells (100 μl/well) and incubated for a further 24 h. Resazurin (10% v/v) was added to each well and incubated with the cells for 24 h. The absorbance was read at 560 nm and 590 nm using a M5 Spectramax Plate Reader (Molecular Devices, USA) and the cell viability calculated as a percentage of the untreated control reading:

% Cell viability = <u>Mean (OD560-590) test agent </u>X 100

                        Mean (OD560-590) untreated control

3.2.2.2 Agar well diffusion assay for antimicrobial activity

Seven microbial strains (section 3.2.1.2) were used in an agar diffusion assay. The microorganisms were grown in Nutrient agar (NA). The growth of microorganism on NA was suspended in saline to adjust the turbidity with 1 McFarland standard $(3x10^8$cfu/ml). The suspension was inoculated onto the surface of the agar with a cotton swab. Cork borer No 3 (7.5 mm diameter) was use to punch wells into the test agar plate containing 20 ml medium agar (NA). The 70 μl of test sample, final concentration 1 mg/ml was loaded into the bored well. The inhibition zone was observed as indicators of antimicrobial activity after 24 h.

3.2.2.3 Anti-inflammatory activity

3.2.2.3.1 Determination of TNF-α from THP-1 cells

3.2.2.3.1.1 THP-1 cell culture

THP-1 cells were maintained in complete RPMI-1640 medium. Complete medium consisted of 500ml RPMI 1640 medium, 50ml FBS, 5ml penicillin/streptomycin and 5ml L-glutamine. Cells were incubated at 37°C, 5% CO_2 and 100% humidity. A suspension of 500 μl of THP-1 cells was seeded in a 24 well plate at a density of $1x10^5$cells/ml with phorbol 12-myristate 13-acetate (PMA) at a concentration of 60 ng/ml in each well, and incubated at 37°C in 5% CO_2 and 100% humidity for 48 h. The differentiated cells were checked and then the medium re-freshed to the same volume without PMA and incubated for a further 24 h. Extracts (500 μl) at different non-toxic concentrations based on the cytotoxicity assay (section 3.2.2.1) were added together with lipopolysaccharide (LPS, 1 μg/ml) and without LPS and then incubated for another 24 h. The supernatants were aspirated and stored at -20 °C until analysed by Enzyme-Linked Immunosorbent Assay (ELISA) (section 3.2.2.3.1.2).

3.2.2.3.1.2 TNF-α ELISA

TNF-α levels were used to investigate the anti-inflammatory activity of supernatants from THP-1 cell following the manufacturer's instructions of a Ready-Set-Go Kit (eBioscience, USA). ELISA plates were coated with 100 μl/well of capture antibody in 1x coating buffer and then the plate was sealed and incubated overnight at 4°C. The supernatants were discarded and the wells washed 3 times with wash buffer (1xPhosphate Buffered Solution (PBS) [Na_2HPO_4 2.3 g, NaCl 8 g, KH_2PO_4 0.2 g and KCl 0.2 g, adjusted pH to 7.2-7.4] plus 0.05%, v/v, Tween-20) and then blocked with 200 μl/well of 1x diluent and incubated at room temperature for 1 h. The supernatants were then discarded and washed at least once with wash buffer and 100 μl of samples were added per well in triplicate wells. Similarly, TNF-α standard at different concentrations were plated out to construct a standard curve. The plates were sealed and incubated at room temperature for 2 h and washed 3-5 times and then 100 μl detection antibody diluted 1x in diluent was added to each well and incubated at room temperature for 1 h. The wells were washed 3-5 times with wash

buffer and Avidin-Horseradish peroxidase (HRP) diluted 1x in ELISA/ELISPOT diluent was added (100 µl/well). After incubation at room temperature for 30 min the wells were washed with wash buffer 5-7 times and 3,3′,5,5′-tetramethylbenzidine solution was added (100 µl/well). The plate was incubated at room temperature for 15 min and 50µl stop solution (2N H_2SO_4) added to each well. The plate was read at 450 nm on a M5 Spectramax Plate Reader (Molecular Devices, USA) and the TNF-α was calculated from the standard curve. Statistical analysis was carried out using with a Dunnett's Multiple Comparison Test.

3.2.2.3.2 NFκB luciferase assay

NCTC cell line transfected with a Nuclear Factor Kappa Beta (NFκB) luciferase reporter vector was used to detect NFκB by luminescence at 961 nm wavelength. The NCTC cell was seeded using 10% (v/v) FBS in M199 medium in a 96 well plate at a density of $1x10^4$cells/well in 200 µl per well and left at room temperature for at least 30 min followed by incubation at 37^0C in 5% CO_2 and 100% humidity for 48 h. The medium was removed and replaced with 50 µl/well of phenol red free Dulbecco's Modified Eagle Medium (DMEM) without FBS and kept in an incubator until the samples or standard MG132 50 µl were added in each well. MG132 was used as a positive control and media with no TNFα was used as a negative control/background. The plate was then incubated at 37^0C for 4 h. The medium was removed and 50 µl per well of Bright-Glo (made up in phenol red free DMEM medium) added and then incubated in the dark for 10 min at room temperature. The plate was read on a Victor Iso96 luminescence plate reader (Perkin Elmer, USA).

3.2.2.3.3 Determination of TNF-α from L929 cells

L929 cells were seeded in a 96 well plate at a density of $1x10^4$cells/well and incubated at 37^0C in 5% CO_2 for 24 h. Twenty five microlitres of medium (DMEM + 2mM Glutamine + 10% FBS) was removed and replaced with samples serially diluted; final concentration 30 µg/ml and incubated 30 min at 37^0C in 5% CO_2. Then 10 µM of Actinomycin D was added to all wells and incubated for 30 min at 37^0C in 5% CO_2. After 30 min, TNF-α (10 pg/ml), was added to all wells and incubated overnight at 37^0C in 5% CO_2. AlamarBlue[TM] (10% v/v) was added to each well and

incubated for 5 h at 37^0C in 5% CO_2. The absorbance was read at Excitation 560 nm and Emission 590 nm using a M5 Spectramax Plate Reader.

3.2.2.5 Potential AD therapeutic screening

3.2.2.5.1 Electric eel anti-AchE activity

The enzymatic activity of Electric eel AchE (100 U/ml) Type VI-S was determined using Amplex Red detection. The reaction was performed in 96 well half area plates. The assay buffer (50 mM Tris-HCl, pH 8) was prepared. The working solution per plate consisted of 2.45 ml buffer, 25µl choline oxidase (20U/ml), 12.5µl HRP (400 U/ml) and 12.5 µl Amplex Red (20 mM). Ten microliters of sample, buffer or reference standard was added to specific wells. Ten microlitres cholinesterase (7 µl AChE 100 U/ml in 1.75 ml buffer) was added per well and incubated for 30 min at room temperature, followed by 20 µl working solution and incubated at room temperature for 20 min. The fluorescence was then measured on a plate reader (Wallac Victor, USA) at absorbance 560nm/590nm (Excitation/Emission).

3.2.2.5.2 Neuroprotective activity

SHSY5Y cells were maintained in complete DMEM medium. Complete medium consisted of 500ml DMEM medium, 50ml FBS and 5ml penicillin/streptomycin. SHSY5Y cells at a density of $1x10^4$cells/ml were seeded in a 96 well plate and incubated at 37^0C in 5% CO_2 and 100% humidity for 24 h. The cells were then treated with samples at different concentrations from 0.05 µg/ml to 100 µg/ml and incubated at 37^0C in 5% CO_2 and 100% humidity for 24 h and then hydrogen peroxide (final concentration 100 µM, 25 µl) was added and incubated at 37^0C for 30 min. The plate was left for a further 30 min at room temperature before adding CellTiter-Glo® Reagent which was mixed for 2 min on an orbital shaker and incubated at room temperature for 10 min. The plate was read on a plate reader (Wallac Victor, USA) using luminescence.

3.3 Results

3.3.1 Cytotoxicity of EtOH crude extract from *P. everhartii*, *P. laevigatus* and *F. cajanderi*

Crude extracts from the three mushrooms were tested against five different cell lines starting from 1.76 μg/ml to 125 μg/ml. Cytotoxicity was defined as decreasing cell viability less than 50% compared with the untreated control and DMSO was used as a negative (solvent) control to ensure that no effect of DMSO as the same concentration of sample on cell viabilty. Cytotoxicity was highest at 125 μg/ml in A2780 (Figure 3.2), A375 (Figure 3.3) and LNCaP (Figure 3.4) cells, but there was no cytotoxicity against ZR75-1 cells (Figure 3.5) nor in the normal cell line PNT2 (Figure 3.6). The crude extracts of *P. laevigatus* and *P. everhartii* were not cytotoxic to the normal cell line at all concentrations while *F. cajanderi* was cytotoxic to PNT2 cells at the highest concentration only. Table 3.2 shows the IC50 values.
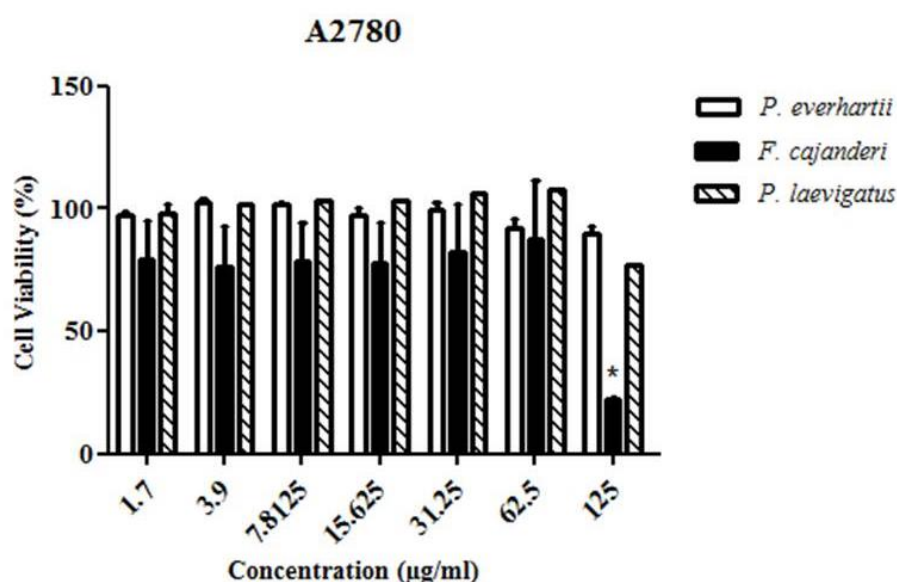
Figure 3.2 Cytotoxicity of EtOH extracts from three mushrooms against ovarian cancer cell line A2780. n=3, * represents a significant (p<0.05) decrease in viability compared with the untreated group.

A375
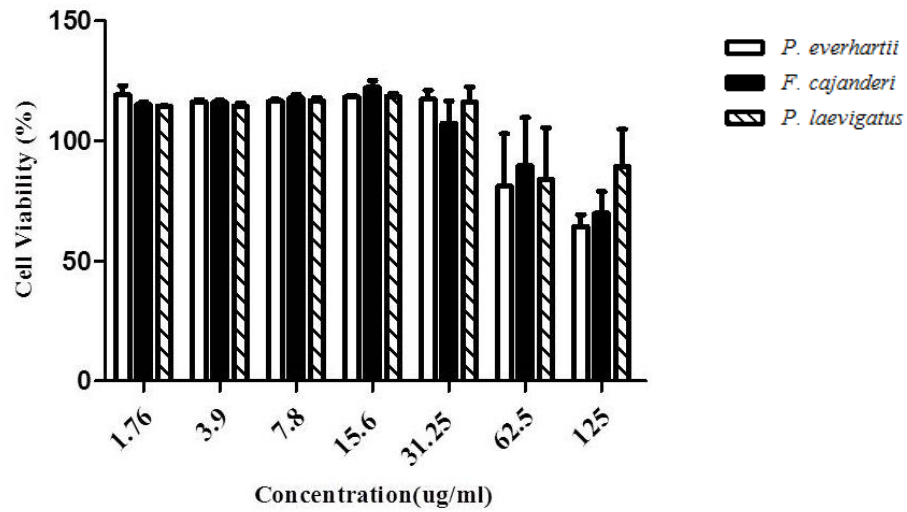
Figure 3.3 Cytotoxicity activity of EtOH extracts from three mushrooms against melanoma cancer cell line A375. n=3

LNCaP
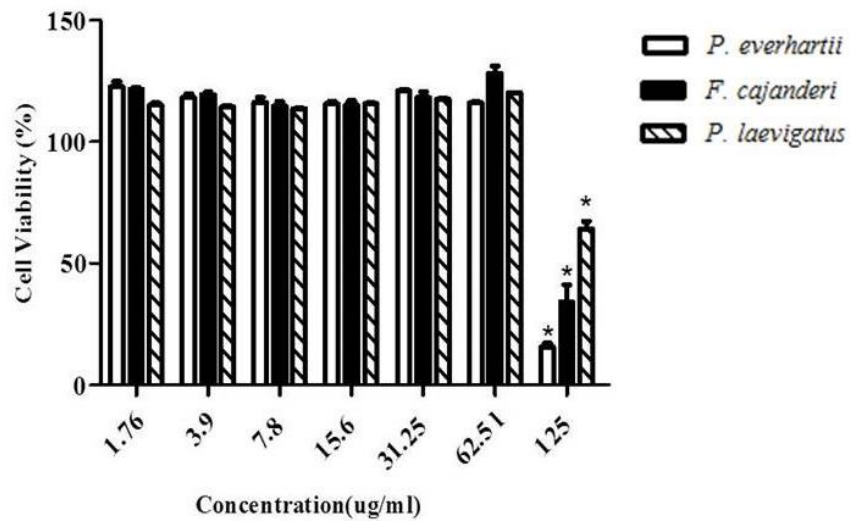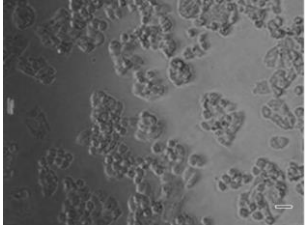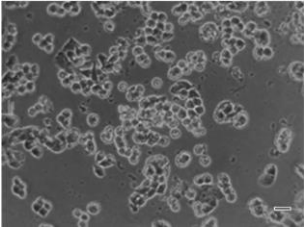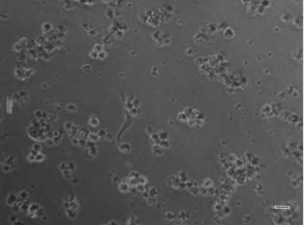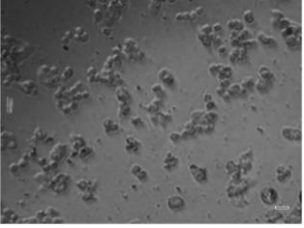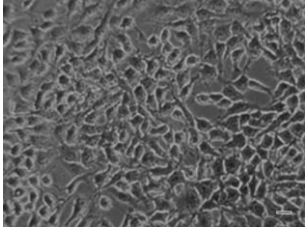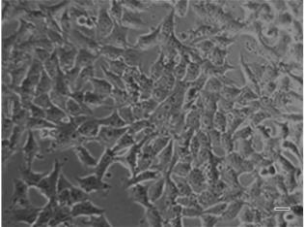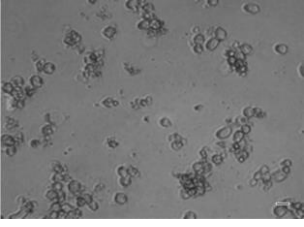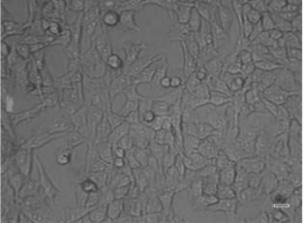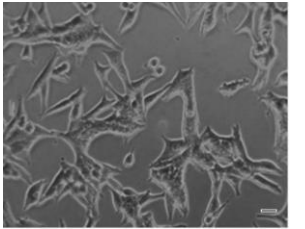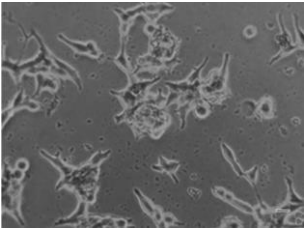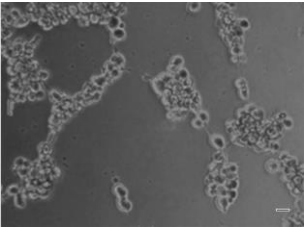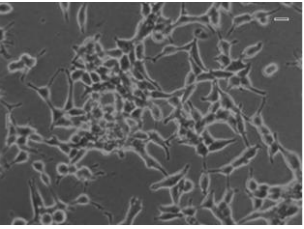
Figure 3.4 Cytotoxicity activity of EtOH extracts from three mushrooms against prostate cancer cell line LNCaP. n=3, * represents a significant (p<0.05) decrease in viability compared with the untreated group.   .
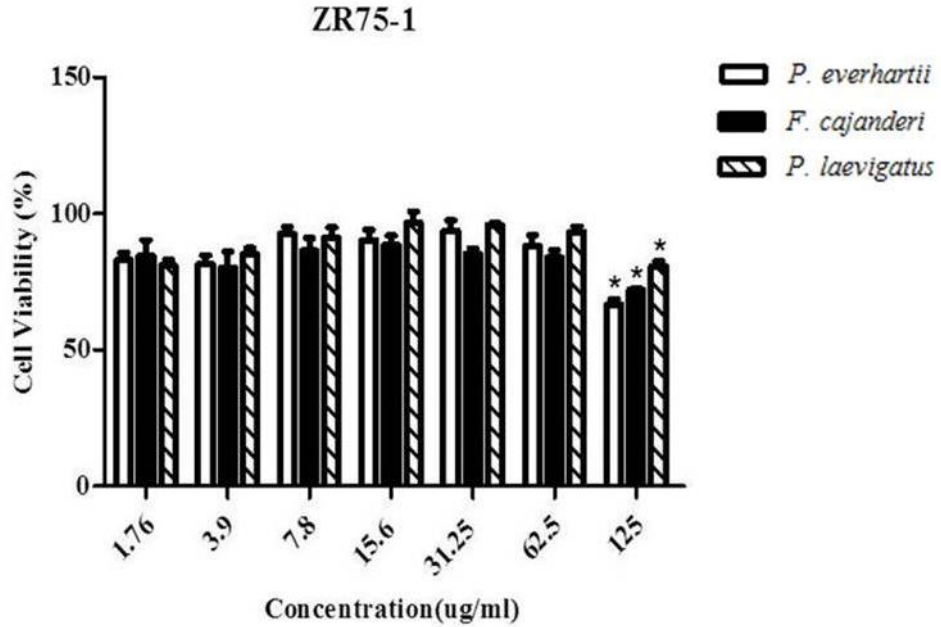
Figure 3.5 Cytotoxicity activity of EtOH extracts from three mushrooms against breast cancer cell line ZR75-1. n=3, * represents a significant (p<0.05) decrease in viability compared with the untreated group.
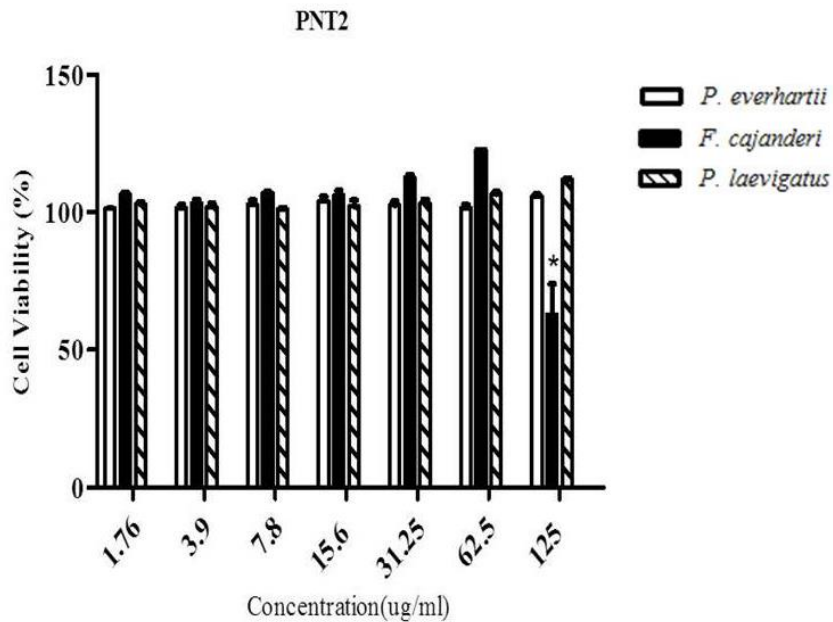
Figure 3.6 Cytotoxicity activity of EtOH extracts from three mushrooms against normal cell line PNT2. n=3, * represents a significant (p<0.05) decrease in viability compared with the untreated group.

	Control	*P. everhartii*	*F. cajanderi*	*P. laevigatus*
A2780				
A375				
LNCaP				

	Control	*P. everhartii*	*F. cajanderi*	*P. laevigatus*
ZR75-1				
PNT2				
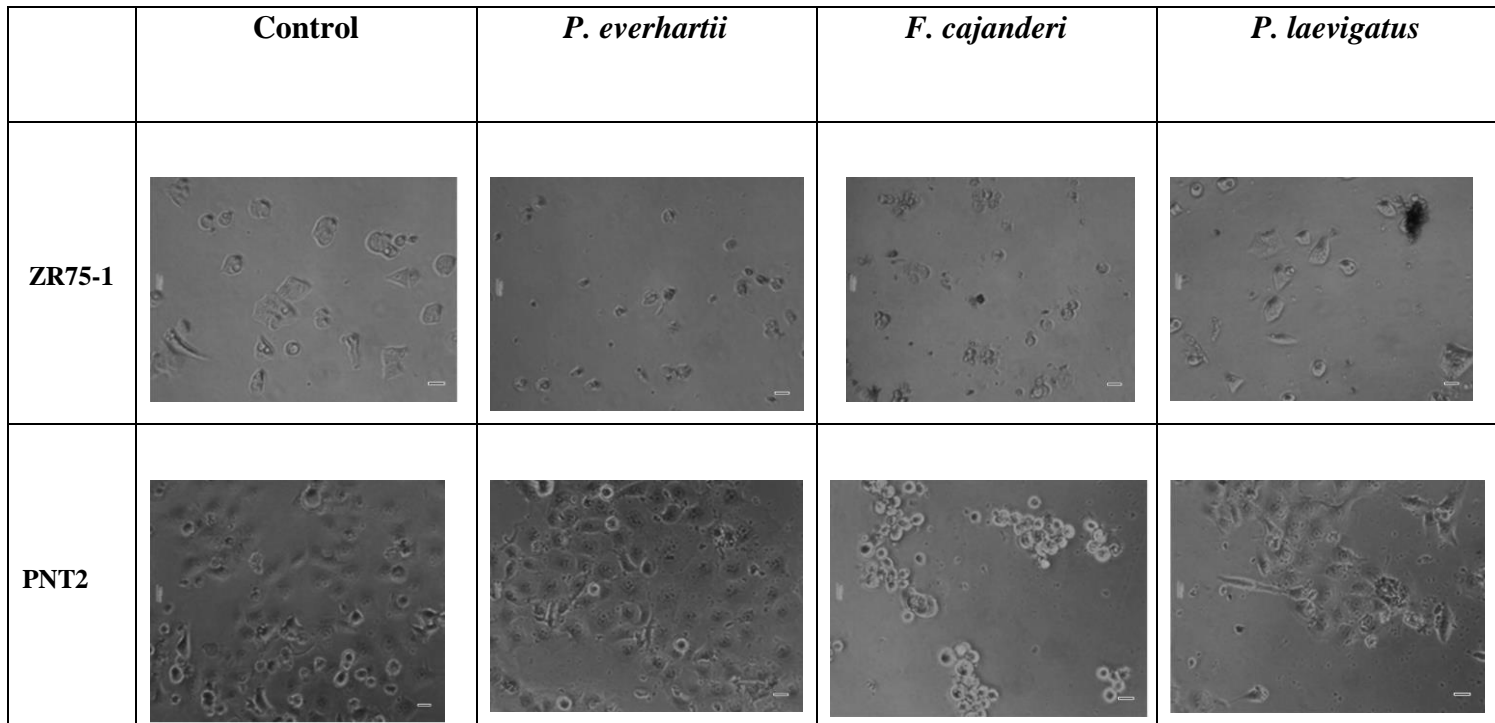
Figure 3.7 Cell morphology of A2780, A375, LNCaP, ZR75-1 and PNT2 cell lines after incubation with crude extracts (EtOH) at concentration 125 µg/ml from *P. everhartii*, *F. cajanderi* and *P. laevigatus* for 24 h (Bar =100µm)**.**

Table 3.2 IC50 (µg/ml) of crude extract (EtOH) of *P. everhartii*, *F. cajanderi* and *P. laevigatus* against a panel of cancer cell lines.

Crude extract	IC50 µg/ml ± SEM			
	LNCaP	A2780	A375	ZR75-1
P. everhartii	80.46±2.07	143.10±0.72	56.99±8.46	>150
F. cajanderi	125.60±9.19	149.70±0.68	57.86±7.16	>150
P. laevigatus	125.90±12.09	118.10±0.78	49.75±5.51	>150

3.3.2 Antimicrobial Activity

An agar well diffusion assay was used for investigating the antimicrobial activity of PE EtOH, PL EtOH and FC EtOH. The results are shown in Table 3.3. Only FC EtOH showed antimicrobial activity against three gram-positive bacteria (*B. subtillis*, *S. aureus*, *and L. monocytogenes*) and one gram-negative strain (*P. aeruginosa*).

Table 3.3 Inhibition zone diameters (mm) in agar well diffusion assay. Data represents mean ± SEM, n=3.

Crude extract	Zone of inhibition mm ± SEM						
	P. aeroginosa	*B. subtillis*	*S. auureus*	*E. coli*	*S.* Typhimurium	*S.* Enteritidis	*L. monocytogenes*
PE EtOH	0	0	0	0	0	0	0
FC EtOH	11.17±0.17	14.17±0.29	14.5±0.29	0	0	0	16±0.17
PL EtOH	0	0	0	0	0	0	0

3.3.4 Anti-Alzheimer's disease activities

3.3.4.1 AChE inhibition assay

The profile of AChE hydrolysis of the standard tacrine and two samples: P and E are presented in Figure 3.8. The percentage inhibition increased when the concentration of tacrine and the two samples increased. The highest percentage of inhibition was around 70% that was observed at concentration 150 µg/ml in both samples.
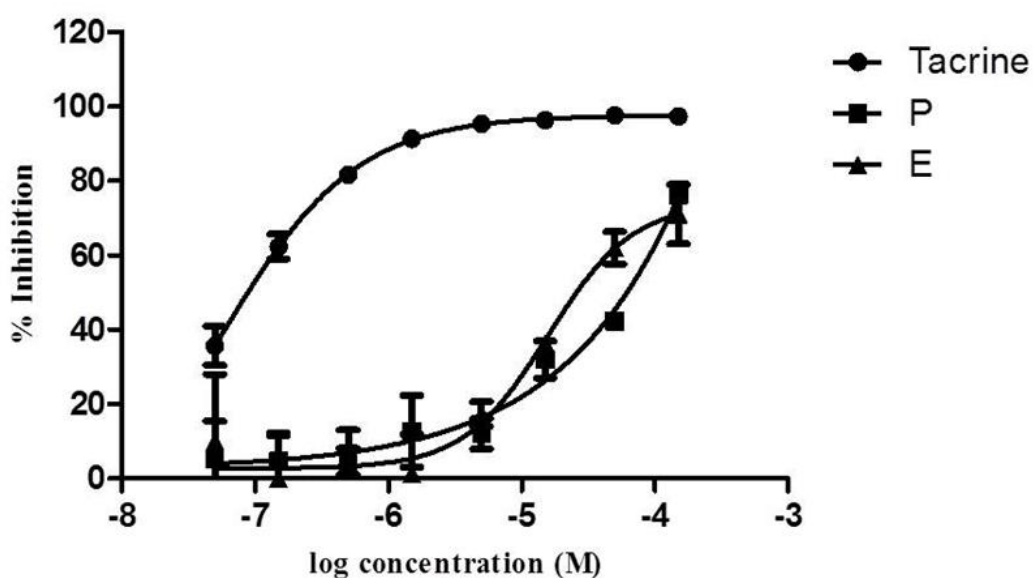
Figure 3.8 Effect of standard tacrine compared with compound E from *P. everhartii* and purchased (P) on AChE activity. Data represents mean ± SEM, n=3.

3.3.4.2 Neuroprotective activity against hydrogen peroxide in SHSY5Y cells

SHSY5Y cells were treated with different concentrations of P and E samples from 0.05 µg/ml to 100 µg/ml and then treated with H_2O_2 (100 µM). The cell viability was investigated using CellTiter-Glo® Reagent. The results in Figure 3.9 show the protection percentage of E increased when the concentration of the compound increased and protection percentage of P was less than 20% from concentration 0.05-100 µg/ml. The highest protection percentage of P was 20% at concentration 1 µg/ml, 5 µg/ml and 10 µg/ml and the highest protective percentage of E was approximately 40% at 50 µg/ml. The protective percentage showed increase significantly (P<0.05) at concentration 50 and 100 µg/ml.
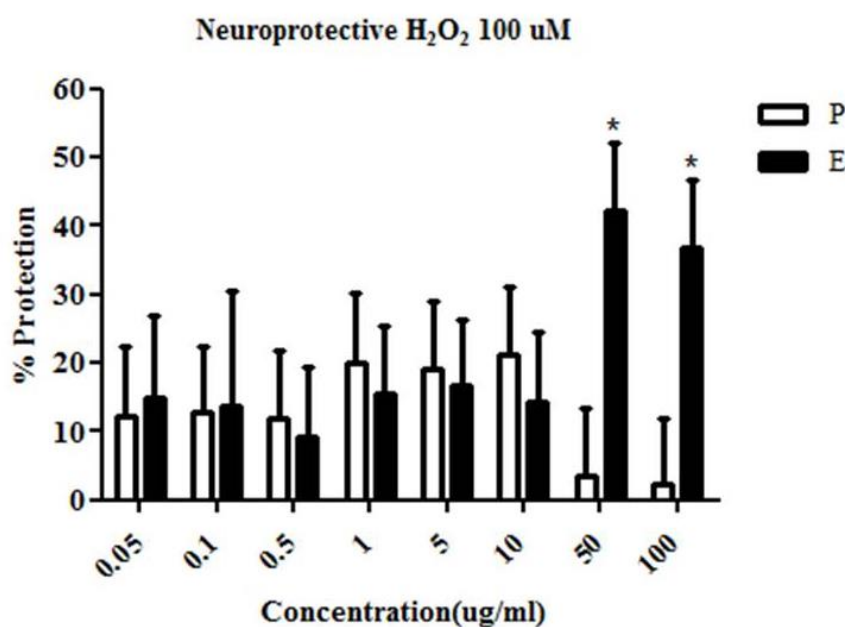
Figure 3.9 Neuroprotective effect of compound E from *P. everhartii* and purchased (P) against H_2O_2 induced cell toxicity. Data represents mean ± SEM, n=3. *P<0.05 is significant increase in % protection.

3.3.5 Anti-inflammatory activity

3.3.5.1 Determination of TNF-α release by ELISA

3.3.5.1.1 TNF-α assessment of PE EtOH, PL EtOH and FC EtOH in differentiated THP-1 cells stimulated with LPS

THP-1 cells were differentiated and then treated with LPS (1μg/ml) in order to investigate the production of TNF-α. If the extract inhibited the production of TNF-α, potential anti-inflammatory activity was deemed present. Three concentrations of ethanol crude extracts (31.25μg/ml, 7.81μg/ml and 1.76μg/ml) that were not toxic to the cells were chosen. PE EtOH without LPS stimulated TNF-α secretion at all concentrations (31.25μg/ml, 7.81μg/ml and 1.76μg/ml). Three of EtOH crude extracts showed a significant ($P<0.05$) decrease in production of TNF-α at concentration 31.25μg/ml for PE EtOH, 31.25μg/ml and 7.81μg/ml for FC EtOH and 1.76μg/ml for PL EtOH compared with the control (THP-1 cells with LPS) (Figure 3.10). The crude extracts of the three mushrooms showed anti-inflammatory activity at all concentrations.
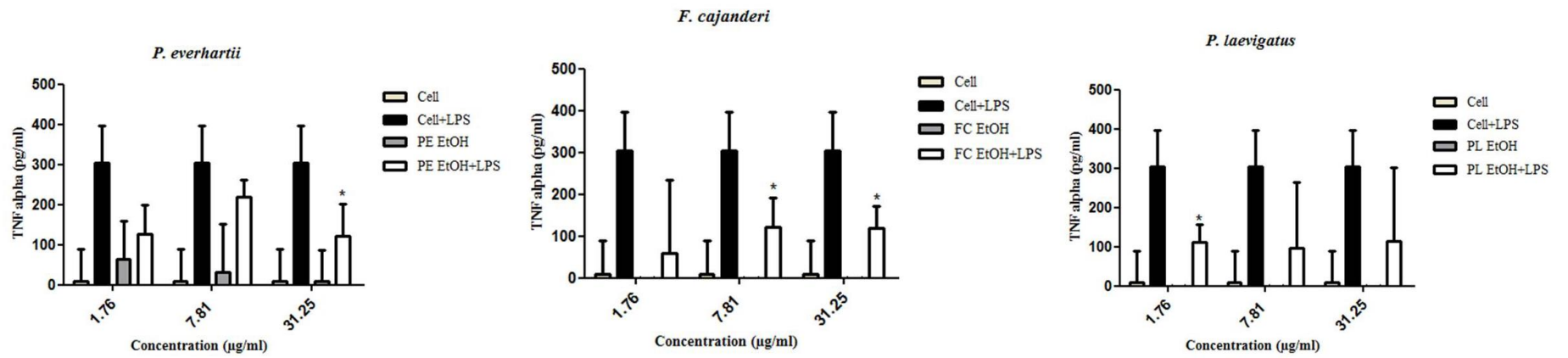
Figure 3.10 TNF-α production of three mushroom crude extracts at three concentrations 1.76 µg/ml, 7.81µg/ml and 31.25 µg/ml, n=3 in the presence and absence of LPS. Data represents mean ± SEM, n=3. Data analysed using One-Way ANOVA with a Dunnett's Multiple Comparison Test.

* indicates significantly ($p<0.05$) lower values compared with the cells with LPS.

3.3.5.1.2 TNF-α assessment of pure compound P and E

TNF-α production from differentiated THP-1 cells treated with LPS and seven concentrations (2, 4, 6, 8, 10, 20 and 30 µg/ml) of P and E are shown in Figures 3.11. The results show that TNF-α production decreased significantly when the concentration of compound increased to 20 µg/ml and 30 µg/ml.
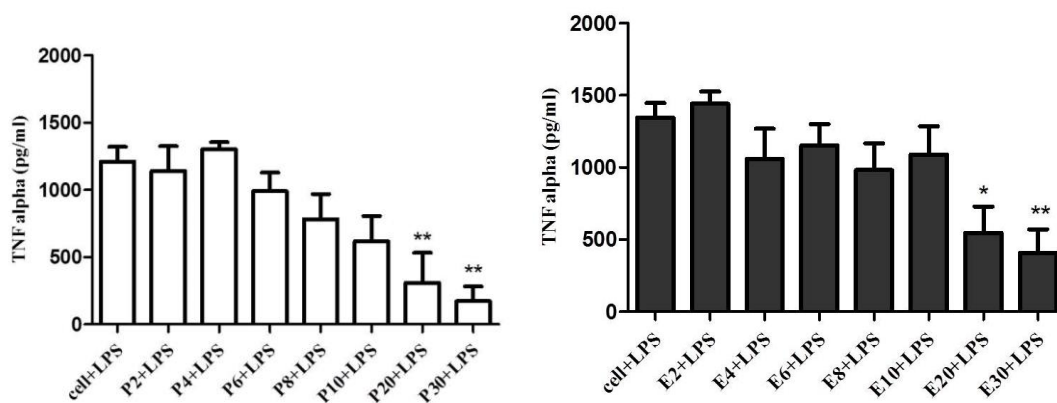
Figure 3.11 TNF-α production of P and E in different concentrations 2, 4, 6, 8, 10, 20 and 30 µg/ml. Data represents mean ± SEM, n=3. Data analysed using One-Way ANOVA with a Dunnett's Multiple Comparison Test. * P<0.05, ** P<0.01 is significant decrease in TNF-α vs control cell with LPS.

3.3.5.2 NFκB Luciferase assay

NCTC cells that include a NFκB reporter gene were treated with TNF-α (10 μg/ml) to induce NFκB. Test compound P and E was assessed at different concentrations (Figures 3.13-3.14). The percentage control of NFκB decreased when the concentration of standard MG132 (Figure 3.12) were increased. P and E decreased the percentage control of NFκB significantly (P<0.05) (less than 50%) at the highest concentration 30 μg/ml in both samples P (Figure 3.13) and E (Figure 3.14).
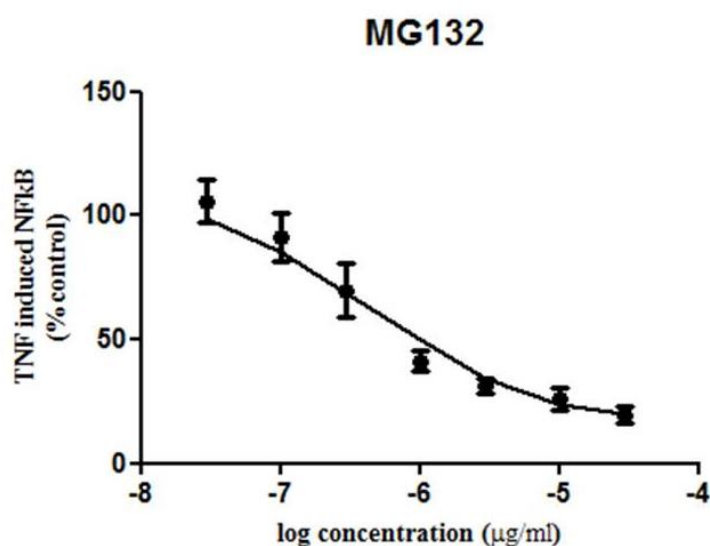
Figure 3.12 Effect of standard MG132 on TNF-α induced in NCTC NFκB cells. Data represents mean ± SEM, n=3.
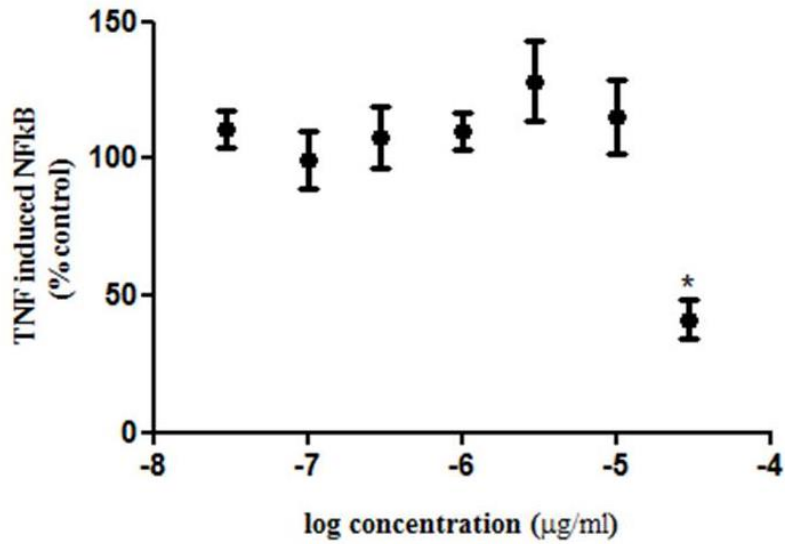
Figure 3.13 Effect of P on TNF-α induced NCTC NFκB cell. Data represents mean ± SEM, n=3. * P < 0.05 shows a significant decrease in NF-ƘB luciferase activity vs control.
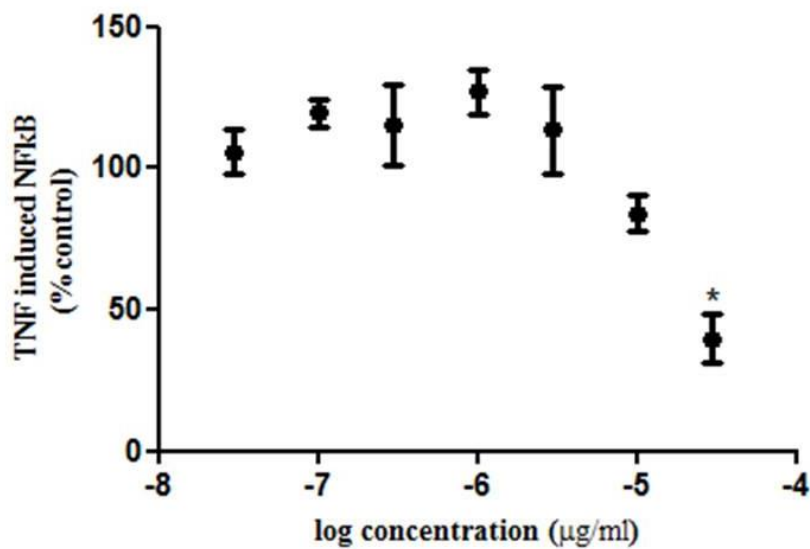
Figure 3.14 Effect of E on TNF-α induced NCTC NFκB cell. Data represents mean ± SEM, n=3. *P < 0.05 is significant decrease in NF-ƘB luciferase activity vs control.

3.3.7 TNF-α Assay in L929 cell

L929 cells were used to investigate test sample protection of the L929 cells against TNF-α. The results in Figure 3.15 showed that the percentage of protection varied around 10-30% at concentration 0.001-30 μg/ml. The highest protection was observed with 7-methoxyindole-3-carboxylic acid methyl ester compound at 10 μg/ml irrespective to the source.
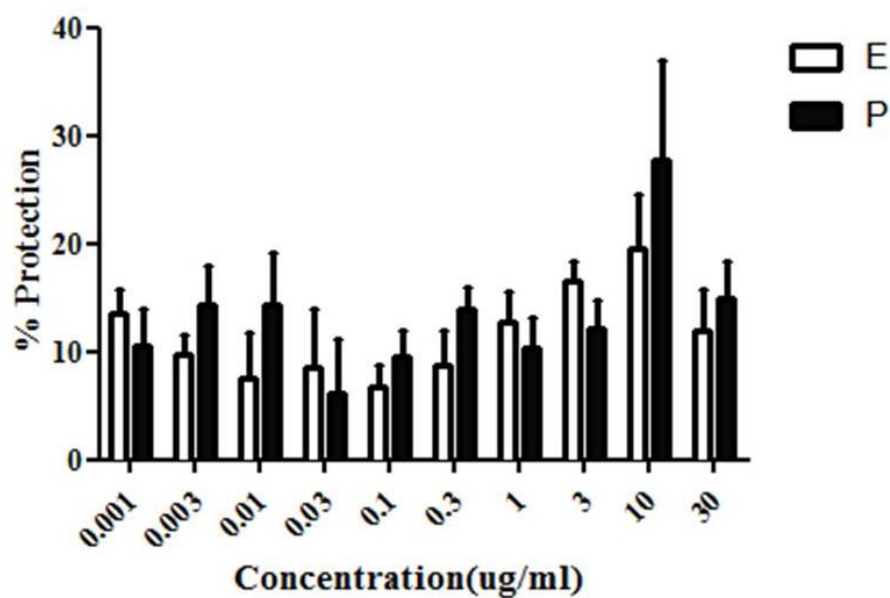
Figure 3.15 Effect of extract E and P on protection percentage against TNF-α on L929 cells. Data represent mean ± SEM, n=3. *P<0.05 is significant increase in % protection.

3.4 Discussion

The study of mushrooms is growing in popularity because of their attributed health benefits. The bioactive molecules found in mushrooms such as polysaccharides, glucans, triterpenes, and alkaloids, contribute greatly to their curative properties like anticancer, anti-inflammatory, antivirus, and even anti-Alzheimer's disease (C.-W. Phan *et al.*, 2018). The crude extract and purified compound from mushrooms were studied the biological activities.

3.4.1 Cytotoxicity

In this study, three crude extracts from three mushrooms PE EtOH, PL EtOH and FC EtOH showed cytotoxic activities against four different human cancer cell lines: ovarian carcinoma (A2780), malignant melanoma (A375), prostate (LNCaP) and breast carcinoma (ZR75-1) only concentration 125 µg/ml. FC EtOH showed significantly cytotoxicity against A2780, LNCaP and ZR75-1 at concentration 125 µg/ml but it was cytotoxic to PNT2A cells also. The morphology of A2780, A375, LNCaP, ZR75-1 and PNT2A changed after treatment with FC EtOH 24 h (Figure 3.6). The process of programmed cell death, or apoptosis, is generally characterised by distinct morphological characteristics. Light and electron microscopy have identified the various morphological changes that occur during apoptosis. In Figure 3.6 the early process of apoptosis, cell shrinkage is visible by light microscopy. No one has reported cytotoxicity of *F. cajanderi* mushroom against any cancer cell lines. However there were the reports of the same genus of Fomitopsis, but a different species investigated for cytotoxicity against cancer cell lines. Sułkowska *et al.* (2018) reported that *F. betulina* (Bull) Bk Cui, M. L. Han&Y.C Daiv mycelium extract exhibited significant cytotoxic activity against DU145 prostate cancer cell at 20 µg/ml and 50 µg/ml and the fruiting body extract showed moderate effects against A375 melanoma cell line at 50 µg/ml. That showed a moderate effect in both cell lines at 50 µg/ml. An EtOH extract from *F. pinicola* showed significant anti-cancer activity by increasing cell apoptosis and decreasing tumor size in different cancer cell lines: mouse sarcoma 180 cells (S-180), human hepatoma (HepG2), lung cancer

(A549), colon cancer (HCT-116) and breast cancer (MDA-MB-231) cell (Wu *et al*., 2014). *F. lilacinogilva* ethanol extracts were highly cytotoxic against the HeLa, HT-29, MCF-7, MIA PaCa-2 and PC-3 cancer cell lines at IC50 ranged between 42.2 and 79.8 μg/mL(Boukes *et al*., 2017). Compound1 has been isolated for the first time from *F. cajanderi* extract in this project so no report studied about purified compound 1 on cytotoxicity. However compound1 has been reported from a mushroom of the *Garnoderma spp* and showed 70% cell viability of anti-tumour promoter activity (Chairul *et al*., 1990). Thus the purified compound 1 from *F. cajanderi* might be a potential compound for anti-tumour and should be continued studying on cytotoxicity against cancer cell line of purified compound 1 in the future.

This is the first time that cytotoxicity activity of *P. everhartii and P. laevigatus* has been studied in human cancer cell lines: ovarian carcinoma (A2780), malignant melanoma (A375), prostate carcinoma (LNCaP) and breast carcinoma (ZR75-1) and showed the cytotoxicity activity at concentration 125 μg/ml after 24 h. In previous studies, *Phellinus* mushrooms have been studied and found to have cytotoxicity activity in different cancer cell lines for example the fruiting bodies from *P. rhabarbarinus* exhibited cytotoxicity against five human cancer cell lines: breast cancer SK-BR-3, hepatocellular carcinoma SMMC-7721, human myeloid leukemia HL-60, pancreatic cancer PANC-1, and lung cancer A-549 cells *(Feng et al*., 2016). Šeklić *et al*. (2016) showed that *P. linteus* (Berk. et Curt) Teng extract significantly decreased cell viability in both tested colon cancer cell lines HCT-116 and SW-480 with IC 50 200.58 μg/ml and 169.80 μg/ml after 72 h. Comparing with the IC 50 of PE EtOH FC EtOH and PL EtOH against cancer cell lines in this study were around 50-150 μg/ml which were lower than previous study. Xue *et al.* (2011) reported that polysaccharide (PB) was isolated and purified from *P. baumii* that induced apoptotic cell death in HepG2 cells after 48 h. Atractylenolide I was a major substance which was isolated from EtOAc extract of *P. linteus* grown on germinated brown rice showed potent anticancer activity against human colon carcinoma (HT-29) cell line at 5-100 μg/ml for 48 h (Jeon *et al*., 2013). Fraction PL-ES from *P. linteus* showed anticancer activities on 10 different human cancer cell lines PC-3 (prostate cancer metastasis to bone), DU-145 (prostate cancer metastasis to brain), and LNCaP

(prostate cancer metastasis to lymph node), bladder cancer T24, kidney cancer ACHN, lung cancer A549, breast cancer MCF-7, stomach cancer AGS, liver cancer HepG2, and brain cancer U-87 cells at concentration 100 µg/ml at 72 h (Konno *et al*., 2015). Comparing the previous studies from *Phellinus*, the incubation time of this study is only 24 h, but in previous studies the incubation was 48 and 72 h. Only EtOH crude extract was investigated in cytotoxicity against cancer cell lines however the purified compound should be tested in the future and it might show cytotoxicity activity at lower concentrations of the pure compound. 7-methoxyindole-3-carboxylic acid methyl ester was isolated for the first time from *P. everhatii* as mentioned in Chapter 2. Samchai *et al*., 2011 isolated 7-methoxyindole-3-carboxylic acid methyl ester from *P. linteus,* but no biological activity has been reported. Therefore, the pure compound 7-methoxyindole-3-carboxylic acid methyl ester should be considered for cytotoxicity activity in future work.

3.4.2 Antimicrobial activity

One of the best natural antimicrobial resources is mushrooms. The crude extract of *F. cajanderi* in this study showed antimicrobial activity against three gram-positive bacteria (*B. subtillis*, *S. aureus*, *and L. monocytogenes*) and one gram-negative strain (*P. aeruginosa*) at 1 mg/ml. Shen *et al*. (2017) reviewed that mushroom 158 species from 88 genera have been reconised to have antimicrobial properties such as *F. pinicola*, *F. officinalis*, *F. lignosus*, *P. baumii*, *and A. bisporus*. In another study, *F. pinicola* demonstrated strong activity against gram-negative bacteria *E. coli*, *K. pneumonia*, *P. aeruginosa*, *Proteus mirabilis* with a MIC value of 0.625-2.5 mg/ml (Nowacka *et al*., 2015). The exopolysaccharide of *F. feei* showed the most effective antimicrobial against gram-negative bacteria, especially *Proteus vulgaris* and *P. aeruginosa* (N *et al*., 2017). *F. pinicola* exhibited antibacterial and antifungal activity of *B. subtilis, E. coli, S. aureus, K. pneumonia, P. aeruginosa, P. vulgaris, C, albicans, S. cerevisiae, A. fumigatus* and *P. chrysogenum* at 150 mg/ml (Pala *et al*., 2019). All previous studies showed the antimicrobial activity of different *Fomitopsis* species at a concentration more than 1 mg/ml compared with the concentration in this study that was 1 mg/ml. Moreover this study produced the first report for antimicrobial activity of EtOH crude extract of *F. cajaderi* on *B. subtillis*, *S. aureus*,

and L. monocytogenes. Further testing should be carried out on the purified compounds and determine the MIC.

3.4.3 Potential AD therapeutic screening

The purified compound P and E were studied for anti-AchE activity and neuroprotective activity. In this study, sample P and E from mushroom *P. everhartii* showed the highest protective percentage against H_2O_2 in SHSY5Y cells at concentration 50 μg/ml after incubation time 24 h. The highest percentage of AChE inhibitory activity was around 70%, which was observed at 150 μg/ml in both samples P and E of *P. everhartii*. Over 20 different brain-improving culinary-medicinal mushrooms and at least 80 different bioactive secondary metabolites isolated from *Hericium erinaceus*, *G. lucidum*, *Sarcodon spp.*, *Antrodia camphorata*, *Pleurotus giganteus*, *Lignosus rhinocerotis*, *Grifola frondosa*, and many more play an important role as therapeutic agents in neurodegenerative diseases such as AD and PD (Phan *et al*., 2015).

There is a significant quantity of research that confirms that bioactive compounds from mushrooms show neuroprotective activity. To begin with triterpene from *G. lucidum* at 10–40 μM could protect H_2O_2-induced cell damage in a dose-dependent relationship, and the survival rates at 40 μM were 62.68 %, 72.57 %, and 78.96 %, respectively (Wang *et al*., 2019). Leucomentins from the mushroom *Paxillus panuoides* showed H_2O_2 neurotoxicity (Lee *et al*., 2003). Compounds 1 and 2 of *G. leucocontextum* fruiting body showed protective effects against H_2O_2 induced damage with survival rates of 83.19±0.92 %, 73.37±1.25 % at 200 μM, respectively on PC12 cells (Chen *et al*., 2018). An EtOAc extract of fruiting bodies from *P. linteus* (PLEA) showed that it dose-dependently reduced the cytotoxicity of H_2O_2 with the pretreatment of human brain neuroblastoma SK-N-MC cells with the PLEA (0.1-5 μg/mL) (Choi *et al*., 2016).

According to the present study, the highest percentage of AChE inhibitory activity was around 70%, which was observed at 150 μg/ml in both samples P and E of *P.*

everhartii. The enzyme cholinesterase (ChE) is a significant therapeutic target for AD. The main cause of AD is the reduction in acetylcholine (ACh) synthesis. Therefore, one of the potential therapeutic strategies is to increase the cholinergic levels in the brain by inhibiting the biological activity of acetylcholinesterase (AChE). A number of ChE inhibitors have been developed such as donepezil, galantamine, rivastigmine and memantine and the four drugs used to treat ad currently available on the market (Sharma, 2019). However, the efficacy of these drugs is limited, and these drugs have shown various dose-associated side-effects, particularly at higher doses. Therefore, there is a need to develop a new drug or multi-functional drugs that are able to target symptoms of AD, including the decreased levels of Ach.

AChE inhibitory activity of fruiting bodies, mycelia and culture filtrate of *P. igniarius* at concentration 25-400 μg/ml exhibited 60.45-90.12, 29.36-72.27 and 22.82-60.76% ,respectively (Jin *et al*., 2014). A Hex extract of *P. pini* exhibited the highest enzyme inhibitory activity against AChE enzyme at 38.15% at concentration 100 μg/ml (Deveci *et al*., 2019). EtOAc extracts of *Funalia trogii* and *G. lucidum* indicated good anti-cholinesterase activity with an IC50 of 94.6 mg/ml and 174.3 mg/ml, respectively (Tel *et al*., 2015).

In this study the concentration of P and E less than 150 μg/ml showed AChE inhibitory activity around 70% compared with the previous study that showed AChE inhibitory activity around 20-70 % at concentration 25-400 μg/ml. Filho *et al.* (2006) reviewed that most AChE inhibitors are known to contain nitrogen; the higher activity of extracts may be due to their rich alkaloidal content. P and E in this study were identified as indole alkaloids (conpound E). The results taken together indicate that the mushrooms in this study exhibited anti-Alzheimer activity by showing AChE inhibitory activity and neuroprotective activity including samples P and E however, the AChE inhibitory activity of P and E were less than tacrine positive control by 1000 times. Therefore, P and E would not be good candidates for AD treatment.

3.4.4 Anti-inflammatory activity

TNF-α is known to cause an inflammatory response and relate to many diseases including AD. In this study three different methods were used to investigate anti-inflammatory property. Firstly TNF-α production from differentiated THP-1 cells stimulated with LPS was used to measure ability of crude extract and a pure compound on potential anti-inflammatory properties. All crude extracts from *P. everhartii*, *F. cajanderi* and *P. laevigatus* and the pure compound P and E significantly decreased TNF-α in comparison to the control (cells with LPS), suggesting it may be possible to use these extracts and compound as anti-inflammatory agents. Only the pure compound P and E were studied in different concentrations by using three assays to confirm anti-inflammatory activity. Moreover, P and E from *P. everhartii* showed a significant decrease in TNF-α compared with the control, but only P showed a dose-dependent effect from low concentration to high concentration. This may have been due to the purity of E, but there is a decreasing trend when the concentration of the compound increases. Mushrooms are rich in anti-inflammatory components such as polysaccharides, phenolic and indolic compounds. Indole compounds are found in mushrooms that have particularly strong effects on the immune and nervous systems of animals and found anti-oxidative and anti-inflammatory properties (Muszyńska *et al*., 2018). Elsayed *et al*., 2014 reviewed that the concentration and efficacy of the bioactive compounds are varied and depend on the type of mushroom, substrate applied, cultivation and fruiting conditions, stage of development, age of the fresh mushroom, storage conditions, and processing and cooking procedures and many bioactive compounds in mushrooms exhibit significant anti-inflammatory properties. According to the result from purified compound E showed unstable result that might relate to the purity of the extraction, the collection time of the mushroom sample. The purification of sample E should be purified more and confirm the anti-inflammatory activity again in the future.

Anti-inflammatory activity of mushrooms is summarised in Table 3.1 and described in a number of publications as follows: The mRNA expression levels of COX-2, iNOS, IL-1α, IL-β, IL-6, and TNF-α decreased in *P. igniarius* (PI) treated groups at concentrations of 50, 100, 200, and 400 μg/mL compared to LPS treated groups in RAW264.7 mouse macrophages (Kim *et al*., 2019). Three phenolic compounds isolated from *P. baumii* showed anti-inflammatory activity by inhibiting NFκβ and LPS-stimulated NO production at IC50<10μM in RAW 264.7 cells (Jang *et al*., 2017). Inotilene from *P. linteus* showed anti-inflammatory activity in RAW 264.7 cells by decreasing NO and TNF-α and *in vivo* in a rat paw oedema test. Polyssaccharide (PSCPL) of cultured *P. linteus* fruiting bodies tested against LPS-induced in THP-1 cells at 5 μg/ml showed inhibition of reactive oxygen species (ROS) formation and cytokine TNF-α, IL-1α, IL-1β and IL4 production (Wu *et al*., 2013). Comparing the anti-inflammatory activity of crude extract of three mushrooms and purified compound P and E of *P. everhartii* with the previous studies found that they use the higher concentration of extract to decrease TNF-α.

A second assay was carried out using L929 cells to confirm the ability of the extracts to protect against TNF-α induced cytotoxicity. The highest protection percentage of the cells against TNF-α and actinomycin D using samples P and E was 30% at 10 μM. Actinomycin D is a transcription inhibitor that inhibits *de novo* protein synthesis. No report studied the ability of the extracts to protect against TNF-α induced cytotoxicity by using L929 but there were the natural product using this cell to investigate anti-inflammatory activity. Kassim *et al*. (2010) showed honey extract significantly protected L929 cells by more than 80% at 250 μg/ml, but no significant protective effects of honey extract on L929 cell treated with TNF-α and actinomycin D.

In a third assay NCTC cells were used to study the ability to inhibit or decrease NF-ƙB expression. NF-ƙB represents a family of inducible transcription factors, which induced the expression of various pro-inflammatory genes including cytokines and chemokines and involved in different processes of the immune and inflammatory responses (T. Liu *et al*., 2017). In this study both P and E were investigated in terms of their ability to inhibit or decrease NF-ƙB expression in NCTC cells. Both P and E

decreased the percentage control of NFκB significantly (P<0.05) at 55% and 70%, respectively at 30 µg/ml. Jedinak *et al*., 2011 studied that edible oyster mushroom (*Pleurotus ostreatus*) suppressed LPS-induced secretion of TNF-α, IL-6, and IL-12p40 and inhibited NF-κB from RAW264.7 macrophages. Shao *et al*. (2014) indicated that hispidin inhibits transcriptional activity of NF-ƙB in a dose-dependent manner.

Nonsteroidal anti-inflammatory drugs (NSAIDs) are usually the most commonly used for treating pain and inflammation (Doña *et al*., 2020). Elsayed *et al*. (2014) reviewed that the long-term administration of NSAIDs has the potential for significant side effects on the gastrointestinal tract (GIT) include numerous harmful effects such as mucosal lesions, bleeding, peptic ulcers, and intestinal perforation. Natural products or natural product-derived compounds represent great structural diversity, which is not commonly seen in synthetic compounds and play a dominant role in the discovery of leads for the development of drugs for treating human diseases. The reported medicinal effects of mushrooms include anti-inflammatory effects, with anti-inflammatory compounds of mushrooms shown in Table 3.1.

From all of the three different assay results and the side effect of the drugs at the present, it can be concluded that the crude extracts of the three mushrooms and pure compound P and E have anti-inflammatory activity and may be an alternative natural product to be developed for anti-inflammatory treatment in the future.

In conclusion, *P. everhartii* and *P. laevigatus* show potential anti-cancer and anti-inflammatory properties, while *F. cajanderi* has potential anti-microbial and anti-inflammatory activity. Furthermore, the purified compound P and E has anti-inflammatory activity and show a dose-dependent effect from low concentration to high concentration by using THP-1 model. To examine the changes in affected pathway and genes caused by purified compound P and E, RNA-Seq was used to investigate the gene expression level supporting the findings obtained in biological activity.

CHAPTER 4 RNA-Sequencing and ELISA

4.1 Introduction

Inflammation is a mechanism that is related to many diseases, such as rheumatoid arthritis, inflammatory bowel disease, disease of the central nervous system (CNS), cardiovascular disease, renal disease, respiratory disease, and psoriasis (Bradley, 2008). The result findings in Chapter 3 suggest that P and E could have potential anti-inflammatory activity and anti-Alzheimers activity. Both P and E inhibited cytokine TNF-α in THP-1 cell, protected against TNF-α mediated cell death in L929 cells and inhibited NFκB in NCTC cell. Following on the findings in Chapter 3, the changes of gene expression in THP-1 cells in response to these compounds were investigated. TNF-α was identified in 1975 as an endotoxin-induced glycoprotein (Bradley, 2008). TNF-α is an inflammatory cytokine or pro-inflammatory mediator. TNF-α has been the centre of study for its roles in normal physiology, acute inflammation, chronic inflammation, autoimmune disease and cancer-related inflammation. IL6 is a pleiotropic cytokine and demonstrated to be a multifunctional cytokine that regulates numerous biological processes including the organ development, acute-phase responses, inflammation, and immune responses (H. Su *et al.*, 2017). Su *et al.* (2016) reviewed the primary pro- and anti-inflammatory cytokines related to AD that include IL1, IL6, TNF-α, IL4, IL10 and transforming growth factor beta (TGFβ). Since the 1990s, studies indicate that anti-inflammatory treatments could be used to reduce the risk of AD developing in patients (Kinney *et al.*, 2018) in particular targeting TNF-α and IL6, pro-inflammatory cytokines, associated with AD. TNF-α has been reported to be found in high levels in both the brains and plasma of AD patients and IL6 is increased in the CNS and serum of AD patients as well, which leads to chronic neuroinflammation and neurodegeneration. TNFSF10 (TRAIL) is a member of the TNF superfamily of cytokines that is involved in different kinds of inflammatory responses and plays an important role in inducing cell death (Zaba *et al.*, 2010). C–X–C motif chemokine 10 (CXCL10) also known as interferon γ-induced protein 10 kDa (IP-10) or small-inducible cytokine B10 is a cytokine belonging to the CXC chemokine family (M. Liu *et al.*, 2011). CXCL10 is associated with a variety of human diseases including infectious diseases, chronic inflammation, immune dysfuntion, tumor development, metastasis and dissemination (M. Liu *et al.*, 2011) . CXCL13, a B-cell chemokine, has been proposed as a biomarker in a variety of conditions and elevated in multiple sclerosis, neuromyelitis optica and other

inflammatory neurological controls compared with noninflammatory controls (Alvarez *et al*., 2013). CCL2 known as monocyte chemoattractant protein-1(MCP-1) is a member of the C-C chemokine family and a highly potent chemo-attractor of monocytes and CD4$^+$ T cells (Ansari *et al*., 2011). CCL2 is one of the most studied pro-inflammatory molecules among the C-C family members and a potential intervention point for the treatment of various inflammatory and autoimmune diseases (Deshmane *et al*., 2009).

Takagi *et al*. (2014) reviewed that *PTX3*, *IL8*, *IL6*, *CXCL10*, *GBP1*, *CHRM3*, *CXCL1*, *IL1R2*, *CCL18*, and *CCL13* were inflammation-related genes. Michlmayr & McKimmie (2014) reviewed that the chemokine CXCL10 is also involved in AD and is highly expression in AD. Kowarik *et al*. (2012) found that CXCL13 was significantly elevated in CSF (cerebrospinal fluid) of all patient groups with inflammatory disease. CCL2-related signalling pathways might be new targets for disease-modifying therapies aimed at slowing down the disease process in patients with pre-dementia stages (Westin *et al*., 2012).

The aim of this chapter was to examine the gene expression of the pure compound P and E from mushroom *P. everhartii* on THP-1 cells and their potential as anti-inflammatory agents. Total RNA was isolated from control and pure extract-treated THP-1 cells and the gene expression changes assessed using RNA-seq and quantitative real-time PCR (RT-qPCR). The biological activities of the *P. everhartii* compound examined in Chapter 3 suggested that they may have anti-inflammatory and anti-cholinesterase properties. In this chapter, RNA-Seq technology were used to understand the genes and pathways involved in the cellular response to this compound. Gene expression analysis using RT-qPCR was chosen on six target genes (*CCL2, CXCL10, CXCL13, TNFSF10, TNFα,* and *IL6*) related to anti-inflammatory activity and anti-Alzheimers activity from the biological activity results in Chapter 3. ELISA was used to investigate the expression of proteins.

4.2 Materials and Methods

4.2.1 Materials

- CXCL10 DuoSet ELISA (R&D SYSTEMS, USA)
- Human IL-6 Uncoated ELISA (Invitrogen, UK)
- Human CCL2 Uncoated ELISA (Invitrogen, UK)
- TNFSF10 DuoSet ELISA (R&D SYSTEMS, USA)
- RNeasy Plus Total RNA Mini Kit (Qiagen, UK)
- QIAshredder (Qiagen, UK)
- Tetro cDNA synthesis kit (Bioline, London, UK).
- Experion™ RNA StdSens Analysis kit (Bio-Rad, UK)
- PowerUp™ SYBR™ Green Master Mix (Applied Biosystems, UK)
- Oligonucleotide PCR primers (Integrated DNA Technologies, Belgium)
- MicroAmp® Fast Optical 96-well reaction plates (Thermo Fisher Scientific, UK)

4.2.2 Methods

4.2.2.1 RNA extraction

THP-1 cell cultures stimulated with LPS were treated with *P. everhartii* extracts as detailed in Chapter 3, Section 3.2.2.3.1.1. The supernatant from the different treatments were harvested and kept at -80ºC for cytokine analysis. Total RNA was isolated from the THP-1 cells using RNeasy® Plus Mini Kit (Qiagen, Manchester, UK) following the manufacturer's instructions. The adherent cells were washed using PBS and aspirated, then 350 µl RPL plus buffer was added to the wells. The cell lysate was pipetted into a QIAshredder spin column and placed into a 2 ml collection tube and centrifuged for 2 min at a maximum speed (16000 x g) to ensure complete disruption to maximise the yield. The homogenised lysate was transferred to a Qiagen gDNA eliminator spin column placed in a 2 ml collection tube and centrifuged for 30s at ≥ 8000 x g. The gDNA eliminator column was discarded and 1 volume of 70% v/v

ethanol was added to the flow-through and mixed by pipetting. Seven hundred microlitres of the sample were transferred to a RNeasy spin column placed in a 2 ml collection tube and then centrifuged for 15 s at ≥ 8000 x g. The flow-through was discarded. The remaining lysate sample was loaded onto a RNeasy spin column and the process repeated. In order to wash the spin column membrane, 700 µl of RW1 buffer provided by the kit was added to a RNeasy spin column and centrifuged for 15 s at ≥ 8000 x g and the flow through discarded. Five hundred microlitres of RPE buffer was added to the RNeasy spin column and centrifuged for 15 s at ≥ 8000 x g. The flow-through was discarded and the RPE buffer step was repeated again, this time with a 2 min spin. The RNeasy spin column was placed in a new 1.5 ml collection tube and then 50 µl RNase-free water was added to the spin column membrane and centrifuged for 1 min at ≥ 8000 x g to elute the RNA.

4.2.2.2 RNA Quality assessment

All of the extracted RNA samples underwent quality assessment to ensure they did not have a negative impact on the gene expression data obtained.

4.2.2.2.1. Spectrophotometry

The total RNA concentration and quality was measured using a Nanodrop™ 2000-C Spectrophotometer (Thermo Fisher Scientific, Loughborough, UK). The absorbance of the RNA sample at 260nm provides a way of obtaining the concentration of the sample. The ratio of absorbance at 260 nm (A_{260}) and 280 nm (A_{280}) was used as an indicator of RNA purity with the A_{260}/A_{280} for pure RNA should be close to 2 The ratio A_{260}/A_{230} was used as a secondary measure of nucleic acid purity providing an indication of salt contamination from the isolation method is commonly in the range close to 2 for pure RNA.

4.2.2.2.2. Automated electrophoresis

The RNA integrity of the extracted THP-1 RNA was assessed using an Experion™ Automated electrophoresis system with a RNA StdSens Analysis kit.

4.2.2.3 RNA Sequencing (RNA-Seq) Analysis

Four RNA samples (control and three extract-treated samples) were submitted to BGI-Tech (Shenzhen, China) for their RNA-Seq (quantification) service. The RNA-Seq was performed using their BGISEQ-500 platform with 20Mb clean reads. Pairwise experiments were carried out on three groups. These were: (1) Control THP-1 cell vs E10; (2) Control vs E30; (3) Control vs P30.

4.2.2.4 Pathway Enrichment Analysis

The RNA-Seq results were analysed and the software that used in the list below.

The list of software:

- GOrilla (http://cbl-gorilla.cs.technion.ac.il/)
- Cytoscape Software (version 3.3.0) with the ClueGO gene ontology plugin (version 2.2.4)
- Primer-BLAST website (https://www.ncbi.nlm.nih.gov/tools/primer-blast/)
- Pathview (https://pathview.uncc.edu/)
- Java Tree View (http://jtreeview.sourceforge.net)

4.2.2.5 Real time Quantitative PCR (RT-qPCR)

4.2.2.5.1 cDNA synthesis

The extracted RNA was transcribed to complementary DNA (cDNA) using a Tetro cDNA synthesis kit. The master mix was prepared using 5 μg of THP-1 total RNA, 1μl Oligo $(dT)_{18}$, 1 μl 10 mM dNTP, 4 μl 5x RT buffer, 1 μl Ribosafe RNase Inhibitor, 1 μl Tetro Reverse Transcriptase (200u/μl) and RNase-free water to bring

the final reaction volume to 20 µl. Reactions containing reverse transcriptase were labelled as RT(+). A reverse transcriptase-minus control (RT(-)) was prepared containing master mix without the reverse transcriptase to act as a genomic DNA carry-over control for RT-qPCR. The reactions were incubated at 45ºC for 30 min, followed by incubating at 85ºC for 5 min. Then samples were cooled on ice. The cDNAs were diluted to 100 µl with 1x RT Buffer and reactions stored at -20ºC until required.

4.2.2.5.2 RT-qPCR primer design

PCR primers for the reference and target genes were designed using the Primer-BLAST website (https://www.ncbi.nlm.nih.gov/tools/primer-blast/ ; Ye *et al*., 2012). The candidate reference gene selection was chosen from those commonly used with THP-1 qRT-PCR studies listed in Table 4.1. The target genes were chosen based on the findings from the RNA-Seq data and analysis of the extract biological activity in Chapter 3.

Table 4.1 Sequences of the qRT-PCR primers for the reference gene assays

Primer Name	Primer Sequence (5'-3')	GenBank Accession	Product Size (bp)
PPIB	Forward:5'-ACCTACGAATTGGAGATGAAGATG-3' Reverse: 5'- TCCTTGATTACACGATGGAATTTG -3'	NM_000942.4	152
HPRT	Forward:5'- CCCTGGCGTCGTGATTAGTG-3' Reverse:5'- TCGAGCAAGACGTTCAGTCC-3'	NM_000194.3	139
RPL37A	Forward:5'- CCGCGTCTCTTCCTTTCTGG-3' Reverse:5'- TTCACCATTTTCCGGAGGGAG-3'	NM_000998.4	123

Table 4.2 Sequences of the qRT-PCR primers for the target gene assays

Primer Name	Primer Sequence (5'-3')	GenBank Accession	Product Size (bp)
Ccl2	Forward:5'- TCCCAAAGAAGCTGTGATCTTCA -3' Reverse: 5'- TGGGTTGTGGAGTGAGTGTT -3'	NM_002982.3	143
Cxcl10	Forward:5'- TGGCATTCAAGGAGTACCTCTC -3' Reverse:5'- GCAATGATCTCAACACGTGGAC -3'	NM_001565.3	141
Cxcl13	Forward:5'- CTAATGAGCCTGGACTCAGAGC -3' Reverse:5'- CACCTCAAGCTTGTGTAATAGACC -3'	NM_006419.2	148
Tnfsf10	Forward:5'- GAGAAGGAAGGGCTTCAGTGAC -3' Reverse:5'- AGGAGCACTGTGAAGATCACG -3'	NM_0011909 43.1	142
Tnf alpha	Forward:5'- AGAACTCACTGGGGCCTACA -3' Reverse:5'- AGGAAGGCCTAAGGTCCACT -3'	NM_000594.3	139
Il6	Forward:5'- TTCTCCACAAGCGCCTTCG -3' Reverse:5'- GAAGAGGTGAGTGGCTGTCTG -3'	NM_000600.4	140

The candidate reference genes were assessed and ranked by their stability of expression following extract treatment on the THP-1 cells using RefFinder (Xie *et al*., 2012). RefFinder uses a number of stability algorithms including GeNorm, BestKeeper, and Normfinder to comprehensively rank the expression of the genes based on their stability of expression between control and treated samples. The most invariant reference gene candidate out of the three was used for normalisation in the relative gene expression calculation.

All of the the PCR primers for this study were synthesised by IDT (Belgium), resuspended in nuclease-free water, and stored at -20ºC until required.

4.2.2.6 SYBR Green quantitative real-time PCR

RT-qPCR was conducted using a SYBR green-based chemistry. Applied Biosystems PowerUp^{TM} SYBR Green Master Mix, was prepared following the manufacturer's instructions. The PCR reaction sets for each gene target consisted of a negative control (no template), a RT (-), and a RT (+) tube. The master mix is shown in Table 4.3. Triple replicate real-time PCR reactions were carried out for each sample. Thermocycling conditions were conducted on a StepOne Plus real-time PCR system (Applied Biosystems, UK) under the fast PCR protocol as shown in Table 4.4.

Table 4. 3 Master Mix components

Component	Volume (10 µl/well)
PowerUp™ SYBR™ Green Master Mix	5 µl
Forward primer (10 pmol/µl)	0.4 µl
Reverse primer (10 pmol/µl)	0.4 µl
DNA template (concentration 50 ng/µl)	1 µl
Nuclease-Free water	3.2 µl

Table 4. 4 PCR thermal cycling and melting curve stage conditions

Step	Temperature	Duration	Cycles
UDG Activation	50°C	2 min	Hold
Dual-Lock™ DNA Polymerase	95°C	2 min	Hold
Denature	95°C	3 sec	40
Anneal/Extend	60°C	30 sec	
Melting curve stage	95°C	95°C	Ramp rate 1.6°C/sec
	60°C	60°C	

4.2.2.7 Gene Expression Analysis

Threshold cycle (Ct) values for each of the reactions were obtained from the StepOne Plus real-time PCR system and used to calculate the gene expression changes following the formula below. Delta-delta Ct ($\Delta\Delta$Ct) was used to calculate the relative gene expression changes of the samples from RT-qPCR between the control and treated samples for target gene and the reference gene (Livak & Schmittgen, 2001).

$$\Delta Ct \text{ Control} = Ct \text{ (Treat Gene)} - Ct \text{ (Ref Gene)}$$

$$\Delta Ct \text{ Treat} = Ct \text{ (Treat Gene)} - Ct \text{ (Ref Gene)}$$

$$\Delta\Delta Ct \text{ Treat Gene} = \Delta Ct \text{ Treat} - \Delta Ct \text{ Control}$$

$$\text{Fold change (FC)} = 2^{(-\Delta\Delta Ct)}$$

4.2.2.8 ELISA

4.2.2.8.1 TNF-α assay

TNF-α levels were used to investigate the anti-inflammatory activity of supernatants from THP-1 cell following the manufacturer's instructions of a Ready-Set-Go Kit. ELISA plates were coated with 100 μl/well of capture antibody in 1x coating buffer and then the plate was sealed and incubated 4°C overnight. The supernatants were discarded and the wells washed 3 times with wash buffer 1x PBS [Na_2HPO_4 2.3 g, NaCl 8 g, KH_2PO_4 0.2 g and KCl 0.2 g, adjusted pH to 7.2-7.4] plus 0.05%, v/v, Tween-20) and then blocked with 200 μl/well of 1x diluent and incubated at room temperature for 1 h. The supernatants were then discarded and washed at least once with wash buffer and 100 μl of samples were added per well in triplicate wells. Similarly, TNF-α standard at different concentrations were plated out to construct a standard curve. The plates were sealed and incubated at room temperature for 2 h and washed 3-5 times and then 100 μl detection antibody diluted 1x in diluent was added to each well and incubated at room temperature for 1 h. The wells were washed 3-5 times with wash buffer and HRP diluted 1x in ELISA/ELISPOT diluent was added (100 μl/well). After incubation at room temperature for 30 min the wells were washed with wash buffer 5-7 times and TMB solution was added (100 μl/well). The plate was incubated at room temperature for 15 min and 50μl stop solution (2N H_2SO_4) added to each well. The plate was read at 450 nm on a M5 Spectramax Plate Reader (Molecular Devices, USA) and the TNF-α levels were calculated from the standard

curve. Statistical analysis was carried out using a Dunnett's Multiple Comparison Test.

4.2.2.8.2 Interleukin-6 (IL6) assay

IL6 was analysed following the manufacturer's instructions of a Human IL-6 Uncoated ELISA. The detail of the procedure was similar to the TNF-α assay (section 4.2.2.8.1).

4.2.2.8.3 CCL2 (MCP1) assay

CCL2 was assayed following the manufacturer's instructions of a Human CCL2 Uncoated ELISA similar to the assay described in section 4.2.2.8.1.

4.2.2.8.4 TRAIL/TNFSF10 assay

TNFSF10 was assessed following the manufacturer's instructions of a DuoSet ELISA. The 96 well microplates were coated with 100 µl/well at a final concentration of 2 µg/ml and then the plate was sealed and incubated overnight at room temperature. The solutions were aspirated and wash 3 times with wash buffer (PBS, see section 4.2.4.5.1) and then blocked with 300 µl/well of Reagent Diluent and incubated at room temperature for a minimum 1 h. The solutions were discarded and the washing step repeated and then 100 µl of samples or standards were added and incubated at room temperature for 2 h. The supernatants were discarded and the plate washed 2-3 times and then 100 µl of detection antibody added, diluted with Reagent Diluent at a final concentration of 12.5 ng/ml. The plate was covered and incubated at room temperature for 2 h. The washing step was repeated and then 100 µl of a working dilution of Streptavidin-HRP added to each well and incubated for 20 min at room temperature. The washing steps were repeated and then 100 µl of Substrate Solution added to each well and incubated for 20 min at room temperature, avoiding direct light. Stop solution 50 µl per well was added. The plate was read using a microplate reader M5 Spectramax Plate Reader (Molecular Devices, USA) set to 450 nm.

4.2.2.8.5 CXCL10/IP-10 assay

CXCL10 was assessed following the manufacturer's instructions of a DuoSet ELISA similar to that described in section 4.2.2.8.4.

4.3 Results

Total RNA from THP-1 cell cultures plus LPS alone (control) or treated for 24 h with P or E plus LPS, were extracted using RNeasy Plus mini kit (Qiagen). The quantity and quality of RNA were checked with Nanodrop™ 2000c Spectrophotometer and the integrity of the RNA was confirmed using an Experion™ RNA StdSens Analysis kit. RNA samples comprising THP-1 cells alone (control), E 10 µg/ml, E 30 µg/ml, and P 30 µg/ml were submitted for RNA-Seq. According to the result from Chapter 4 and the RNA-Seq data, six genes (*CCL2, CXCL10, TNFSF10, CXCL13, IL6* and *TNFα*) were related to inflammation and AD were chosen to confirm by using RT-qPCR and ELISA.

4.3.1 Quantification and quality control of RNA Extraction

4.3.1.1 Nanodrop analysis

The NanoDrop spectrophotometer 2000c is used to quantify and can assess the purity of DNA, RNA, and protein samples. The RNA concentrations as well as the A_{260}/A_{280} and A_{260}/A_{230} ratios is this study's samples are shown in Table 4.5 and their UV absorption curves are shown in Figure 4.1. All of the samples quality ratios are within the expected acceptable ranges and all display expected RNA absorption curves.

Table 4.5 The concentration and quality of RNA samples determined using a NanoDrop 2000c spectrophotometer.

Sample	OD 260/280	OD260/230	Concentration (ng/µL)
Cells+LPS	2.07	0.33	144.6
E10	2.07	0.40	115.5
E30	2.03	0.51	67.0
P30	2.05	0.67	143.3
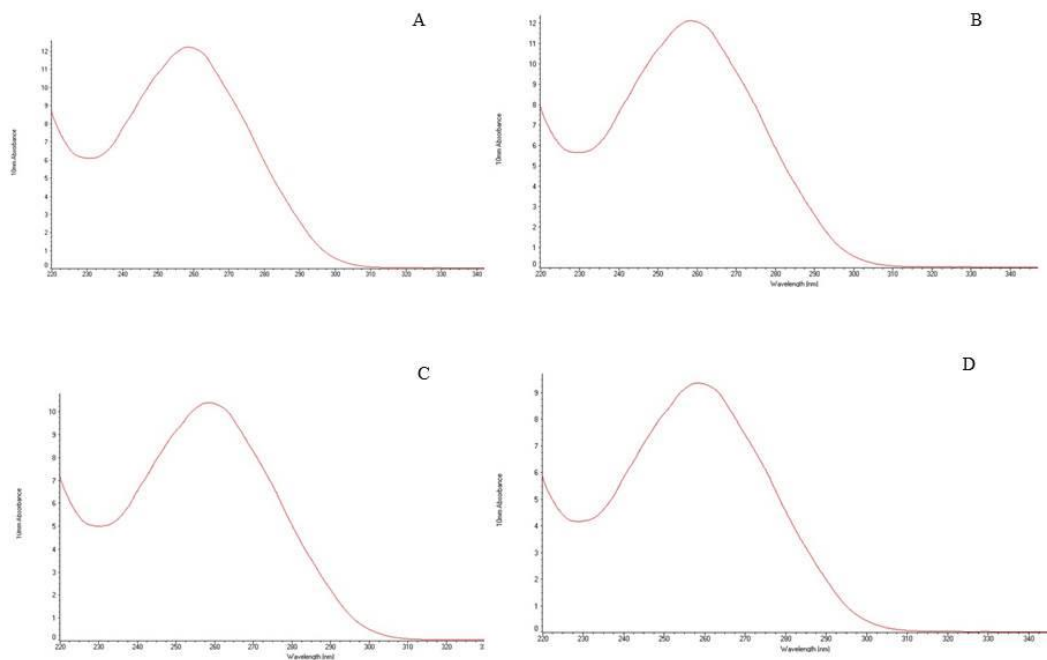
Figure 4.1 Nanodrop UV-region absorption spectra for total RNA isolated from (A) THP-1 Cells+LPS; (B) E10+LPS; (C) E30+LPS; and (D) P30+LPS samples.

4.3.1.2 Experion^{TM} RNA StdSens Analysis

RNA integrity was determined by the Experion^{TM} automated electrophoresis system. This system can provide an indication of RNA integrity, providing a RNA quality indicator (RQI). The 28s:18s ratio is also an indicator of RNA integrity and a 2:1 ration is typical of intact RNA. The RQI threshold for samples submitted for RNA-Seq was 7 or more. In the Experion virtual gel image of the RNA samples is shown in Figure 4.2 and their 28s:18s ratio and RQI scores are shown in Table 4.6.
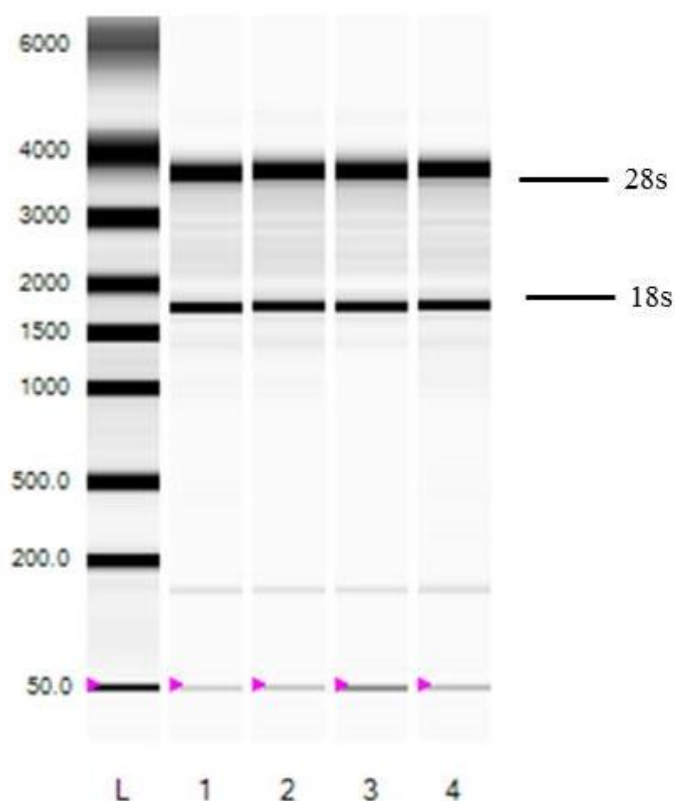
Figure 4.2 Experion^{TM} RNA StdSsens virtual gel reports showing the 18s and 28s bands from the control and treated THP-1 cell RNAs. Lane L: StdSens RNA Ladder, Lane 1: E10+LPS; Lane 2: E30+LPS; Lane 3: P30+LPS; and Lane 4: Cell+LPS.
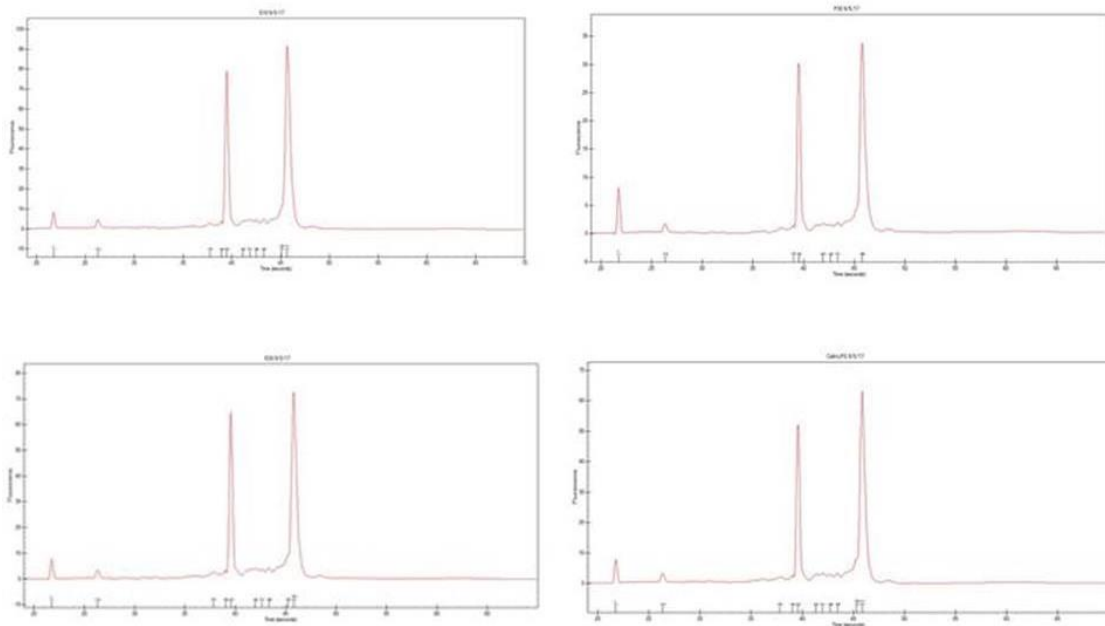
Figure 4.3 Electropherogram from an RNA StdSens analysis of total RNA samples; Cells+LPS, E10+LPS, E30+LPS and P30+LPS.

Table 4.6 Experion™ results of 28S:18S ratio and RQI for each THP-1 RNA samples

Sample	ID	28S:18S ratio	RQI
1	Cells+LPS	1.51	9.8
2	E10+LPS	1.61	9.9
3	E30+LPS	1.44	9.7
4	P30+LPS	1.50	9.8

4.3.2 RNA Seq

Three samples of extracts and control THP-1 RNA were sequenced by using RNA-Seq, the summarised information of sequencing data of each sample is shown in Table 4.7. The alignment of clean reads to the human GRCh38/hg38 reference genome was used for quality control analysis by BGI-Tech. The average number of raw sequencing reads was 24,136,618 and after clean read filtering was 24,085,765. Mapping quality parameter is the percentage of mapped read, which is indicator of the sequencing accuracy and the presence of contaminating DNA. In this study the total mapped read showed high percentage 94% and percentage of total unmapped read was around 5%.

Table 4.7 RNA Seq alignment statistics of read align to reference genome by BGI-Tech

Sample	Total Reads	Total Mapped Reads (%)	Unique Match (%)	Multi-position Match (%)	Total Unmapped Reads (%)
Control THP-1	24,085,768	94.23	73.05	21.18	5.77
E 10 µg/ml	24,082,732	94.79	73.81	20.98	5.21
E 30 µg/ml	24,084,835	94.88	73.26	21.62	5.12
P 30 µg/ml	24,089,727	94.54	71.76	22.78	5.46

4.3.2.1 RNA Seq Analysis

4.3.2.1.1 Pearson correlation heat map between samples

The correlation heat map between the number of gene expression changes is shown in Figure 4.4. Comparison of the control THP-1 and treated RNA samples, the coefficient value of E 10 μg/ml, 30 μg/ml and P 30 μg/ml was 0.988, 0.959, and 0.867, respectively. If one sample is highly similar to another one, the correlation value between them is very close to 1. According to the result in Figure 4.4, sample P showed the most difference with control THP-1 whereas E 10 μg/ml was similar to the control as the correlation value was 0.988.
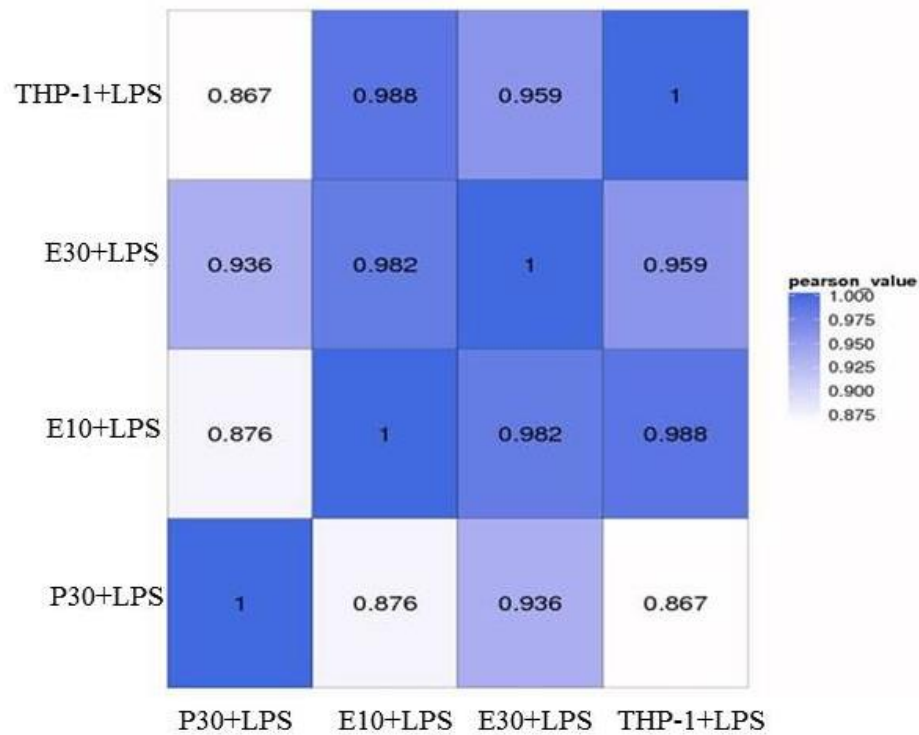
Figure 4.4 Heat map of correlation coefficient values across control and treated THP-1 RNA samples as provided by BGI-Tech.

4.3.2.1.2 Differential Expression Genes (DEGs)

DEG analysis was used to determine the number of genes affected by each treatment and comparison between treatment groups. The total number of genes expressed in each group was shown in Figure 4.5 and the number of differentially expressed genes between each pairwise comparison were shown in Figure 4.6. The number of expressed genes in each group was around 18000 genes (44%) from the reference transcriptome 41268 genes. When comparing the treated group with control THP-1, P30 appear to up-regulated and down-regulated more genes than the control group in comparison to the E10 and E30 group. Otherwise in comparison between treatment groups E10 vs P30 showed up-regulated and down-regulated more different number of genes than E10 vs E30 and E30 vs P30.
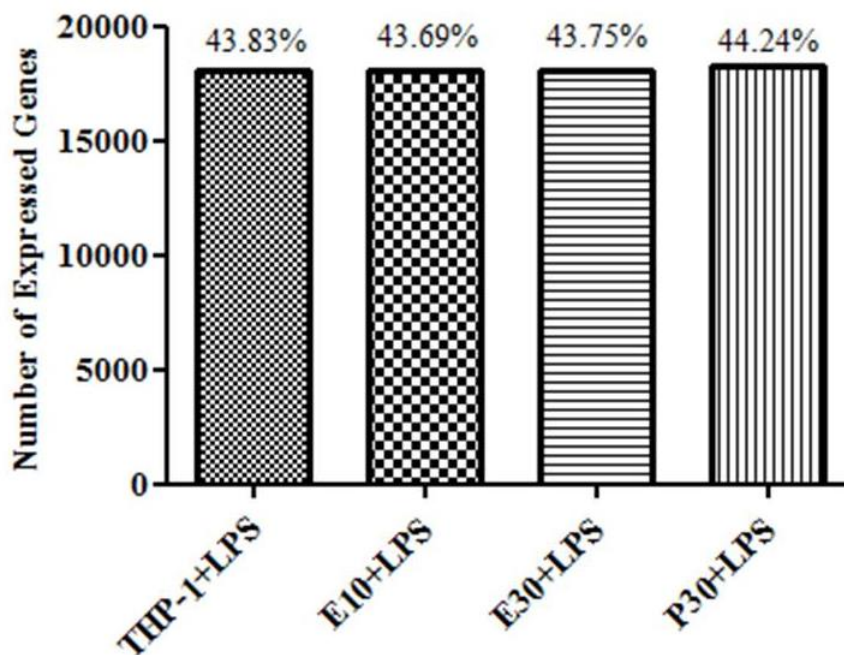
Figure 4.5 The number of identified expressed genes in control THP-1 and three treatment groups.
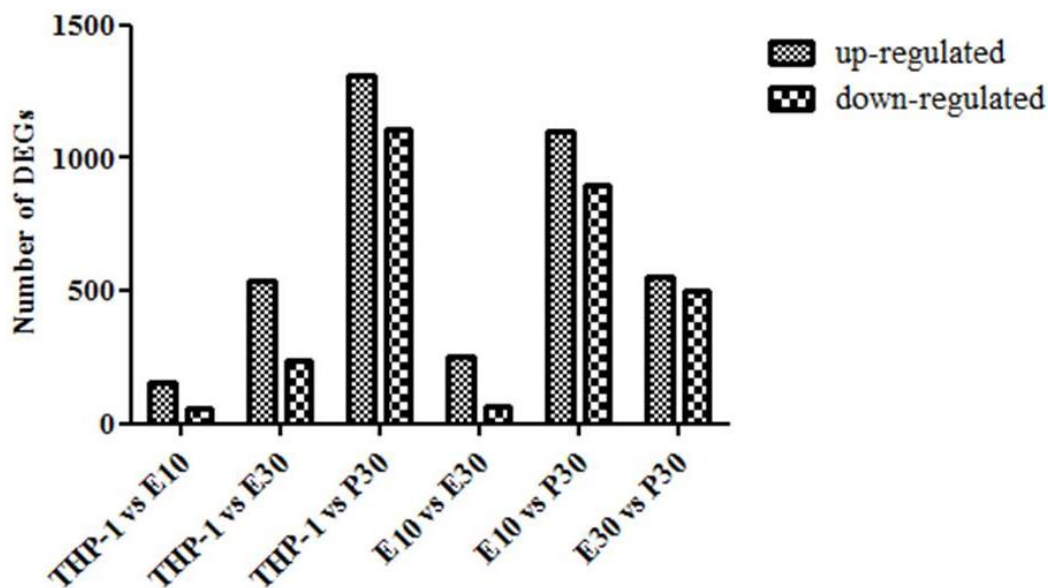
Figure 4.6 Differential expression genes in each pairwise comparison. X axis represents pairwise and Y axis means number of screened DEGs.

Genes with similar expression patterns usually have same functional correlation. We also provide clustering analysis of DEGs with cluster and JavaTree view according to the provided cluster plans for DEGs. Heatmaps of clustering analysis of DEGs using Java Tree View (http://jtreeview.sourceforge.net) (Eisen *et al*., 1998) were generated showing an intersection heat map (Figure 4.7 A) and a union heat map (Figure 4.7 B), with red showing up-regulated genes and blue showing down-regulated genes. Each pairwise comparison consisted of control vs P 30 µg/ml, control vs E 10 µg/ml and control vs E 30 µg/ml. It is evident that the three treatments (E10, E30 and P30) groups cause numerous effects of gene expression in both directions.

Only genes that were differentially expressed in all pairwises of the cluster plans were used to build the intersection heatmap and at least one pairwise that were differentially expressed in all pairwises of cluster plan was used to build the union heatmap.
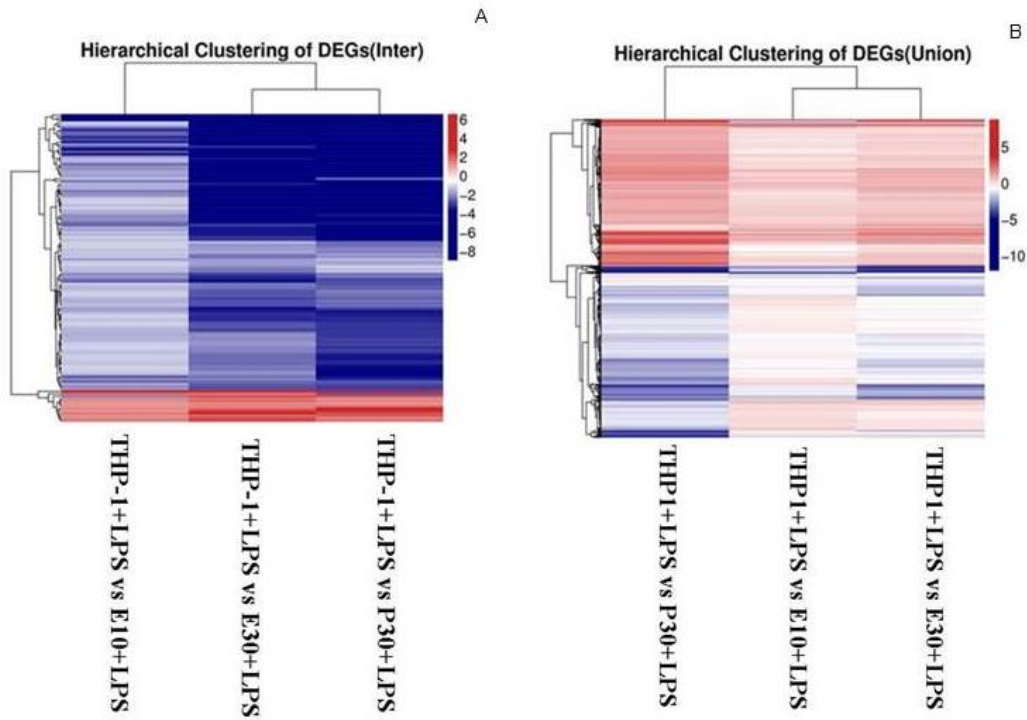
Figure 4.7 DEGs analysis intersection (A) and union(B) heat map generated using TreeView. Gradient colour barcode at the right top indicates log2 (FC) value (FC is fold change of expression in treatment case to expression in control case). Upregulated genes show in red and downregulated in blue. Each column represents a pairwise comparison and each row represents differentially expressed genes. DEGs with similar FC value are clustered both at row and column level.

4.3.2.1.3 Pathway Enrichment Analysis

Cytoscape and ClueGO plugin were used for pathway enrichment analysis by using RNA-Seq data. Cytoscape ClueGO cluster results using DEGs in the P 30 µg/ml vs THP-1 cell control (Figures 4.8), E 30 µg/ml vs THP-1 cell control (Figures 4.9) and the E 10 µg/ml vs THP-1 cell control (Figures 4.10). The cytokine-cytokine receptor interaction KEGG chart with log 2 FC values of THP-1 with LPS and E10, E30 and P30 were analysed by using Pathview (https://pathview.uncc.edu/) (Figure 4.11-4.13) The cytokine-cytokine receptor interaction pathway was significantly (p value ≤ 0.05) down-regulated in both P 30 µg/ml and E 30 µg/ml compare with the THP-1 cell control.

Significantly (P<0.05) enriched Kyoto Encyclopedia of Genes and Genomes (KEGG) pathways associated with all genes that were up-regulated and down-regulated by more than 2-fold were selected. Gene Ontology (GO) is an international standard gene functional classification system that provides a dynamically up-to-date vocabulary. GO covers three ontologies: molecular function, cellular component, and biological process. There were 11 GO terms associated with both up-regulated and down-regulated genes in the P 30 µg/ml vs THP-1 cell control (Appendix Table 1B) and only 6 GO terms related with up-regulated genes (Appendix Table 2B) and 14 GO terms related with down-regulated genes (Appendix Table 3B). There were 12 GO terms associated with both up-regulated and down- regulated genes in the E 30 µg/ml vs THP-1 cell control (Appendix Table 4B) and only 1 GO term related with up-regulated genes (Appendix Table 5B) and 21 GO terms related with down-regulated genes (Table 6B). In contrast, only 1 GO term was associated with both up-regulated and down-regulated genes in E 10 µg/ml vs THP-1 cell control (Appendix Table 7B), 2 GO terms were related with down-regulated genes (Appendix Table 8B) and one with up-regulated genes.
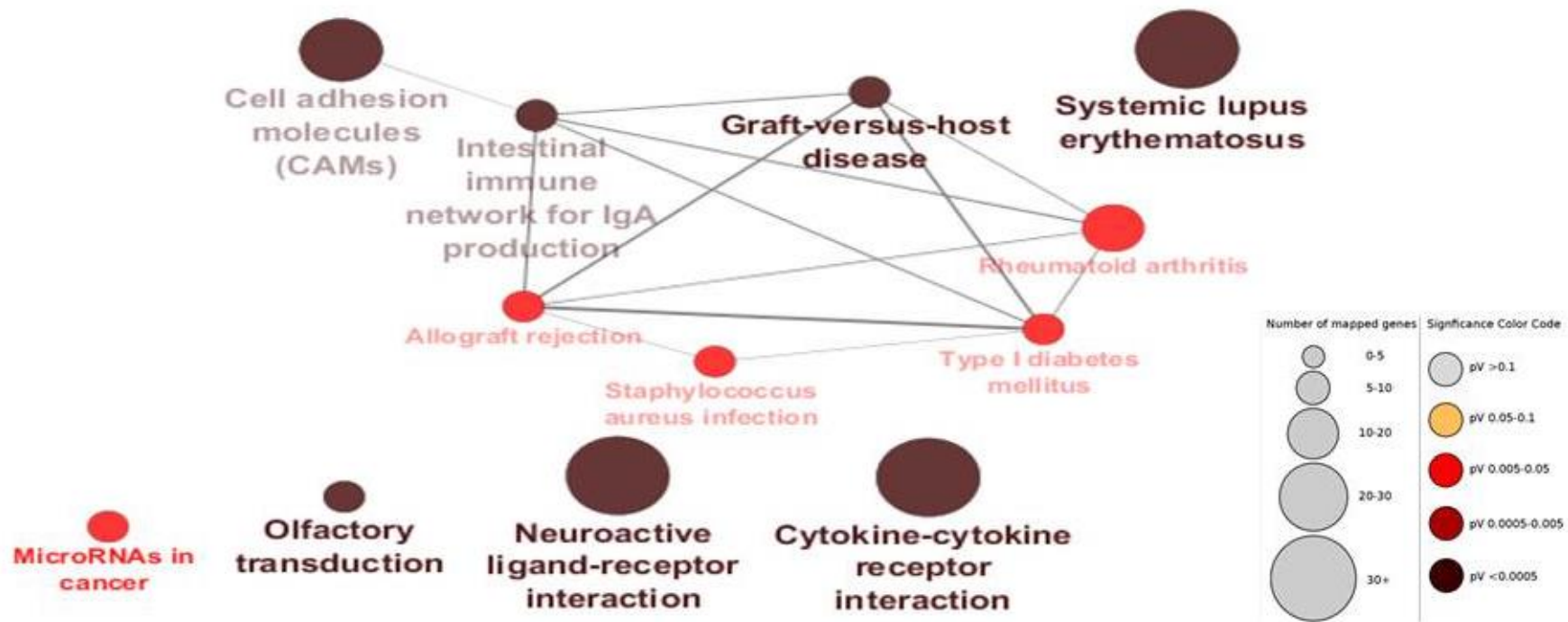
Figure 4.8 Cytoscape ClueGO cluster results using the DEGs from the RNA-seq data of the THP-1 cells treated with P 30 µg/ml vs THP-1 cell control. ClueGO legend (shown on the right of the figure) – circle size represents the number of genes, colours represent the significantly enriched KEGG pathways associated with all genes up-regulated and down regulated genes by more than 2-fold.
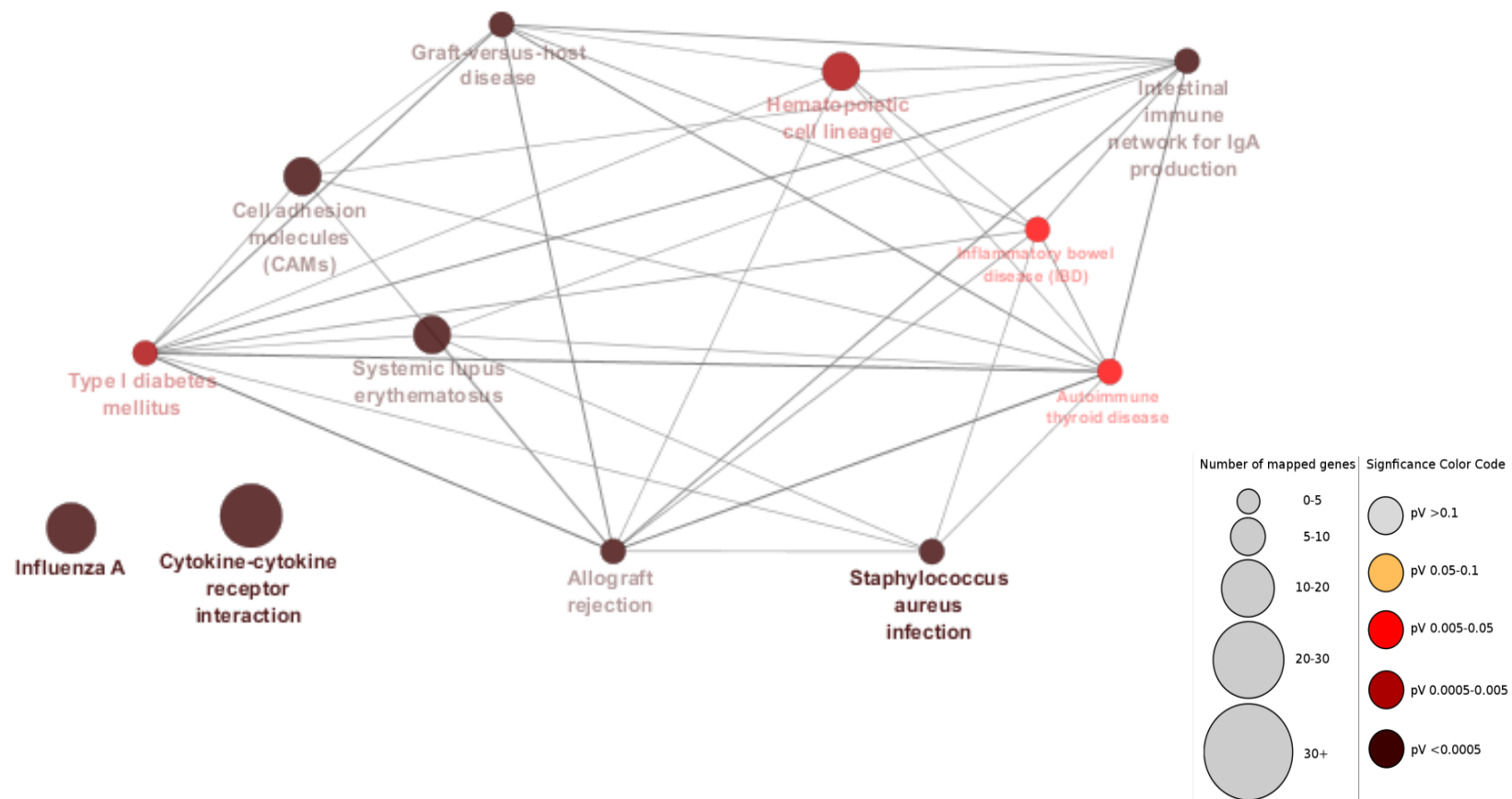
Figure 4.9 Cytoscape ClueGO cluster results using the differentially expressed genes from the RNA-seq data of the THP-1 cells treated with E 30 µg/ml vs. THP-1 cell control. ClueGO legend (shown on the right of the figure) – circle size represents the number of genes, colours represent the significantly enriched KEGG pathways associated with all genes up-regulated and down regulated by more than 2-fold.
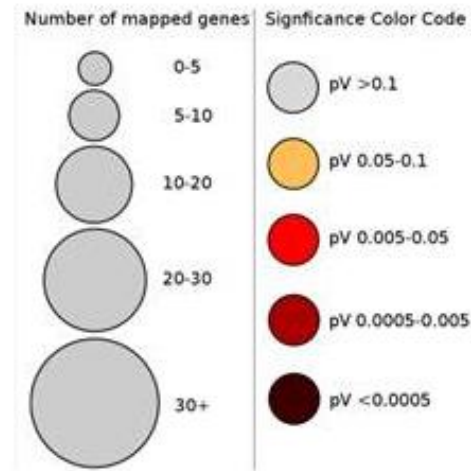
Figure 4.10 Cytoscape ClueGO cluster results using the differentially expressed genes from the RNA-seq data of the THP-1 cells treated with E 10 μg/ml vs THP-1 cell control. ClueGO legend (shown on the right of the figure) – circle size represents the number of genes, colours represent the significantly enriched KEGG pathways associated with all genes up-regulated and down regulated by more than 2-fold.

Following the results using Cytoscape ClueGo plugin, cytokine-cytokine receptor interaction was the only KEGG pathway significantly affected among the control THP-1 cell and THP-1 treated with E10, E30 and P30. The involvement of a number of pathways that related to the changes gene expression was identified and the specific genes and their Log2 ratio according to the RNA-Seq data were shown in Table 4.8. All five genes showed down-regulated in THP-1 treated with E10, E30 and P30.

From the results in Chapter 3 and the analysis above, six genes *CCL2*, *CXCL10*, *CXCL13*, *TNFSF10*, *IL6*, *and TNF-α* related to inflammation and AD were chosen to confirm gene expression analysis using RT-qPCR.

Figure 4.11 The cytokine-cytokine receptor interaction KEGG chart with log 2 FC values of THP-1 with LPS vs E10 with LPS. Upregulated genes show in red and downregulated in green.

Figure 4.12 The cytokine-cytokine receptor interaction KEGG chart with log 2 FC values of THP-1 with LPS vs E30 with LPS.

Upregulated genes show in red and downregulated in green.
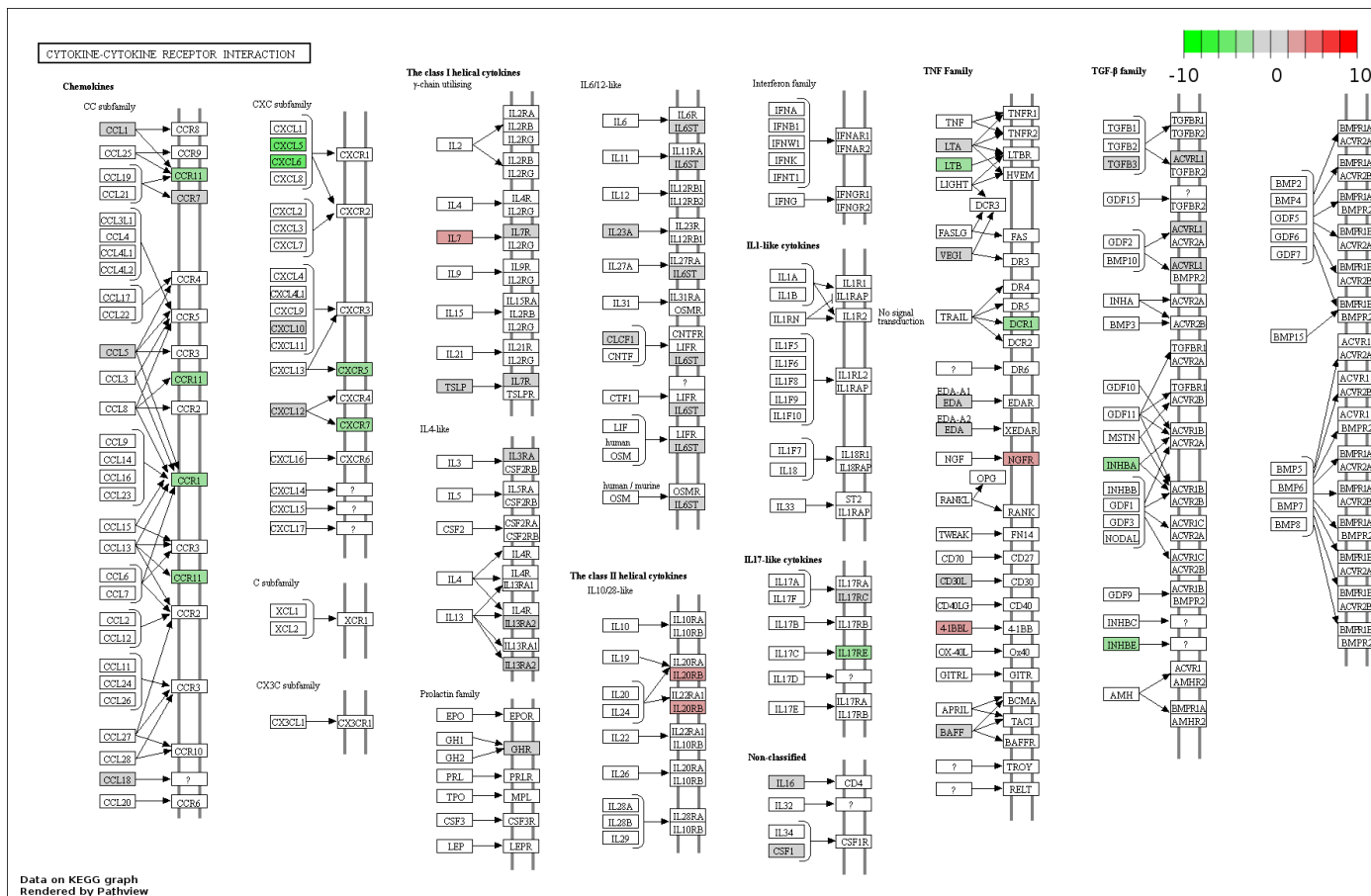
Figure 4.13 The cytokine-cytokine receptor interaction KEGG chart with log 2 FC values of THP-1 with LPS vs P30 with LPS. Upregulated genes show in red and downregulated in green.

Table 4.8 The details of selected gene and pathway enrichment in the clusters of THP-1 cell treated with E10, E30 and P30.

Genes	Log$_2$ Fold change			Related function (GO term/KEGG)
	E10	E30	P30	
CCL2	-1.41076	-3.29392	-3.29392	Glycosaminoglycan binding CCR chemokine receptor binding Cytokine activity Kinase activity
CXCL10	-3.42336	-4.54006	-5.57921	Cytokine activity Protein kinase regular activity
CXCL13	-2.45943	-7.82564	-8.02564	CXCR chemokine receptor binding Glycosaminoglycan binding

				CCR chemokine receptor binding
				Cytokine
TNFSF10	-2.11662	-4.10831	-4.61973	Cation binding
				Tumor necrosis factor receptor superfamily binding
				Tumor necrosis factor receptor
IL6	-3.6477	-5.38466	-5.74723	Cytokine receptor binding

4.3.2.2 Stability of candidate reference genes

Three candidate reference genes were selected to be screened for their suitability in RT-qPCR relative gene expression analysis for this study. RefFinder was used to examine and rank the expression stability of the candidate reference genes in the control and extract-treated samples. The most stable reference gene out of the three was *PP1B* whereas *RPL37A* was the least stable (Figure 4.14). Reliable relative gene expression analysis is dependent on the selection of a good, invariant normalising gene, thus *PP1B* was used as the reference gene in this study.
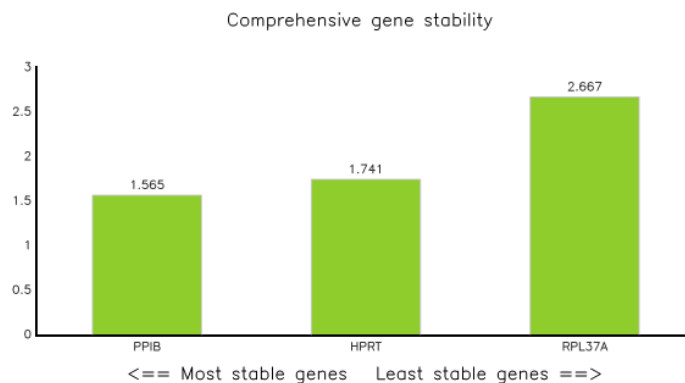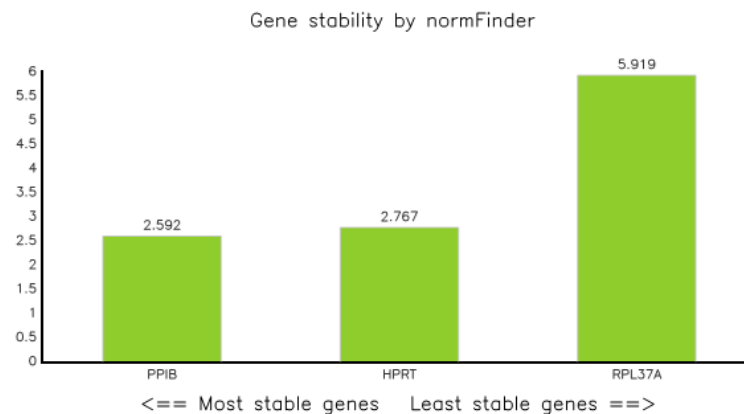
Figure 4.14 Stability of Reference Genes using RefFinder

4.3.2.3 Gene Expression analysis

RT-qPCR was carried out on six target genes which were selected from the RNA-Seq results. Melting curve analysis (MCA) is a simple way to check real-time PCR reactions for primer-dimer artifacts and to ensure reaction specificity. The different PCR products can be distinguished by their melting characteristics because the melting temperature of nucleic acids is affected by length, GC content, and presence of base mismatches. All samples were tested with (RT+), without (RT-) reverse transcriptase and a no-template control (NTC). No amplification was observed in NTC and RT-, thus there were no genomic DNA contamination from the reaction or reaction components and no false positive signals affecting the results. In the MCA of NTC samples (Figure 4.15) and RT- samples (Figure 4.16), there were no sharp single peaks generated by any of the primers indicating that they were not contaminated with genomic DNA and would not produce false positive PCR amplicons. All samples RT+ showed single sharp peaks on the MCA as shown in Figure 4.17-4.22 indicating that the designed primers were specific and selective to their target genes of interest.
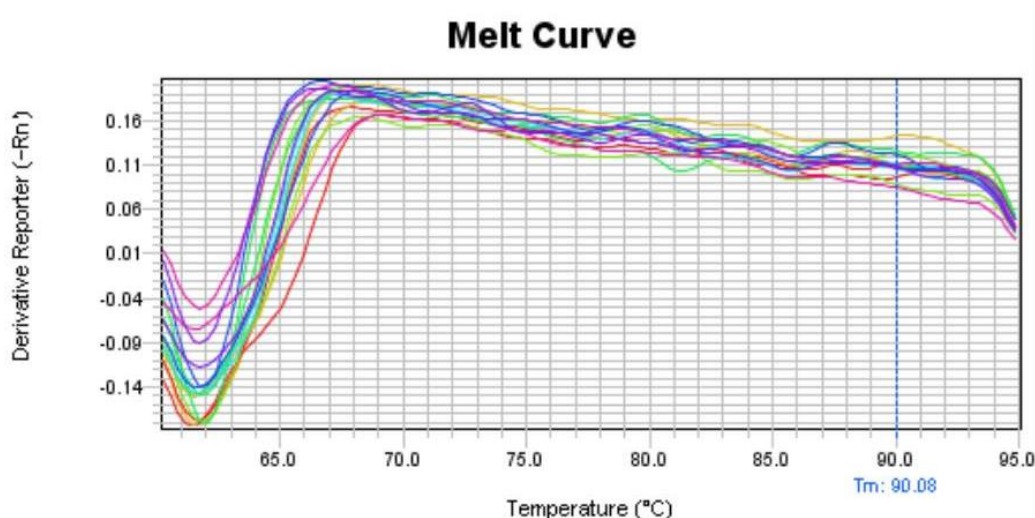
Figure 4.15 MCA of RT-qPCR products of NCT from *CCL2*, *CXCL10*, *CXCL13*, *IL6*, *TNF-α* and *TNFSF10*. Curves are representative of NTC samples in the RT-qPCR assay analyses.
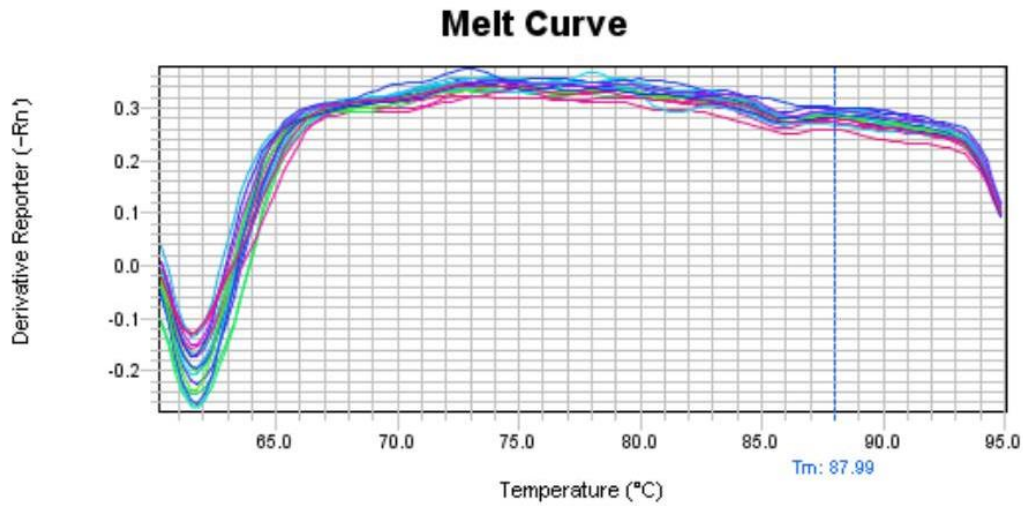
Figure 4.16 MCA of RT-qPCR products of RT- from *CCL2*, *CXCL10*, *CXCL13*, *IL6*, *TNF-α* and *TNFSF10*. Curves are representative of RT- samples in the RT-qPCR assay analyses.
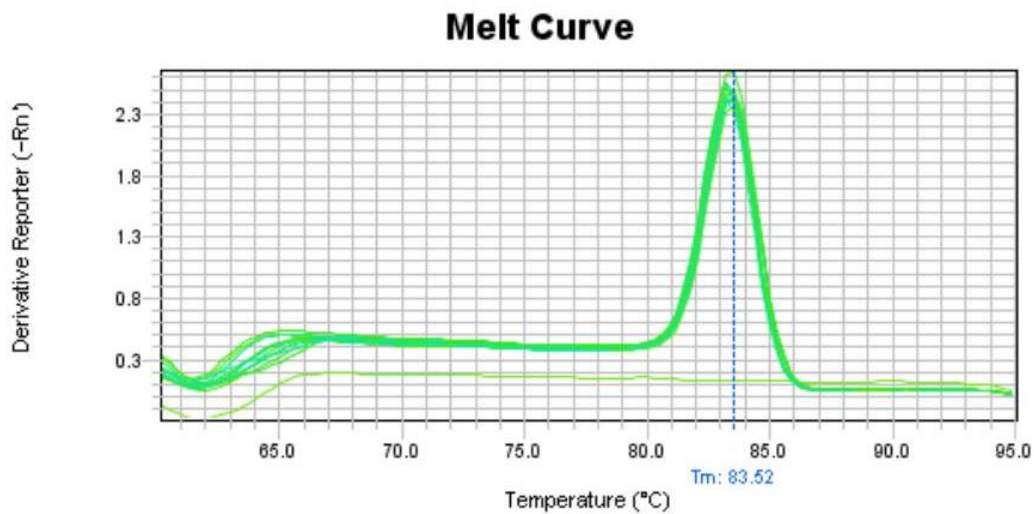
Figure 4.17 MCA of RT-qPCR products of RT+ from *CCL2* gene expression assay. Curves are representative of RT+ samples in the RT-qPCR assay analyses which produced single peaks in melt curve analyses.
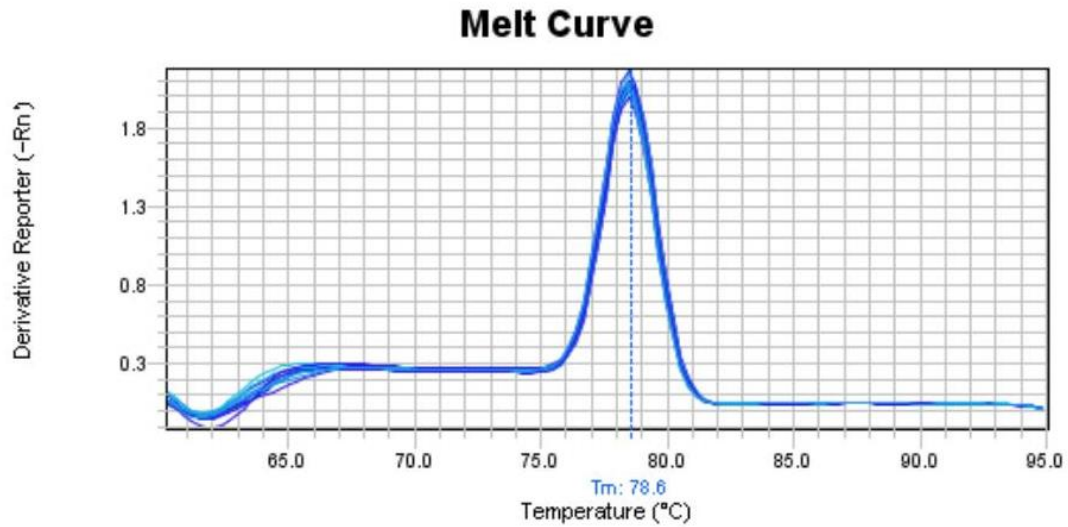
Figure 4.18 MCA of RT-qPCR products of RT+ from *CXCL10* gene expression assay. Curves are representative of RT+ samples in the RT-qPCR assay analyses which produced single peaks in melt curve analyses.
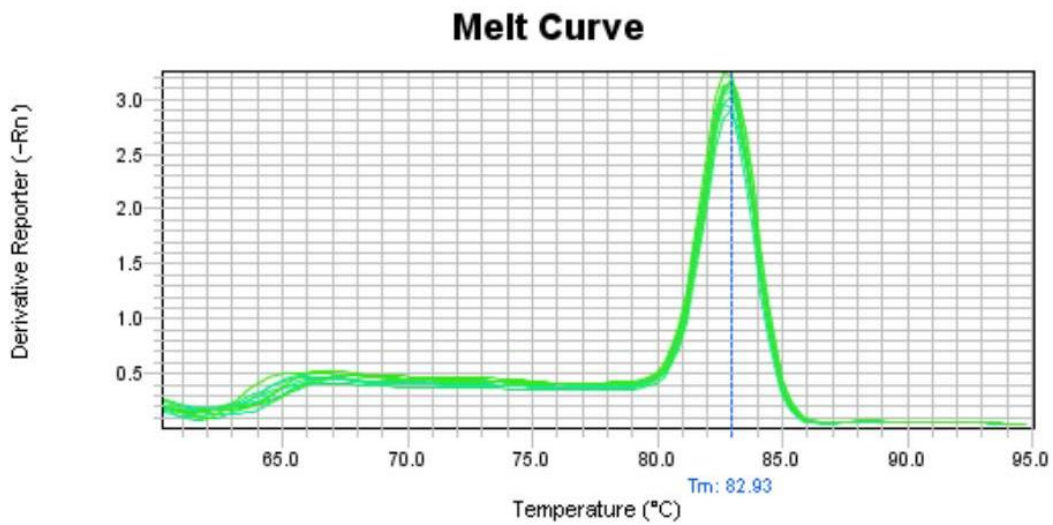
Figure 4.19 MCA of RT-qPCR products of RT+ from *CXCL13* gene expression assay. Curves are representative of RT+ samples in the RT-qPCR assay analyses which produced single peaks in melt curve analyses.
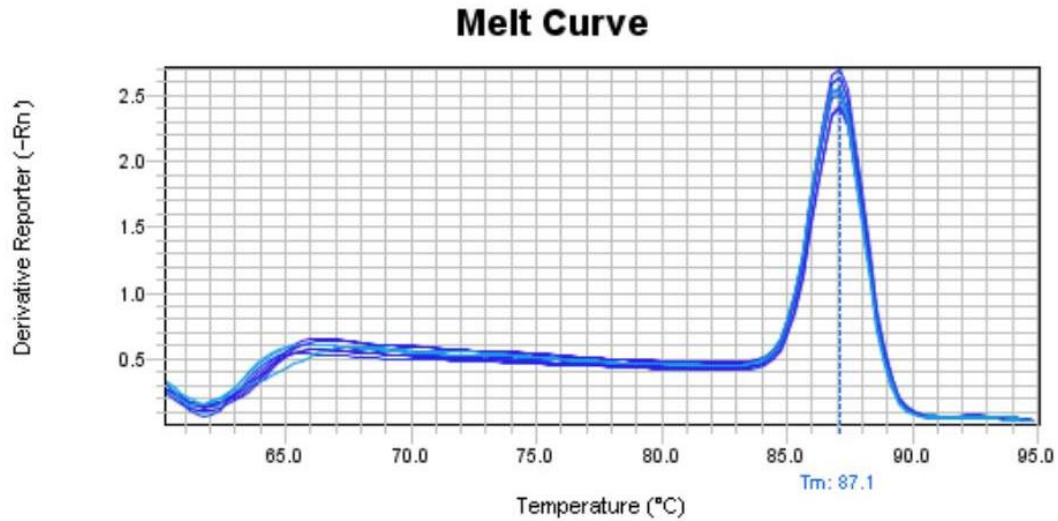
Figure 4.20 MCA of RT-qPCR products of RT+ from *IL6* gene expression assay.
Curves are representative of RT+ samples in the RT-qPCR assay analyses which produced single peaks in melt curve analyses.
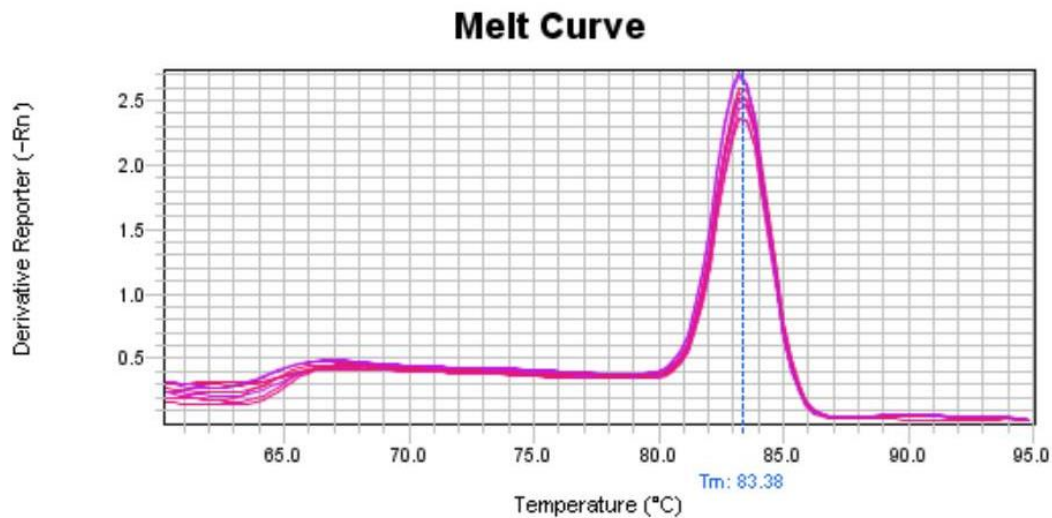
Figure 4.21 MCA of RT-qPCR products of RT+ from *TNF-α* gene expression assay.
Curves are representative of RT+ samples in the RT-qPCR assay analyses which produced single peaks in melt curve analyses.
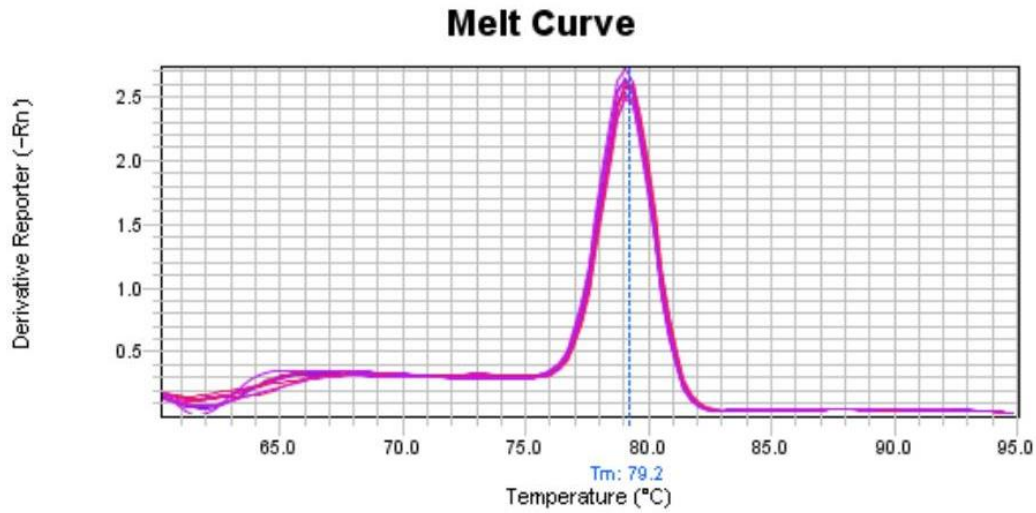
Figure 4.22 MCA of RT-qPCR products of RT+ from *TNFSF10* gene expression assay. Curves are representative of RT+ samples in the RT-qPCR assay analyses which produced single peaks in melt curve analyses.

PP1B was used as the reference gene in this study. The direction of gene expression change is shown in Figure 4.23. *TNF-α*, *IL6,* and *CCL2* were shown to be up-regulated in three samples around 1-2 fold and *CXCL13*, *CXCL10* and *TNFS10* were shown to be down-regulated around 1-2 fold.
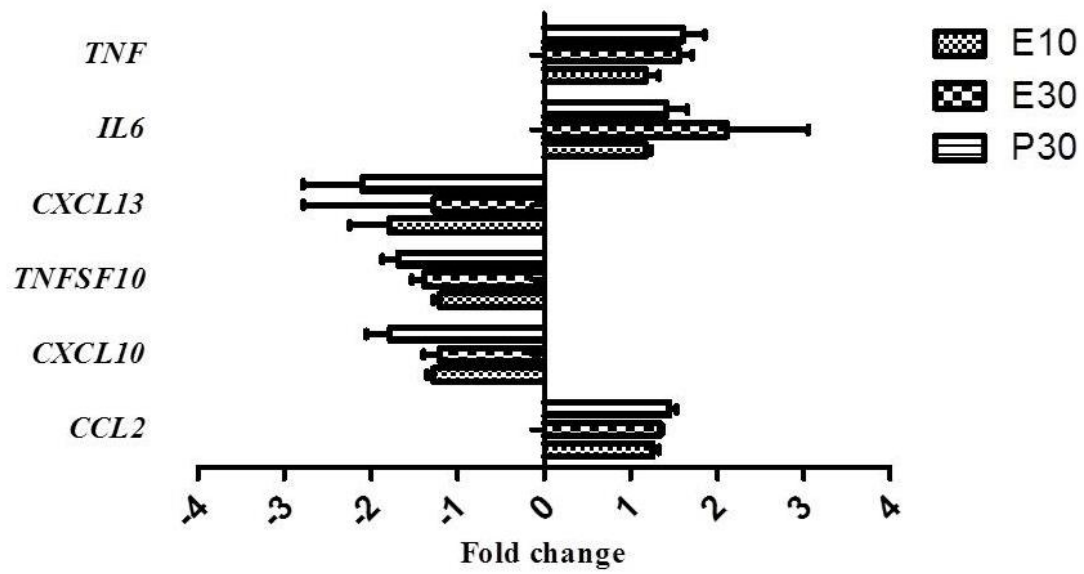
Figure 4.23 RT-qPCR relative gene expression changes (Fold change) of six target genes in three samples E10, E30, and P30 compared with control THP-1 cells. Data represents mean ± SEM. n=3.

4.3.2.4 THP-1 cytokines and chemokines release assay

The protein expression of the genes of interest that were chosen from RNA-Seq and RT-qPCR results were investigated using ELISA. The ELISA results for IL6, CXCL10, CCL2, TNFSF10 and CXCL13 are shown in Figures 4.24-4.28, respectively. No significant increase or decrease of cytokines and cheomokines release were observed in IL6, CCL2, TNFSF10 and CXCL13 production by E and P at all different concentrations (10 µg/ml and 30 µg/ml) compared with cells alone. Only CXCL10 showed a slight difference between the control and E and P (Figure 4.25).
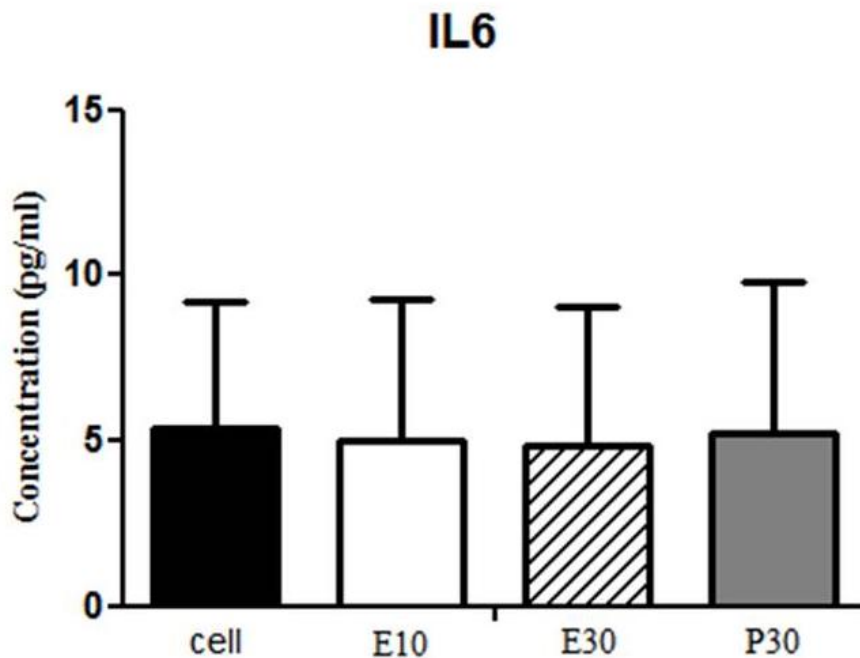
Figure 4.24 IL6 productions of P and E at different concentrations E10, E30 and P30 compared with THP-1 cell. Data represents mean ± SEM, n=3. Data was analysed using One-Way ANOVA with a Dunnett's Multiple Comparison Test.
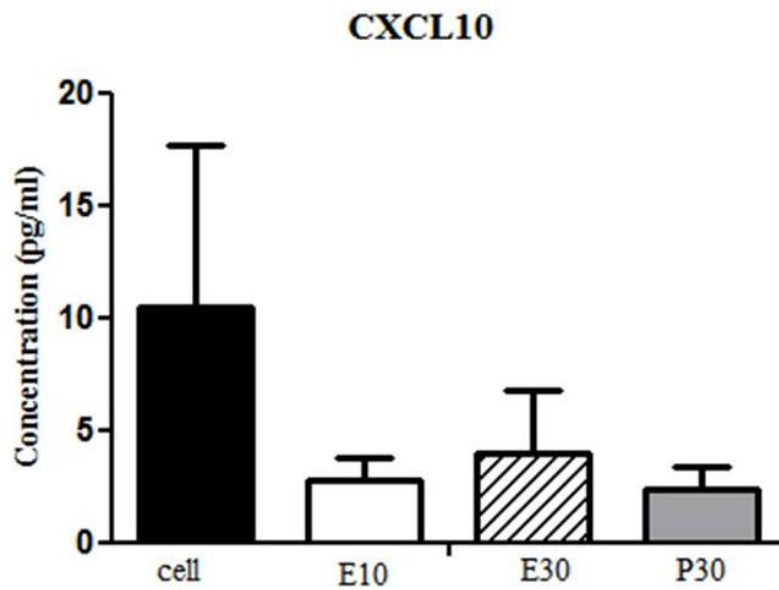
CXCL10

Figure 4.25 CXCL10 productions of P and E at different concentrations E10, E30 and P30 compared with THP-1 cell. Data represents mean ± SEM, n=3. Data analysed using One-Way ANOVA with a Dunnett's Multiple Comparison Test.
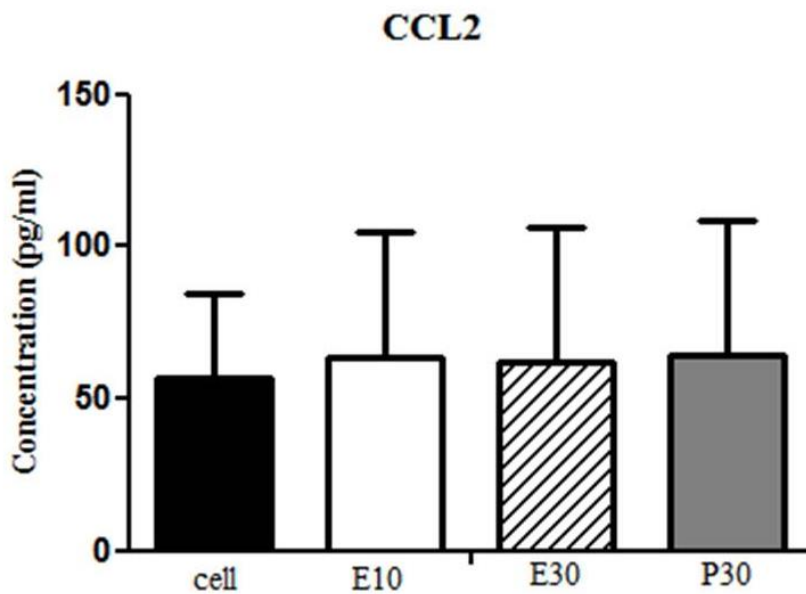
CCL2

Figure 4.26 CCL2 productions of P and E at different concentrations E10, E30 and P30 compared with THP-1 cell. Data represents mean ± SEM, n=3. Data analysed using One-Way ANOVA with a Dunnett's Multiple Comparison Test.
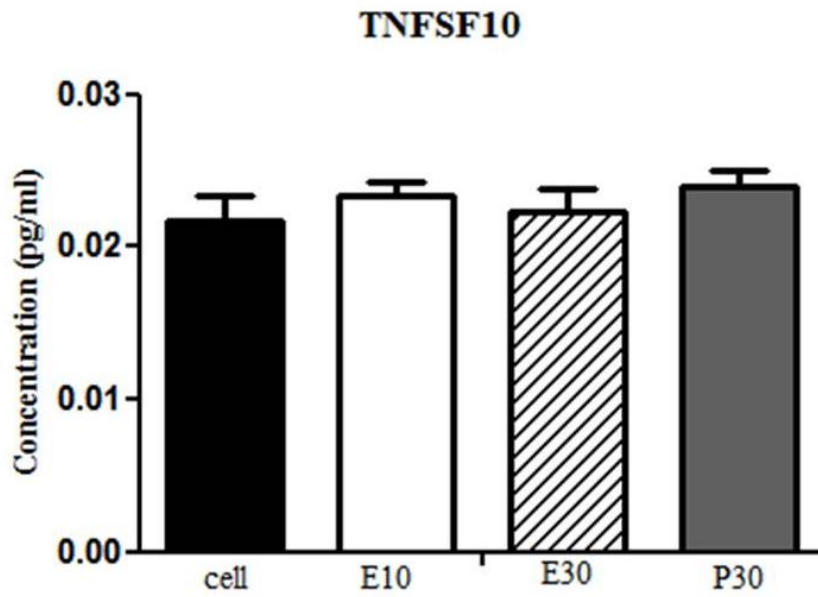
TNFSF10

Figure 4.27 TNFSF10 productions of P and E at different concentrations E10, E30 and P30 compared with THP-1 cell. Data represents mean ± SEM, n=3. Data analysed using One-Way ANOVA with a Dunnett's Multiple Comparison Test.
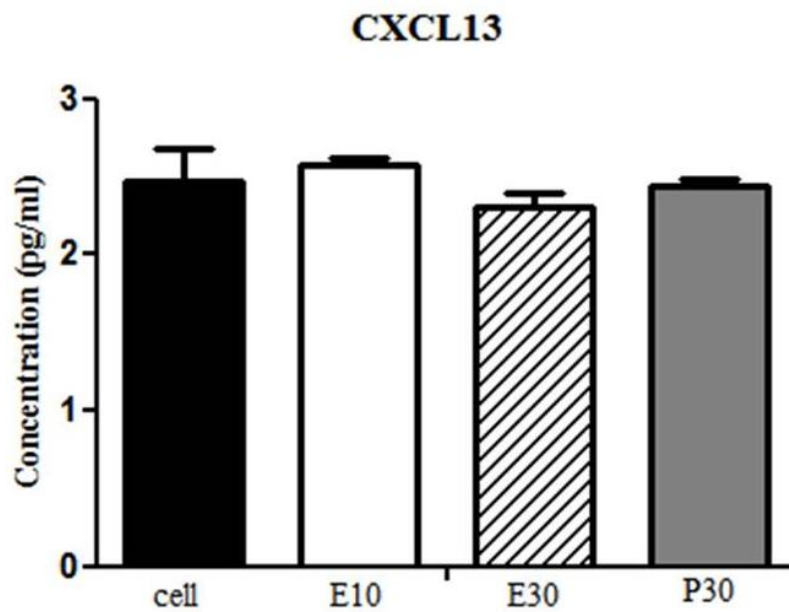
CXCL13

Figure 4.28 CXCL13 productions of P and E at different concentrations E10, E30 and P30 compared with THP-1 cell. Data represents mean ± SEM, n=3. Data analysed using One-Way ANOVA with a Dunnett's Multiple Comparison Test.

4.3.2.3.1 Comparison of gene expression determined by RNA-Seq data with the relative gene expression (2^$^{-\Delta\Delta CT}$) and with protein expression determined by ELISA

Validation of the RNA-Seq data was conducted using RT-qPCR. RNA-Seq data showed down-regulation in all genes (Table 4.9), but only *CXCL10*, *CXCL13* and *TNFSF10* genes were down-regulated as determined by RT-qPCR, which was the same as the RNA-Seq analysis. *CCL2*, *IL6* and *TNF-α* expression was up-regulated which was the opposite to the RNA-Seq data. According to the ELISA result, only *TNF-α* and *CXCL10* were down-regulated, which was the same as the RNA-Seq data, but there was no change in expression of *CCL2*, *CXCL13*, *IL6* and *TNFSF10*.

Table 4.9 Comparison of THP-1 cell gene expression determined by RNA-Seq data with RT-qPCR relative gene expression ($2^{-\Delta\Delta CT}$) data and with protein expression determined by ELISA.

Gene/Protein	RNA-Seq			RT-qPCR			ELISA		
	E10	**E30**	**P30**	**E10**	**E30**	**P30**	**E10**	**E30**	**P30**
CCL2	ND	↓	↓	⇧	⇧	⇧	-	-	-
CXCL10	↓	↓	↓	↓	↓	↓	↓	↓	↓
CXCL13	↓	↓	↓	↓	↓	↓	-	-	-
IL6	↓	↓	↓	⇧	⇧	⇧	-	-	-
TNF- α	ND	ND	ND	⇧	⇧	⇧	↓	↓	↓
TNFSF10	↓	↓	↓	↓	↓	↓	-	-	-

ND: no data

- : no change

⇧ : up regulated

↓ : down regulated

4.4 Discussion

RNA-Seq is a high throughput technique that is used to analyse gene expression of biological objects under specific conditions and have become the gold standard for in depth characterization of novel transcript isotherm in tissue samples (Manchon *et al*., 2017). Therefore RNA-Seq was used in this study in order to examine the transcriptome of THP-1 cells treated with pure compound (7-methoxydole-3-carboxylic acid methyl ester) extracted from *P. everhartii* (E) and purchased (P). The isolated RNA samples showed RQI of 9 which indicated the high quality of the RNA samples.   Following the results obtained from the biological activity studies in Chapter 3, RNA-Seq was carried out. The RNA-Seq data revealed a number of key inflammatory pathways associated with disease pathologies affected by each treatment. The cytokine-cytokine receptor interaction pathway was the only pathway that was differentially affected by the E30 and P30 treatments with up-regulation and down-regulation. Six genes from this cytokine-cytokine receptor interaction pathway associated with inflammation and AD genes that were chosen for further investigation by RT-qPCR and ELISA.

THP-1 cells were used as the *in vitro* model cell system in this study. Chanput *et al*. (2014) reviewed that THP-1 cells have been widely used as an *in vitro* model of human macrophages in mechanism studies of inflammatory disease and gene expression of THP-1 macrophages appeared to be at a maximum after 6 h. In this study, there were two substances on trial: E10 µg/ml and E30 µg/ml; P30 µg/ml and the incubation time of treatment was 24 h. *CXCL10, CXCL13* and *TNFSF10* were down-regulated for all the techniques used (RNA-Seq, RT-qPCR, and ELISA), but *CCL2*, *TNFSF10* and *TNF-α* demonstrated different expression responses to the compounds between RNA-Seq data, RT-qPCR, and ELISA (Table 4.16). Mismatches between RNA-Seq and RT-qPCR has been observed; Taylor, *et al*. (2017) mentioned that when comparing changes in protein levels with changes in transcriptional levels, not all changes were concordant with the utility of a 'multi-omics' approach to further elucidate the mechanism behind complex biological responses. Cheng *et al*. (2007) studied the effect of the collection time point on gene

expression of *G. lucidum* polysaccharide in THP-1 cells using microarray and qPCR, and found that different time points showed differing effects on gene expression. The Taylor, *et al*. (2017) review might relate to this study in that the results from RNA-Seq, RT-qPCR and ELISA showed opposite findings. In addition, Fassbinder-orth, (2014) reviewed that three additional sources of variation exist in studies of gene expression: technical variation which occurs after collection of samples, biological variation which is due to difference in gene expression within an organism, or difference among individuals in a population or among species, and environmental variation. Therefore, these might be the cause of opposing results in each method.

4.4.1 Effect of P and E on *TNF-α*

No *TNF-α* gene showed in DEGs list from RNA-Seq, however the biological results from Chapter 3 showed anti-inflammatory activity of sample P and E so the *TNF-α* gene was investigated for anti-inflammatory properties using RT-qPCR and ELISA techniques. The *TNF-α* gene showed up-regulation by RT-qPCR and down-regulation by ELISA. In this study, the incubation time with treated samples was only 24 h which may be the reason that the result from RT-qPCR and ELISA were different. Chanput *et al*. (2014) mentioned that gene expression of THP-1 macrophages appeared to be maximum after 6 h so the collection time point should be studied in further experiments. However the mechanism behind such a complex biological response might be a factor for differences in direction of the results obtained between RT-qPCR and ELISA techniques. Berti *et al*. (2002) mentioned that the peak level of TNF-α mRNA was observed at the 6 h time point. The expression levels of IL-8, ICAM-1, IP-10, MCP-1, TNF-α and MMP-1 were significantly reduced after phosphatidylcholine (PC) pre-treatment for at least 2 h (Treede *et al*., 2009). All these findings support the sampling time of treatment may affect the detected expression level of TNF-α. Polysaccharide extracts from the medicinal mushroom *C. militaris* showed anti-inflammatory effects at 50 μg/ml by inhibiting mRNA expression levels of *IL-1β*, *TNF-α* and *COX2* after incubation for 3

h with THP-1 cells (Smiderle *et al*., 2014). The ELISA result in this study showed a down-regulation of TNF-α that correlated with a number of studies reporting a decrease of TNF-α. Maxia *et al*. (2011) mentioned that a decrease of TNF-α and IL6 levels in a rat paw oedoma assay by *Pistacia lentiscus* oil may be useful in treatment of inflammatory conditions. Triterpene extract from the medicinal mushroom *G. lucidum* (GLT) supressed the inflammatory response in LPS-dependent secretion of TNF-α, IL6, NO and prostaglandin E2 (PGE$_2$) from murine RAW 264.7 macrophages (Dudhgaonkar *et al*., 2009). Dichloromethane extract of *Auricularia auricula-judae* markedly reduced the expressions of inflammatory cytokines (IL-6, TNF-α and IL-1β) mRNA in LPS-treated RAW 264.7 macrophages at concentrations of 10, 30, 100, and 300 μg/ml at 24 h (Damte *et al*., 2011). As mentioned earlier, the RT-qPCR analysis of P and E effects on THP-1 cell gene expression showed *TNF-α* up-regulation while the ELISA study in Chapter 3 showed down-regulation of TNF-α. Further investigation of these compounds would benefit from time-response gene expression and ELISA studies to improve understanding of their mechanism of action on these cells.

4.4.2 Effect of P and E on *TNFSF10*

TNFSF10 (TRAIL) is a member of the TNF superfamily of cytokines that is involved in different kinds of inflammatory responses (Zaba *et al*., 2010). TNFSF10 is not detectable in healthy human brain; its expression is upregulated in several neurodegenerative diseases including AD (Cantarella *et al*., 2015). RNA-Seq and RT-qPCR results indicated that all treatments showed down-regulated *TNFSF10* expression, however there were no changes observed in the ELISA experiments. Choi (2013) indicated that an extract from the root bark *Moutan Cortex Radicis* (MCR), can inhibit the up-regulation of *Tnfsf10* by LPS stimulation in cultured human gingival fibroblasts (HGFs). Brazilian red propolis (BRP) showed anti-inflammatory properties by inhibiting genes that activate NF-κB and MAPK pathways such as *Mapk1*, *Il1b*, *Tnfsf10*, and *Txn1* in LPS activated peritoneal

macrophages at a concentration of 60 μg/ml (Bueno-silva *et al.*, 2017). Neutralisation of TNFSF10 improved and controlled immune/inflammatory responses in the brain of 3xTg-AD mice that was a potential target for efficacious treatment of amyloid related disorders (Cantarella *et al.*, 2015). These parallels suggest that P and E are acting like other ant-inflammatory and potential anti-Alzheimer agents.

4.4.3 Effect of P and E on *CXCL10*

CXCL10 was originally identified as a proinflammatory chemokine mediating leukocyte trafficking and *Cxcl10* mRNA and protein expression have been associated with pathogenesis of various infectious diseases, chronic inflammatory, and autoimmune diseases as well as cancer (M. Liu *et al.*, 2011). Following the treatment of activated THP-1 cells with P and E, *CXCL10* expression showed down-regulation in RNA-Seq data, RT-qPCR, and ELISA analysis. Takagi *et al.* (2014) reported that inflammation-related genes are *Ptx3*, *Il8*, *Il6*, *Cxcl10*, *Gbp1*, *Chrm3*, *Cxcl1*, *Il1r2*, *Ccl18*, and *Ccl13* and showed up-regulation. CXCL10 related to anti-inflammatory and human disease has been mentioned in many published papers. *Vitex trifolia* extract showed anti-inflammatory effects by the significant inhibition of *Ccl3* and *Cxcl10* mRNA production in LPS-stimulated RAW264.7 cells at 2500 mg/ml (Matsui *et al.*, 2012). EPZ-6438 is a small molecule which is used for inhibiting EZH2 (Enhancer of Zeste Homolog 2) that plays a role in inflammation and significantly suppressed the expression of key LPS-inducible inflammation and immunity-related genes, including *Ccl3*, *Ccl4*, *Ccl8*, *Ccl12*, *Cxcl2*, *Cxcl10*, *Tnf-α*, *Irg1* and *Setdb2* in mice (Arifuzzaman *et al.*, 2017). An azaphenothiazine derivative, 6-chloroethylureidoethyldiquino [3,2-b;2',3'-e][1,4]thiazine(DQT) inhibited the

expression of CXCL10 at the protein level in mouse models. Gonomycin isolated from fermentations of the basidiomycete *G. applanatum* reduced LPS/IFN-γ induced CXCL10 protein synthesis and excretion (Jung *et al*., 2011). Antroquinonol significantly attenuated histopathologic changes in mouse skin and inhibited the infiltration of CD8$^+$ T cells and expression of chemokines CXCL10 and CXCR3 (Guan *et al*., 2017). Therefore, down-regulation of *CXCL10* by P and E suggests that this compound could be considered for development of potential anti-inflammatory and anti-Alzheimers treatment in the future.

In addition, CXCL10 represents a potential pharmacologic target for other human diseases such as infectious diseases and cancer. BXL-01-0029 is a prodrug of BXL-2198 that was used for immunosuppressive activity and reported to decrease the expression of CXCL10 in human renal tubular cells and reduce kidney allograft rejection (Liu *et al*., 2011). Michlmayr & McKimmie (2014) found that CXCL10 can mediate leukocyte influx in a variety of inflammatory CNS diseases (such as AD) as shown in Figure 4.18 and could be a potential drug target to block functional CXCL10 in these diseases. M. Liu *et al*. (2011) reviewed that CXCL10 is recognised as a biomarker that predicts severity of various diseases. CXCL10 has been reported in higher levels in patients with IBD and associated with inflammatory disease therefore CXCL10 might be an attractive target for the development of new therapeutics against various inflammatory conditions (Jung *et al*., 2011). In this study THP-1 cells treated with P and E samples showed down-regulation of *CXCL10* in

RNA-Seq, RT-qPCR and ELISA so it may be good starting point for further study to use in anti-inflammatory and anti-Alzheimers treatment.
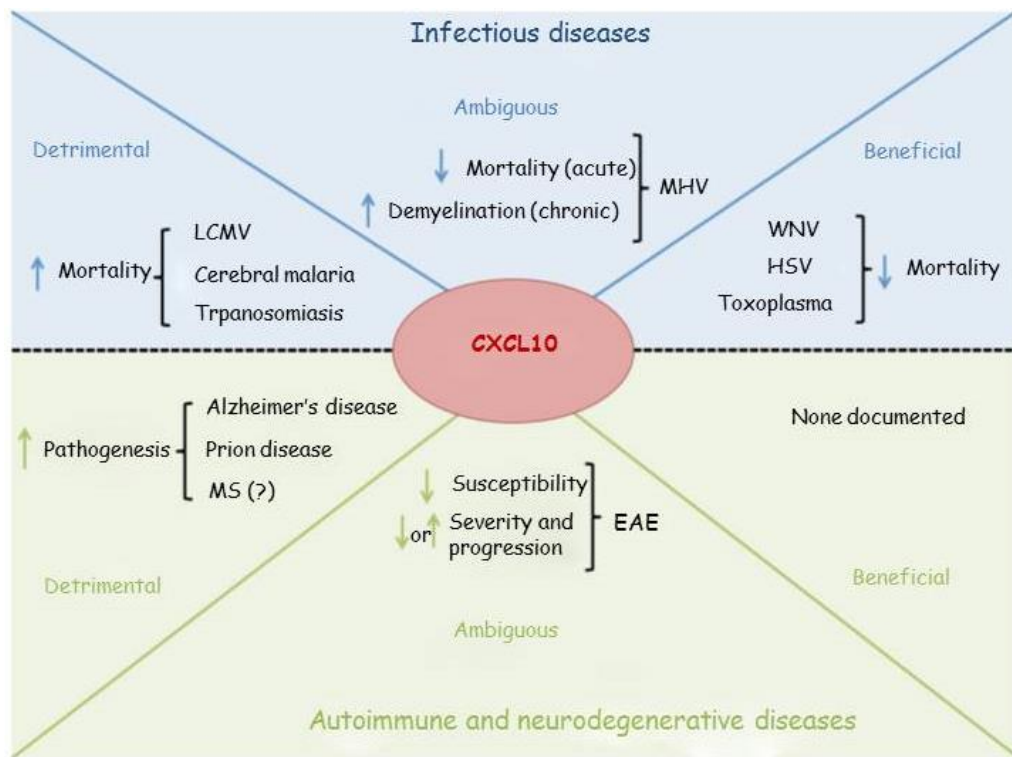
Figure 4.29 CXCL10 function can be either beneficial or detrimental to the host depending on the disease and context (Michlmayr & McKimmie, 2014).

Abbreviations: EAE, experimental autoimmune encephalomyelitis; MS, multiple sclerosis; MHV, mouse hepatitis virus; LCMV, lymphocytic choriomeningitis virus; WNV, West Nile virus; HSV, herpes simplex virus.

4.4.4 Effect of P and E on *CXCL13*

CXCL13 is chemotactic for B cells, which is produced in ectopic lymphoid follicles in the pathogenesis of MS and neuromyelitis optica (NMO) (Alvarez *et al*., 2013). The RNA-Seq data and RT-qPCR indicated that *Cxcl13* was down-regulated in THP-1 cells treated with P and E. However, no changes in ELISA protein levels were observed. CXCL13 seems to be the major determinant for B cell recruitment to the CNS compartment in different neuroinflammatory diseases (Kowarik *et al*., 2012). Data & Kurth (2013) reported that one or more inflammatory disease markers consisting of CXCL9, CXCL10, CXCL11, CXCL13, CXCR3 and CXCR5. CXCL13 is associated with worse outcomes in MS patients and higher levels may help predict who will develop MS amongst those with clinically isolated demyelinating syndromes (Alvarez *et al*., 2013). According to the result from RNA-Seq data and RT-qPCR indicated that P and E showed down-regulation; it may be helpful for AD treatment as CXCL13 is a potential pharmacologic target for the disease.

4.4.5 Effect of P and E on *CCL2*

CCL2 is a pro-inflammatory chemokine that is a potential intervention point for the treatment of various inflammatory and autoimmune diseases. In this study, *CCL2* showed down-regulation from RNA-Seq data and up-regulation from RT-qPCR in THP-1 cells treated with P and E. Takei *et al*. (2006) reported that glycyrrhizin (GL) has the capacity to suppress systemic inflammatory response syndrome (SIRS) associated with an anti-inflammatory response manifestation through the inhibition of CCL2 production by polymorphonuclear neutrophils (PMN). Latil *et al*., (2012) found that a hexanic lipidosterolic extract of *Serenoa repens* (hexanic LSESr)

reduced the expression of two key inflammatory mediators, *Mcp-1*/*Ccl2* mRNA levels in both epithelial (BPH-1) and myofibroblastic (WPMY-1) prostate cell lines. Westin *et al*. (2012) found that elevated CCL2-signaling in the brain might exacerbate the progression rate of AD-related pathology during pre-dementia stages. Ansari *et al*. (2011) reviewed that CCL2 can be induced during several human acute and chronic viral infections and could be an anti-inflammatory target in the treatment of HIV-1 infection. All of these findings support that *CCL2* is the chemokine that correlated with AD and inflammation and the RNA-Seq showed down-regulation so requires more study. However, the result in this study showed the opposite result that may happen from the mechanism behind complex biological responses as mentioned at the beginning.

4.4.6 Effect of P and E on *IL6*

IL6 is a pleiotropic cytokine and demonstrated to be a multifunctional cytokine that regulates numerous biological processes including organ development, acute-phase responses, inflammation, and immune responses (H. Su *et al*., 2017). In this study, *IL6* was down-regulated in RNA-Seq data and up-regulated in RT-qPCR and no change in ELISA. The triterpene extract from *G. lucidum* (GLT) suppressed the secretion of inflammatory cytokines TNF-α and IL-6, and inflammatory mediators NO and PGE2 from LPS-stimulated RAW264.7 cells (Dudhgaonkar *et al*., 2009). A protein (PEP) from *Pleurotus eryngii*, exhibited an anti-inflammatory effect on LPS-stimulated RAW264.7 macrophages by inhibiting the overproduction of IL-1β, TNFα, and COX2 (Yuan *et al*., 2017). Chlorojanerin isolated from *Saussurea heteromalla* was shown to be significantly effective in inhibiting TNF-α and IL-6 production in LPS-stimulated THP-1 cells (IC50 = 2.3 ± 0.2 μM and 1.8 ± 0.7 μM, respectively) and inhibited LPS-induced mRNA transcription of NF-κB dependent genes for *Tnfsf10*, *Il6*, *Tnf-α*, *Irf1*, *Ptgs2*, *Bcl-2*, *Il-18*, and *Nfκb1a* which can be developed into better therapeutic molecules targeted towards some specific inflammatory diseases (Saklani *et al*., 2012). All these findings support that

inhibition of IL6 can be used for inflammatory disease treatment. In this study *IL6* revealed conflicting gene expression results between the two techniques used, exhibiting down-regulation in RNA-Seq, but up-regulation in RT-qPCR. Due to limitation of time, it would be appropriate to repeat the anti-inflammatory activity in the future. Moro *et al*. (2012) reported that results obtained with the same extract from different assays, could be mediated by the selective inhibition of different upstream factors in macrophage activation by LPS.

In conclusion, RNA-Seq, RT-qPCR and ELISA findings from THP-1 macrophages stimulated with LPS showed that purified sample P and E may have potential for anti-inflammatory and anti-Alzheimers activities. There are no published scientific reports of the effects of pure compound 7-methoxyindole-3-carboxylic acid methyl ester on gene expression in THP-1 cells. *CCL2*, *CXCL10*, *CXCL13*, *IL6,* and *TNFSF10* have roles in inflammatory diseases and AD. These genes showed down-regulation in RNA-Seq and TNF-α were decreased from biological activity result (Chapter3) in both P and E. This compound appears to be an attractive one to consider further investigation as an inflammatory and anti-Alzheimers agent due to its inhibitory action on *CXCL10*, *CXCL13* and *TNFSF10* gene expression in RT-qPCR and decreased *CCL2*, *IL6* expression in RNA-Seq including inhibition of TNF-α in ELISA. The occasional conflicting results obtained from gene and protein expression techniques used in this study highlights the challenges faced in obtaining clarity in the mechanisms of action of drugs on cells. The correlation between the processes behind complex biological responses as mentioned previously and the period of gene expression time and gene expression level changes may not exhibit temporal alignment with that of protein expression. Chanput *et al*. (2014) reviewed that gene expression of THP-1 macrophages appeared to be maximum after 6 h therefore the different collection time points of gene expression should be investigated in the future. Analysis of the RNA-Seq data analysis reveals a complex network of affected pathways and there is a massive amount of data that could be studied in the future such as acetylcholine receptor (*chrna* gene) in neuroactive ligand-receptor interaction (Appendix B): a pathway that was related to AD.

CHAPTER 5 Summary, Future Work and Conclusions

5.1 Summary

Three mushrooms were chosen for study in this project. According to the previous study carried out at TISTR, genus *Phellinus* had shown good biological activity and *F. cajanderi* can be cultivated in the laboratory so two species of *Phellinus* mushrooms (*P. everhartii* and *P. laevigatus*) and one of *F. cajanderi* were investigated. Soxhlet was used for extraction; column chromatography was used for purification of the compounds and NMR was used to identify the compounds E, an alkaloid compound was isolated for the first time from *P. everhartii*, while compound1 was isolated for the first time from *F. cajanderi* mushroom.

The biological activities (cytotoxicity, anti-microbial, anti-inflammatory and anti-Alzhiemers) of EtOH crude extract and purified compound P and E were examined. EtOH crude extract of *F. cajanderi* showed cytotoxicity against ovarian carcinoma (A2780), prostate carcinoma (LNCap) and breast carcinoma (ZR75-1) at IC50 149.70 µg/ml, 125.60 µg/ml and more than 150 µg/ml, respectively. EtOH crude extract from *P. everhartii* and *P. laevigatus* showed cytotoxicity against LNCap at IC50 80.46 µg/ml and 125.90 µg/ml and ZR75-1 at IC50 more than 150 µg/ml. EtOH crude extract of *F. cajanderi* showed antimicrobial activity against three gram-positive bacteria (*B. subtillis*, *S. aureus*, *and L. monocytogenes*) and one gram-negative strain (*P. aeruginosa*) at 1 mg/ml. Three crude extracts from mushroom *F. cajanderi*, *P. everhartii* and *P. laevigatus* showed the anti-inflammatory activity in THP-1 cell at concentration 31.25µg/ml, 7.81µg/ml and 1.76µg/ml. This study suggests a potential use of EtOH crude extract of *F. cajanderi* as a source of anticancer activity for ovarian, prostate, breast cancers, and antimicrobial and anti-inflammatory activity. *P. everhartii* and *P. laevigatus* could be used for anticancer treatment of prostate and breast cancers and as an anti-inflammatory agent. However the purified compound of EtOH crude extracts from *P. everhartii*, *P. laevigatus* and *F. cajanderi* should be isolated and purified and the activity evaluated again.

The pure compounds P and E were studied for anti-inflammatory properties using three different methods. P and E both showed significant anti-inflammatory activity at 20 µg/ml and 30 µg/ml in THP-1 cells and in NCTC cells at 30 µg/ml. However, in L929 cells the percentage of the highest protection was slightly lowered around 30% at 10 µg/ml.

Anti-Alzheimer activity was investigated using AChE inhibitory activity and a neuroprotectivity assay. The result showed that the highest percentage of AChE inhibitory activity was 70% observed at 150 µg/ml for P and E and the highest protective percentage against H_2O_2 in SHSY5Y cells was around 40% at 50 µg/ml after 24 h for both sample P and E. However the AChE inhibitory activity showed an inhibitory percentage less than the positive control so P and E would not be good candidates for AD treatment.

P and E were then investigated by RNA-Seq and RT-qPCR to examine any gene expression changes and ELISA was used to confirm the result. RNA-seq data found that the cytokine-cytokine receptor interaction pathway was affected in almost treatment samples. Six genes (*Ccl2*, *Cxcl10*, *Cxcl13*, *Tnfsf10*, *Il6*, *and Tnf-α*) from RNA-seq analysis and the result from Chapter 3 were chosen for validation by RT-qPCR and ELISA. All six genes showed down-regulation in all samples with a 1 to 8 log 2-fold change. RT-qPCR showed that *TNFα*, *IL6* and *CCL2* were up-regulated in three samples (E10, E30 and P30) with 1-2 fold and *CXCL13*, *CXCL10* and *TNFS10* were down-regulated 1-2 fold.

The purified compound 7-methoxyindole-3-carboxylic acid methyl ester by extraction (E) and purchased (P) showed identical results and biological activity was similar but only E showed slightly higher than P in the neuroprotective activity.

This suggests that 7-methoxyindole-3-carboxylic acid methyl ester may be developed for ant-inflammatory treatment in the future.

5.2 Future work

- Purification of crude extract from *F. cajanderi* and investigation of biological activity such as anti-cancer, anti-inflammatory and anti-microbial from pure compounds of *F. cajanderi*

- In this study only cytokine-cytokine receptor interaction pathway and only six genes were investigated therefore the different pathways and genes from the RNA-Seq result should be examined further.

- The different collection time points of the samples should be carried out to investigate gene expression using RT-qPCR.

- Only fruiting bodies of the mushrooms were used for extraction in this study, but the filamentous part should be cultivated in the laboratory and the biological activity studied too in order to support commercial development in the future.

- The safety of 7-methoxydole-3-carboxylic acid methyl that showed anti-inflammatory activity should be considered in *in vivo* studies before being investigated further.

5.3 Conclusion

The local people in North-East of Thailand believed that genus *Phellinus* and genus *Fomitopsis* can use the mushrooms for treatment by boiling and drinking the water and some finely grate and mould the material into a bolus and eat it like a tablet. In the previous study by TISTR, they found that mushrooms in the genus *Phellinus* had good biological properties and the genus *Fomitopsis* in its filamentous form can be stored in 15% glycerol at -80ºC and still be alive after 2 years. In the present study, the compounds from three mushrooms *P. everhartii*, *P. laevigatus* and *F. cajanderi* were extracted and biological activity evaluated.

The main findings of the study were:

- *F. cajanderi* showed cytotoxicity against ovarian carcinoma (A2780), prostate carcinoma (LNCap) and breast carcinoma (ZR75-1) at IC50 149.70 μg/ml, 125.60 μg/ml and more than 150 μg/ml, respectively.

- *F. cajanderi* showed antimicrobial activity against three gram-positive bacteria (*B. subtillis*, *S. aureus*, *and L. monocytogenes*) and one gram-negative strain (*P. aeruginosa*) at 1 mg/ml.

- *P. everhartii* and *P. laevigatus* showed cytotoxicity against LNCap at IC50 80.46 μg/ml and 125.90 μg/ml and ZR75-1 at IC50 more than 150 μg/ml, respectively.

- The crude extracts from mushroom *F. cajanderi*, *P. everhartii* and *P. laevigatus* showed the anti-inflammatory activity in THP-1 cell at concentration 31.25μg/ml, 7.81μg/ml and 1.76μg/ml.

- The pure compounds P and E showed significant anti-inflammatory activity at 20 μg/ml and 30 μg/ml in THP-1 cells.

- P and E decreased the percentage control of NFκB significantly ($P<0.05$) were approximately 55% and 75%, respectively at 30 μg/ml.

- P and E showed the percentage of protection L929 ($P<0.05$) from cytotoxic effects of 10 μg/ml TNF-α were around 10-30%.

- P and E showed the protective percentage against H2O2 in SHSY5Y cells was around 40% at 50 μg/ml

- RNA-Seq data found that the cytokine-cytokine receptor interaction pathway was affected in P and E sample.

- RT-qPCR showed that TNFα, IL6 and CCL2 were up-regulated in three samples (E10, E30 and P30) with 1-2 fold and CXCL13, CXCL10 and TNFS10 were down-regulated 1-2 fold.

This study was in response to the lack of scientific data on mushroom *P. everhartii*, *P. laevigatus* and *F. cajanderi* use by the local people. Therefore this research produced findings that the mushroom could be valuable sources of some new potential anti-inflammatory and anti-cancer treatment.

References

Akihisa, T., Nakamura, Y., Tagata, M., Tokuda, H., Yasukawa, K., Uchiyama, E., … Kimura, Y. (2007). Anti-inflammatory and anti-tumor-promoting effects of triterpene acids and sterols from the fungus Ganoderma lucidum. *Chemistry and Biodiversity*, *4*(2), 224–231. https://doi.org/10.1002/cbdv.200790027

Alvarez, E., Piccio, L., Mikesell, R. J., Klawiter, E. C., Parks, B. J., Naismith, R. T., & Cross, A. H. (2013). CXCL13 is a biomarker of inflammation in multiple sclerosis, neuromyelitis optica, and other neurological conditions. *Multiple Sclerosis Journal*, *19*(9), 1204–1208. https://doi.org/10.1177/1352458512473362

Ansari, A. W., Heiken, H., Meyer-Olson, D., & Schmidt, R. E. (2011). CCL2: A potential prognostic marker and target of anti-inflammatory strategy in HIV/AIDS pathogenesis. *European Journal of Immunology*, *41*(12), 3412–3418. https://doi.org/10.1002/eji.201141676

Arifuzzaman, S., Das, A., Kim, S. H., Yoon, T., Lee, Y. S., Jung, K. H., & Chai, Y. G. (2017). Selective inhibition of EZH2 by a small molecule inhibitor regulates microglial gene expression essential for inflammation. *Biochemical Pharmacology*, *137*, 61–80. https://doi.org/10.1016/j.bcp.2017.04.016

Azmir, J., Zaidul, I. S. M., Rahman, M. M., Sharif, K. M., Mohamed, A., Sahena, F., … Omar, A. K. M. (2013). Techniques for extraction of bioactive compounds from plant materials: A review. *Journal of Food Engineering*, *117*(4), 426–436. https://doi.org/10.1016/j.jfoodeng.2013.01.014

Balouiri, M., Sadiki, M., & Ibnsouda, S. K. (2016). Methods for in vitro evaluating antimicrobial activity : A review $. *Journal of Pharmaceutical Analysis*, *6*, 71–79. https://doi.org/10.1016/j.jpha.2015.11.005

Barbosa Filho, J. M., Medeiros, K. C. P., Diniz, M. D. F. F. M., Batista, L. M., Athayde-Filho, P. F., Silva, M. S., … Quintans-Júnior, L. J. (2006). Natural products inhibitors of the enzyme acetylcholinesterase. *Revista Brasileira de Farmacognosia*, *16*(2), 258–285. https://doi.org/10.1590/S0102-695X2006000200021

Berti, R., Williams, A. J., Moffett, J. R., Hale, S. L., Velarde, L. C., Elliott, P. J., … Tortella, F. C. (2002). Quantitative real-time RT–PCR analysis of inflammatory gene expression associated with ischemia – reperfusion brain injury. *Journal of Cerebral Blood Flow & Metabolism*, *22*(9), 1068–1079.

Bobek, P., Nosálová, V., & Cerná, S. (2001). Effect of pleuran (β-glucan from Pleurotus ostreatus) in diet or drinking fluid on colitis in rats. *Nahrung - Food*, *45*(5), 360–363. https://doi.org/10.1002/1521-3803(20011001)45:5<360::AID-FOOD360>3.0.CO;2-C

Boukes, G. J., Koekemoer, T. C., van de Venter, M., & Govender, S. (2017). Cytotoxicity of

thirteen South African macrofungal species against five cancer cell lines. *South African Journal of Botany*, *113*, 62–67. https://doi.org/10.1016/j.sajb.2017.07.010

Bradley, J. R. (2008). TNF-mediated inflammatory disease. *J Pathol*, *214*, 149–160. https://doi.org/10.1002/path

Bueno-silva, B., Kawamoto, D., Ando-suguimoto, E. S., Casarin, R. C. V, Alencar, S. M., Rosalen, P. L., & Mayer, M. P. A. (2017). Brazilian red propolis effects on peritoneal macrophage activity : Nitric oxide , cell viability , pro-inflammatory cytokines and gene expression. *Journal of Ethnopharmacology*, *207*(June), 100–107. https://doi.org/10.1016/j.jep.2017.06.015

Cantarella, G., Di Benedetto, G., Puzzo, D., Privitera, L., Loreto, C., Saccone, S., … Bernardini, R. (2015). Neutralization of TNFSF10 ameliorates functional outcome in a murine model of Alzheimer's disease. *Brain*, *138*(1), 203–216. https://doi.org/10.1093/brain/awu318

Carbonero, E. R., Gracher, A. H. P., Komura, D. L., Marcon, R., Freitas, C. S., Baggio, C. H., … Iacomini, M. (2008). Lentinus edodes heterogalactan: Antinociceptive and anti-inflammatory effects. *Food Chemistry*, *111*(3), 531–537. https://doi.org/10.1016/j.foodchem.2008.04.015

Cha, W., Ding, J., Shin, H., Kim, J., Kim, Y., Choi, D., … Lee, C. (2009). Effect of *Fomitopsis pinicola* extract on blood glucose and lipid metabolism in diabetic rats, *26*(6), 1696–1699. https://doi.org/10.1007/s11814-009-0340-2

Chairul, Tokuyama, T., Nishizawa, M., Shiro, M., Tokuda, H., & Hayashiji, Y. (1990). Malonate half-esters of homolanostanoid from an asian Ganoderma fungus. *Phytochemistry*, *29*(3), 923–928. https://doi.org/10.1016/0031-9422(90)80047-K

Chang, H.-Y., Huang, G.-J., Chang, Y.-S., Ho, Y.-L., Sheu, M.-J., Lin, Y.-H., … Wu, S.-H. (2007). Antioxidant and free radical scavenging activities of *Phellinus merrillii* extracts. *Botanical Studies*, *48*(4), 407–417.

Chanput, W., Mes, J. J., & Wichers, H. J. (2014). THP-1 cell line: An in vitro cell model for immune modulation approach. *International Immunopharmacology*, *23*(1), 37–45. https://doi.org/10.1016/j.intimp.2014.08.002

Chen, H., Zhang, J., Ren, J., Wang, W., & Xiong, W. (2018). Triterpenes and Meroterpenes with Neuroprotective Effects from Ganoderma leucocontextum. *Chem. Biodiversity*, *55*, 2–10. https://doi.org/10.1002/cbdv.201700567

Cheng, K. C., Huang, H. C., Chen, J. H., Hsu, J. W., Cheng, H. C., Ou, C. H., … Juan, H. F. (2007). *Ganoderma lucidum* polysaccharides in human monocytic leukemia cells: From gene expression to network construction. *BMC Genomics*, *8*, 1–17. https://doi.org/10.1186/1471-2164-8-411

Choi, C. Y. Y. (2013). Moutan Cortex Radicis inhibits inflammatory changes of gene expression in lipopolysaccharide-stimulated gingival fibroblasts, 576–589. https://doi.org/10.1007/s11418-012-0714-3

Damte, D., Reza, A., Lee, S., Jo, W., & Park, S. (2011). Anti-inflammatory activity of dichloromethane extract of *Auricularia auricula-judae* in RAW264 . 7 Cells. *Toxicol. Res.*, *27*(1), 11–14. https://doi.org/10.5487/TR.2011.27.1.011

Data, R. U. S. A., & Kurth, A. (2013). (12) United States Patent, *2*(12).

De Silva, D. D., Rapior, S., Fons, F., Bahkali, A. H., & Hyde, K. D. (2012). Medicinal mushrooms in supportive cancer therapies: An approach to anti-cancer effects and putative mechanisms of action. *Fungal Diversity*, *55*, 1–35. https://doi.org/10.1007/s13225-012-0151-3

Deshmane, S. L., Kremlev, S., Amini, S., & Sawaya, B. E. (2009). Monocyte chemoattractant protein-1 (MCP-1): An overview. *Journal of Interferon and Cytokine Research*, *29*(6), 313–325. https://doi.org/10.1089/jir.2008.0027

Deveci, E., Tel, G., Mehmet, Ç., Duru, E., & Öztürk, M. (2019). Chemical constituents of Porodaedalea pini mushroom with cytotoxic , antioxidant and anticholinesterase activities. *Journal of Food Measurement and Characterization*, *13*(4), 2686–2695. https://doi.org/10.1007/s11694-019-00189-2

Doña, I., Pérez-Sánchez, N., Eguiluz-Gracia, I., Muñoz-Cano, R., Bartra, J., Torres, M. J., & Cornejo-García, J. A. (2020). Progress in understanding hypersensitivity reactions to nonsteroidal anti-inflammatory drugs. *Allergy: European Journal of Allergy and Clinical Immunology*, *75*(3), 561–575. https://doi.org/10.1111/all.14032

DuBok Choi, Sang-Shin Park, Ji-Lu Ding, and W.-S. C. (2007). Effects of *Fomitopsis pinicola* extracts on antioxidant and antitumor activities. *Biotechnology and Bioprocess Engineering*, *12*, 516–524.

Dudhgaonkar, S., Thyagarajan, A., & Sliva, D. (2009). Suppression of the inflammatory response by triterpenes isolated from the mushroom *Ganoderma lucidum*. *International Immunopharmacology*, *9*(11), 1272–1280. https://doi.org/10.1016/j.intimp.2009.07.011

Eisen, M. B., Spellman, P. T., Brown, P. O., & Botstein, D. (1998). Cluster analysis and display of genome-wide expression patterns. *Proceedings of the National Academy of Sciences of the United States of America*, *95*(25), 14863–14868. https://doi.org/10.1073/pnas.95.25.14863

El Enshasy, H. a, & Hatti-Kaul, R. (2013). Mushroom immunomodulators: unique molecules with unlimited applications. *Trends in Biotechnology*, *31*(12), 668–77. https://doi.org/10.1016/j.tibtech.2013.09.003

Elsayed, E. A., El Enshasy, H., Wadaan, M. A. M., & Aziz, R. (2014). Mushrooms: A potential natural source of anti-inflammatory compounds for medical applications. *Mediators of Inflammation*. https://doi.org/10.1155/2014/805841

Fangkrathok, N., Junlatat, J., & Sripanidkulchai, B. (2013). In vivo and in vitro anti-inflammatory activity of Lentinus polychrous extract. *Journal of Ethnopharmacology*, *147*(3), 631–637. https://doi.org/10.1016/j.jep.2013.03.055

Fassbinder-orth, C. A. (2014). Integrative and comparative biology methods for quantifying gene expression in ecoimmunology : from qPCR to RNA-Seq. *Integrative and Comparative Biology*, *54*(3), 396–406. https://doi.org/10.1093/icb/icu023

Feng, T., Cai, J., Li, X., Zhou, Z., Li, Z., & Liu, J. (2016). Chemical Constituents and Their Bioactivities of Mushroom Phellinus rhabarbarinus. *Journal of Agricultural and Food Chemistry*, *64*, 1945–1949. https://doi.org/10.1021/acs.jafc.6b00176

Filho, J. M. B., Medeiros, K. C. P., & Diniz, M. D. F. F. M. (2006). Natural products inhibitors of the enzyme acetylcholinesterase Revisão, *16*(2), 258–285.

Ge, Q., Mao, J. wei, Zhang, A. qiang, Wang, Y. jiang, & Sun, P. long. (2013). Purification, chemical characterization, and antioxidant activity of a polysaccharide from the fruiting bodies of sanghuang mushroom (*Phellinus baumii* Pilát). *Food Science and Biotechnology*, *22*(2), 301–307. https://doi.org/10.1007/s10068-013-0081-1

Greice, A., Leite, B., Tereza, E., Farias, N., & Paula, A. (2019). Phytochemical screening and antimicrobial activity testing of crude hydroalcoholic extract from leaves of Sphagneticola trilobata (Asteraceae).

Grienke, U., Zöll, M., Peintner, U., & Rollinger, J. M. (2014). European medicinal polypores--a modern view on traditional uses. *Journal of Ethnopharmacology*, *154*(3), 564–83. https://doi.org/10.1016/j.jep.2014.04.030

Grzywacz-kisielewska, A., Ka, K., & Gdula-argasi, J. (2018). Anti-inflammatory properties of edible mushrooms : A review. *Food Chemistry*, *243*(September 2017), 373–381. https://doi.org/10.1016/j.foodchem.2017.09.149

Guan, C., Li, Q., Song, X., Xu, W., Li, L., & Xu, A. (2017). Antroquinonol exerts immunosuppressive effect on CD8+ T cell proliferation and activation to resist depigmentation induced by H_2O_2. *Oxidative Medicine and Cellular Longevity*, *2017*. https://doi.org/10.1155/2017/9303054

Han, C., & Cui, B. (2012). Pharmacological and pharmacokinetic studies with agaricoglycerides, extracted from grifola frondosa, in animal models of pain and inflammation. *Inflammation*, *35*(4), 1269–1275. https://doi.org/10.1007/s10753-012-9438-5

Han, J., Chen, Y., Bao, L., Yang, X., Liu, D., Li, S., … Liu, H. (2013). Anti-inflammatory and cytotoxic cyathane diterpenoids from the medicinal fungus Cyathus africanus. *Fitoterapia*, *84*(1), 22–31. https://doi.org/10.1016/j.fitote.2012.10.001

Ismail, N., Stevenson, H. L., & Walker, D. H. (2006). Role of tumor necrosis factor alpha (TNF-α) and interleukin-10 in the pathogenesis of severe murine monocytotropic ehrlichiosis: Increased resistance of TNF receptor p55- and p75-deficient mice to fatal ehrlichial infection. *Infection and Immunity*, *74*(3), 1846–1856. https://doi.org/10.1128/IAI.74.3.1846-1856.2006

Jang, T. S., & Kang, K. S. (2017). Anti-inflammatory phenolic metabolites from the Edible fungus *Phellinus baumii* in LPS-stimulated RAW264.7 cells. *Molecules*, *22*. https://doi.org/10.3390/molecules22101583

Jared F Taylor, Ramin Goudarzi, Puya G Yazdi1, and B. A. P. (2017). In *vitro* effects of arthrocen, an avocado/soy unsaponifiables agent, on inflammation and global gene expression in human monocytes. *Int J Chem.*, *9*(4), 31–39. https://doi.org/doi:10.5539/ijc.v9n4p31

Jedinak, A., Dudhgaonkar, S., Wu, Q., Simon, J., & Sliva, D. (2011). Anti-inflammatory activity of edible oyster mushroom is mediated through the inhibition of NF- B and AP-1 signaling. *Nutrition Journal*, *10*(1), 52. https://doi.org/10.1186/1475-2891-10-52

Jeon, T. Il, Jung, C. H., Cho, J. Y., Park, D. K., & Moon, J. H. (2013). Identification of an anticancer compound against HT-29 cells from *Phellinus linteus* grown on germinated brown rice. *Asian Pacific Journal of Tropical Biomedicine*, *3*(10), 785–789. https://doi.org/10.1016/S2221-1691(13)60156-2

Jiang, P., Yuan, L., Cai, D., Jiao, L., & Zhang, L. (2015). Characterization and antioxidant activities of the polysaccharides from mycelium of Phellinus pini and culture medium. *Carbohydrate Polymers*, *117*, 600–604. https://doi.org/10.1016/j.carbpol.2014.10.013

Jin, D., Cho, S., Yeon, J., Burm, H., & Il, Y. (2016). Neuroprotective effects of the Phellinus linteus ethyl acetate extract against H_2O_2 -induced apoptotic cell death of SK-N-MC cells. *Nutrition Research*, *36*(1), 31–43. https://doi.org/10.1016/j.nutres.2015.11.005

Jin, G., Lee, M. W., Im, K. H., & Lee, T. S. (1988). Inhibitory activities of three extracts from *Phellinus igniarius*, (Grice), 1–7.

Jiao, C., Xie, Y. Z., Yang, X., Li, H., Li, X. M., Pan, H. H., … Yang, B. B. (2013). Anticancer Activity of Amauroderma rude. *PLoS ONE*, *8*(6). https://doi.org/10.1371/journal.pone.0066504

Jung, M., Liermann, J. C., Opatz, T., & Erkel, G. (2011). Ganodermycin, a novel inhibitor of CXCL10 expression from *Ganoderma applanatum. Journal of Antibiotics*, *64*(10),

683–686. https://doi.org/10.1038/ja.2011.64

Kassim, M., Achoui, M., & Rais, M. (2010). Ellagic acid , phenolic acids , and flavonoids in Malaysian honey extracts demonstrate in vitro anti-inflammatory activity. *Nutrition Research*, *30*(9), 650–659. https://doi.org/10.1016/j.nutres.2010.08.008

Kidd, P. M. (2000). The use of mushroom glucans and proteoglycans in cancer treatment. *Alternative Medicine Review*, *5*(1), 4–27.

Kim, E. H., Choi, Y. S., & Kim, Y. M. (2019). Antioxidative and anti-inflammatory effect of *Phellinus igniarius* on RAW 264.7 macrophage cells. *Journal of Exercise Rehabilitation*, *15*(1), 2–7. https://doi.org/10.12965/jer.1938010.005

Kim, S., Song, Y., Kim, S., Kim, B., Lim, C., & Park, E. (2004). Anti-inflammatory and related pharmacological activities of the n -BuOH subfraction of mushroom Phellinus linteus, *93*, 141–146. https://doi.org/10.1016/j.jep.2004.03.048

Kinney, J. W., Bemiller, S. M., Murtishaw, A. S., Leisgang, A. M., Salazar, A. M., & Lamb, B. T. (2018). Inflammation as a central mechanism in Alzheimer ' s disease. *Alzheimer's & Dementia: Translational Research & Clinical Interventions*, *4*, 575–590. https://doi.org/10.1016/j.trci.2018.06.014

Konno, S., Chu, K., Feuer, N., Phillips, J., & Choudhury, M. (2015). Potent anticancer effects of bioactive mushroom extracts (*Phellinus linteus*) on a variety of human cancer cells. *J Clin Med Res*, *7*(2), 76–82. https://doi.org/10.14740/jocmr1996w

Kowarik, M. C., Cepok, S., Sellner, J., Grummel, V., Weber, M. S., Korn, T., … Hemmer, B. (2012). CXCL13 is the major determinant for B cell recruitment to the CSF during neuroinflammation. *Journal of Neuroinflammation*, *9*, 1–11. https://doi.org/10.1186/1742-2094-9-93

Kozarski, M., Klaus, A., Niksic, M., Jakovljevic, D., Helsper, J. P. F. G., & Van Griensven, L. J. L. D. (2011). Antioxidative and immunomodulating activities of polysaccharide extracts of the medicinal mushrooms *Agaricus bisporus*, *Agaricus brasiliensis*, *Ganoderma lucidum* and *Phellinus linteus*. *Food Chemistry*, *129*(4), 1667–1675. https://doi.org/10.1016/j.foodchem.2011.06.029

Krediet, E., Bostoen, T., Breeksema, J., van Schagen, A., Passie, T., & Vermetten, E. (2020). Reviewing the Potential of Psychedelics for the Treatment of PTSD. *International Journal of Neuropsychopharmacology*, *23*(6), 385–400. https://doi.org/10.1093/ijnp/pyaa018

Krohn, K., Cludius-brandt, S., Schulz, B., Sreelekha, M., & Shafi, P. M. (2011). Isolation, structure elucidation, and biological activity of a new alkaloid from *Zanthoxylum rhetsa*, 12–13. https://doi.org/10.1177/1934578X1100601110

Krsti, D. Z., Lazarevi, T. D., Bond, A. M., & Vasi, V. M. (2013). Acetylcholinesterase Inhibitors : Pharmacology and Toxicology. *Curr Neuropharmacol*, *11(3)*, 315–335. https://doi.org/doi: 10.2174/1570159X11311030006

Kurapati, K. R. V., Atluri, V. S. R., Samikkannu, T., & Nair, M. P. N. (2013). Ashwagandha (*Withania somnifera*) reverses β-amyloid1-42 induced toxicity in human neuronal cells: implications in HIV-associated neurocognitive disorders (HAND). *PLoS ONE*, *8*(10), 1–15. https://doi.org/10.1371/journal.pone.0077624

Laovachirasuwan, P., Judprakob, C., Sinaphet, B., & Phadungkit, M. (2016). In vitro antioxidant and antimutagenic activities of different solvent extracts of *Phellinus spp.* *International Food Research Journal*, *23*(6), 2608–2615.

Latil, A., Libon, C., Templier, M., Junquero, D., Lantoine-Adam, F., & Nguyen, T. (2012). Hexanic lipidosterolic extract of *Serenoa repens* inhibits the expression of two key inflammatory mediators, MCP-1/CCL2 and VCAM-1, in vitro. *BJU International*, *110*(6B). https://doi.org/10.1111/j.1464-410X.2012.11144.x

Lavi, I., Levinson, D., Peri, I., Nimri, L., Hadar, Y., & Schwartz, B. (2010). Orally administered glucans from the edible mushroom Pleurotus pulmonarius reduce acute inflammation in dextran sulfate sodium-induced experimental colitis. *British Journal of Nutrition*, *103*(3), 393–402. https://doi.org/10.1017/S0007114509991760

Lavi, I., Nimri, L., Levinson, D., Peri, I., Hadar, Y., & Schwartz, B. (2012). Glucans from the edible mushroom Pleurotus pulmonarius inhibit colitis-associated colon carcinogenesis in mice. *Journal of Gastroenterology*, *47*(5), 504–518. https://doi.org/10.1007/s00535-011-0514-7

Li, H., Lu, X., Zhang, S., Lu, M., & Liu, H. (2008). Anti-inflammatory activity of polysaccharide from Pholiota nameko. *Biochemistry (Moscow)*, *73*(6), 669–675. https://doi.org/10.1134/S0006297908060060

Lee, I., Yun, B., Kim, J., Ryoo, I., Kim, Y., & Yoo, I. (2003). Neuroprotective activity of p - Terphenyl leucomentins from the mushroom *Paxillus panuoides*. *Biosci. Biotechnol. Biochem*, *67*(8), 1813–1816. https://doi.org/10.1271/bbb.67.1813

Lee, S., Lee, D., Jang, T. S., Kang, K. S., Nam, J. W., Lee, H. J., & Kim, K. H. (2017). Anti-inflammatory phenolic metabolites from the edible fungus *Phellinus baumii* in LPS-stimulated RAW264.7 Cells. *Molecules*, *22*(10). https://doi.org/10.3390/molecules22101583

Li, X., Jiao, L. L., Zhang, X., Tian, W. M., Chen, S., & Zhang, L. P. (2008). Anti-tumor and

immunomodulating activities of proteoglycans from mycelium of *Phellinus nigricans* and culture medium. *International Immunopharmacology*, *8*(6), 909–915. https://doi.org/10.1016/j.intimp.2008.02.008

Lee, Y. J., Han, S. B., Nam, S. Y., Oh, K. W., & Hong, J. T. (2010). Inflammation and Alzheimer's disease. *Archives of Pharmacal Research*, *33*(10), 1539–1556. https://doi.org/10.1007/s12272-010-1006-7

Lisa C. Zaba , Judilyn Fuentes-Duculan , Narat John Eungdamrong , Leanne M. Johnson-Huang , Kristine E. Nograles , Traci R. White , Katherine C. Pierson , Tim Lentini , Mayte Suárez-Fariñas , Michelle A. Lowes, J. G. K. (2010). Identification of TNF-related apoptosis-inducing ligand and other molecules that distinguish inflammatory from resident dendritic cells in patients with psoriasis. *Journal of Allergy and Clinical Immunology*, *125*(6), 1261-1268.e9. https://doi.org/10.1016/j.jaci.2010.03.018

Liu, M., Guo, S., Hibbert, J. M., Jain, V., Singh, N., Wilson, N. O., & Stiles, J. K. (2011). CXCL10/IP-10 in infectious diseases pathogenesis and potential therapeutic implications. *Cytokine and Growth Factor Reviews*, *22*(3), 121–130. https://doi.org/10.1016/j.cytogfr.2011.06.001

Liu, T., Zhang, L., Joo, D., & Sun, S. (2017). NF- κ B signaling in inflammation. *Signal Transduct Target Ther*, *2*(April). https://doi.org/10.1038/sigtrans.2017.23

Livak, K. J., & Schmittgen, T. D. (2001). Analysis of relative gene expression data using real-time quantitative PCR and the 2(-Delta Delta C(T)) Method. *Methods (San Diego, Calif.)*, *25*(4), 402–408. https://doi.org/10.1006/meth.2001.1262

Llauradó, G., Morris, H. J., Lebeque, Y., Gutiérrez, A., Fontaine, R., Bermúdez, R. C., & Perraud-Gaime, I. (2013). Phytochemical screening and effects on cell-mediated immune response of Pleurotus fruiting bodies powder. *Food and Agricultural Immunology*, *24*(3), 295–304. https://doi.org/10.1080/09540105.2012.686988

Lu, Y. Y., Ao, Z. H., Lu, Z. M., Xu, H. Y., Zhang, X. M., Dou, W. F., & Xu, Z. H. (2008). Analgesic and anti-inflammatory effects of the dry matter of culture broth of Termitomyces albuminosus and its extracts. *Journal of Ethnopharmacology*, *120*(3), 432–436. https://doi.org/10.1016/j.jep.2008.09.021

Lull, C., Wichers, H. J., & Savelkoul, H. F. J. (2005). Antiinflammatory and immunomodulating properties of fungal metabolites. *Mediators of Inflammation*, *2005*(2), 63–80. https://doi.org/10.1155/MI.2005.63

Ma, L., Chen, H., Dong, P., & Lu, X. (2013). Anti-inflammatory and anticancer activities of extracts and compounds from the mushroom Inonotus obliquus. *Food Chemistry*, *139*(1–4), 503–508. https://doi.org/10.1016/j.foodchem.2013.01.030

Majekodunmi, S. O. (2015). Review of extraction xtraction of medicinal plants lants for pharmaceutical harmaceutical research, *3*(November), 521–527.

Manchon, L., Chebli, K., Papon, L., Paul, C., Garcel, A., Campos, N., … Tazi, J. (2017). RNA sequencing analysis of activated macrophages treated with the anti-HIV ABX464 in intestinal inflammation. *Scientific Data*, *4*, 1–11. https://doi.org/10.1038/sdata.2017.150

Matsui, M., Adib-Conquy, M., Coste, A., Kumar-Roiné, S., Pipy, B., Laurent, D., & Pauillac, S. (2012). Aqueous extract of *Vitex trifolia* L. (Labiatae) inhibits LPS-dependent regulation of inflammatory mediators in RAW 264.7 macrophages through inhibition of Nuclear Factor kappa B translocation and expression. *Journal of Ethnopharmacology*, *143*(1), 24–32. https://doi.org/10.1016/j.jep.2012.05.043

Maxia, A., Sanna, C., Frau, M. A., Piras, A., Karchuli, M. S., & Kasture, V. (2011). I Anti-inflammatory activity of *Pistacia lentiscus* essential oil:involvement of IL-6 and TNF-α. *Natural Product Communications* , 6(10), 7–8.https://doi.org/10.1177/1934578X1100601033

Mehta, M., Adem, A., & Sabbagh, M. (2012). New acetylcholinesterase inhibitors for alzheimer's disease. *International Journal of Alzheimer's Disease*, *2012*. https://doi.org/10.1155/2012/728983

Michlmayr, D., & McKimmie, C. S. (2014). Role of CXCL10 in central nervous system inflammation. *International Journal of Interferon, Cytokine and Mediator Research*, *6*(1), 1–18. https://doi.org/10.2147/IJICMR.S35953

Ming Yeou Lung, J. C. T. and P. C. H. (2010). Antioxidant properties of edible basidiomycete *Phellinus igniarius* in submerged cultures. *Journal of Food Sciences*, *75*(1), 18–24. https://doi.org/10.1111/j.1750-3841.2009.01384.x

Moro, C., Palacios, I., Lozano, M., D'Arrigo, M., Guillamón, E., Villares, A., … García-Lafuente, A. (2012). Anti-inflammatory activity of methanolic extracts from edible mushrooms in LPS activated RAW 264.7 macrophages. *Food Chemistry*, *130*(2), 350–355. https://doi.org/10.1016/j.foodchem.2011.07.049

Munir, M. T., Pailhories, H., Eveillard, M., Irle, M., Aviat, F., Dubreil, L., … Belloncle, C. (2020). Testing the antimicrobial characteristics of wood materials: A review of methods. *Antibiotics*, *9*(5), 12–16. https://doi.org/10.3390/antibiotics9050225

Muszyńska, B., Grzywacz-Kisielewska, A., Kała, K., & Gdula-Argasińska, J. (2018). Anti-inflammatory properties of edible mushrooms: A review. *Food Chemistry*, *243*(September 2017), 373–381. https://doi.org/10.1016/j.foodchem.2017.09.149

N, S. V. S. S. S. L. H. B., Charya, M. A. S., & State, T. (2017). Biological Activities of Exopolysaccharide from Fomitopsis feei. *International Journal of Microbiological Research*, *8*(2), 48–58. https://doi.org/10.5829/idosi.ijmr.2017.48.58

Niemelä, T. (1972). On Fennoscandian Polypores. II. *Phellinus laevigatus* (Fr.) Bourd. & Galz. and P. lundellii Niemelä, n.sp. *Annales Botanici Fennici*, *9*(1), 41–59.

Nn, A. (2015). A review on the extraction methods use in medicinal plants, principle, strength and limitation. *Medicinal & Aromatic Plants*, *04*(03), 3–8. https://doi.org/10.4172/2167-0412.1000196

Nowacka, N., Nowak, R., Drozd, M., Olech, M., & Los, R. (2015). Antibacterial , antiradical potential and phenolic compounds of thirty-One polish mushrooms, 1–13. https://doi.org/10.1371/journal.pone.0140355

Núñez, M.; Ryvarden, L. (2000). East Asian polypores. *Synopsis Fungorum*, *13*, 1–168.

Ohta, Y., Lee, J. B., Hayashi, K., Fujita, A., Dong, K. P., & Hayashi, T. (2007). In vivo anti-influenza virus activity of an immunomodulatory acidic polysaccharide isolated from Cordyceps militaris grown on germinated soybeans. *Journal of Agricultural and Food Chemistry*, *55*(25), 10194–10199. https://doi.org/10.1021/jf0721287

Pace, R. T., & Burg, K. J. L. (2013). Toxic effects of resazurin on cell cultures. *Cytotechnology*, *67*(1), 13–17. https://doi.org/10.1007/s10616-013-9664-1

Pala, S. A., Wani, A. H., & Ganai, B. A. (2019). Antimicrobial potential of some wild collected from *Kashmir Himalayas*. *Plant Science Today*, *6*, 137–146.

Palacios, I., Lozano, M., Moro, C., D'Arrigo, M., Rostagno, M. a., Martínez, J. a., … Villares, a. (2011). Antioxidant properties of phenolic compounds occurring in edible mushrooms. *Food Chemistry*, *128*(3), 674–678. https://doi.org/10.1016/j.foodchem.2011.03.085

Park, Y. M., Won, J. H., Kim, Y. H., Choi, J. W., Park, H. J., & Lee, K. T. (2005). In vivo and in vitro anti-inflammatory and anti-nociceptive effects of the methanol extract of Inonotus obliquus. *Journal of Ethnopharmacology*, *101*(1–3), 120–128. https://doi.org/10.1016/j.jep.2005.04.003

Patel, S., & Goyal, A. (2012). Recent developments in mushrooms as anti-cancer therapeutics: a review. *3 Biotech*, *2*(1), 1–15. https://doi.org/10.1007/s13205-011-0036-2

Phan, C.-W., Tan, E. Y.-Y., & Sabaratnam, V. (2018). Bioactive Molecules in Edible and Medicinal Mushrooms for Human Wellness, 1–24. https://doi.org/10.1007/978-3-319-54528-8_83-1

Phan, C., David, P., Naidu, M., & Wong, K. (2015). Therapeutic potential of culinary-

medicinal mushrooms for the management of neurodegenerative diseases: diversity, metabolite, and mechanism. *Critical Reviews in Biotechnology*, *35(3)*, 355–368. https://doi.org/10.3109/07388551.2014.887649

Qazzaz, M. E., Raja, V. J., Lim, K., Kam, T., Bong, J., Gershkovich, P., & Bradshaw, T. D. (2016). In vitro anticancer properties and biological evaluation of novel natural alkaloid jerantinine B. *Cancer Letters*, *370*(2), 185–197. https://doi.org/10.1016/j.canlet.2015.10.013

Qian, G. M., Pan, G. F., & Guo, J. Y. (2012). Anti-inflammatory and antinociceptive effects of cordymin, a peptide purified from the medicinal mushroom Cordyceps sinensis. *Natural Product Research*, *26*(24), 2358–2362. https://doi.org/10.1080/14786419.2012.658800

Quang, D. N., Hashimoto, T., Arakawa, Y., Kohchi, C., Nishizawa, T., Soma, G. I., & Asakawa, Y. (2006). Grifolin derivatives from Albatrellus caeruleoporus, new inhibitors of nitric oxide production in RAW 264.7 cells. *Bioorganic and Medicinal Chemistry*, *14*(1), 164–168. https://doi.org/10.1016/j.bmc.2005.08.005

Queiroz, L. S., Nascimento, M. S., Cruz, A. K. M., Castro, A. J. G., Moura, M. D. F. V, Baseia, I. G., … Leite, E. L. (2010). Glucans from the Caripia montagnei mushroom present anti-inflammatory activity. *International Immunopharmacology*, *10*(1), 34–42. https://doi.org/10.1016/j.intimp.2009.09.015

Rampersad, S. N. (2012). Multiple applications of alamar blue as an indicator of metabolic function and cellular health in cell viability bioassays. *Sensors (Switzerland)*, *12*(9), 12347–12360. https://doi.org/10.3390/s120912347

Rincao, V. P., Yamamoto, K. A., Ricardo, N. M. P. S., Soares, S. A., Paccola Meirelles, L. D., Nozawa, C., & Linhares, R. E. C. (2012). Polysaccharide and extracts from Lentinula edodes: Structural features and antiviral activity. *Virology Journal*, *9*(1), 37. https://doi.org/10.1186/1743-422X-9-37

Riss, T. L., Moravec, R. A., & Niles, A. L. (2011). Cytotoxicity Ttesting: measuring viable cells, dead cells, and detecting mechanism of cell death. *Mammalian Cell Viability: Methods and Protocols* (pp. 103–114). Totowa, NJ: Humana Press. https://doi.org/10.1007/978-1-61779-108-6_12

Roupas, P., Keogh, J., Noakes, M., Margetts, C., & Taylor, P. (2012). The role of edible mushrooms in health: Evaluation of the evidence. *Journal of Functional Foods*, *4*(4), 687–709. https://doi.org/10.1016/j.jff.2012.05.003

Ruthes, Andrea C., Rattmann, Y. D., Malquevicz-Paiva, S. M., Carbonero, E. R., Córdova,

M. M., Baggio, C. H., … Iacomini, M. (2013). Agaricus bisporus fucogalactan: Structural characterization and pharmacological approaches. *Carbohydrate Polymers*, *92*(1), 184–191. https://doi.org/10.1016/j.carbpol.2012.08.071

Ruthes, Andrea Caroline, Carbonero, E. R., Córdova, M. M., Baggio, C. H., Santos, A. R. S., Sassaki, G. L., … Iacomini, M. (2013). Lactarius rufus (1→3),(1→6)-β-d-glucans: Structure, antinociceptive and anti-inflammatory effects. *Carbohydrate Polymers*, *94*(1), 129–136. https://doi.org/10.1016/j.carbpol.2013.01.026

Ryvarden, L.; Gilbertson, R. L. (1993). European polypores. Part 1. *Synopsis Fungorum*, *6*, 1–387.

Saklani, A., Hegde, B., Mishra, P., Singh, R., Mendon, M., Chakrabarty, D., … Kulkarni-Almeida, A. A. (2012). NF-κB dependent anti-inflammatory activity of chlorojanerin isolated from Saussurea heteromalla. *Phytomedicine*, *19*(11), 988–997. https://doi.org/10.1016/j.phymed.2012.05.016

Samchai, S., Seephonkai, P., & Kaewtong, C. (2011). Two Indole Derivatives and Phenolic Compound Isolated from Mushroom Phellinus linteus. *Chinese Journal of Natural Medicines*, *9*(3), 173–175. https://doi.org/http://dx.doi.org/10.3724/SP.J.1009.2011.00173

Santillo, M. F., & Liu, Y. (2015). A fluorescence assay for measuring acetylcholinesterase activity in rat blood and a human neuroblastoma cell line (SH-SY5Y). *Journal of Pharmacological and Toxicological Methods*, *76*, 15–22. https://doi.org/10.1016/j.vascn.2015.07.002

Seephonkai, P., Samchai, S., Thongsom, A., Sunaart, S., Kiemsanmuang, B., & Chakuton, K. (2011). DPPH Radical scavenging activity and total phenolics of Phellinus mushroom extracts collected from northeast of Thailand. *Chinese Journal of Natural Medicines*, *9*(6), 441–445. https://doi.org/10.3724/SP.J.1009.2011.00441

Šeklić, D. S., Stanković, M. S., Milutinović, M. G., Topuzović, M. D., Štajn, A. Š., & Marković, S. D. (2016). Cytotoxic , antimigration , pro-and antioxidative activities of extracts from medicinal mushrooms on colon cancer cell lines. *Arch. Biol. Sci., Belgrade, 68*(1), 93–105. https://doi.org/10.2298/ABS150427131S

Shao, H. J., Jeong, B., Kim, K., & Lee, S. (2014). Anti-inflammatory activity of mushroom-derived hispidin through blocking of NF-κB activation. *J Sci Food Agric*, *95*(November), 2482–2486. https://doi.org/10.1002/jsfa.6978

Sharma, K. (2019). Cholinesterase inhibitors as Alzheimer's therapeutics (Review). *Molecular Medicine Reports*, *20*(2), 1479–1487. https://doi.org/10.3892/mmr.2019.10374

Shen, H., Shao, S., Chen, J., & Zhou, T. (2017). Antimicrobials from Mushrooms for

Assuring Food Safety. *ComprehensiveReviewsinFoodScienceandFoodSafety*, *16*, 316–329. https://doi.org/10.1111/1541-4337.12255

Silva, A. M., Alvarado, H. L., Abrego, G., Martins-Gomes, C., Garduño-Ramirez, M. L., García, M. L., … Souto, E. B. (2019). In vitro cytotoxicity of oleanolic/ursolic acids-loaded in PLGA nanoparticles in different cell lines. *Pharmaceutics*, *11*(8), 1–11. https://doi.org/10.3390/pharmaceutics11080362

Sittiwet, C., & Puangpronpitag, D. (2008). Antibacterial activity of *Phellinus gilvus* aqueous extract. *International Journal of Pharmacology*, *4*(6), 500–502. https://doi.org/10.3923/ijp.2008.500.502

Sliva, D. (2010). Medicinal mushroom *Phellinus linteus* as an alternative cancer therapy (review). *Experimental and Therapeutic Medicine*, *1*(3), 407–411. https://doi.org/10.3892/etm_00000063

Smiderle, F. R., Baggio, C. H., Borato, D. G., Santana-Filho, A. P., Sassaki, G. L., Iacomini, M., & Van Griensven, L. J. L. D. (2014). Anti-Inflammatory properties of the medicinal mushroom *Cordyceps militaris* might be related to its linear (1→3)-β-D-Glucan. *PLoS ONE*, *9*(10), e110266. https://doi.org/10.1371/journal.pone.0110266

Smiderle, F. R., Alquini, G., Tadra-Sfeir, M. Z., Iacomini, M., Wichers, H. J., & Van Griensven, L. J. L. D. (2013). Agaricus bisporus and Agaricus brasiliensis (1 → 6)-β-d-glucans show immunostimulatory activity on human THP-1 derived macrophages. *Carbohydrate Polymers*, *94*(1), 91–99. https://doi.org/10.1016/j.carbpol.2012.12.073

Song, H. H., Chae, H. S., Oh, S. R., Lee, H. K., & Chin, Y. W. (2012). Anti-inflammatory and anti-allergic effect of Agaricus blazei extract in bone marrow-derived mast cells. *American Journal of Chinese Medicine*, *40*(5), 1073–1084. https://doi.org/10.1142/S0192415X12500796

Stanikunaite, R., Khan, S. I., Trappe, J. M., & Ross, S. A. (2009). Cyclooxygenase-2 inhibitory and antioxidant compounds from the truffle elaphomyces granulatus. *Phytotherapy Research*, *23*(4), 575–578. https://doi.org/10.1002/ptr.2698

Su, F., Bai, F., & Zhang, Z. (2016). Inflammatory cytokines and Alzheimer ' s disease : A review from theperspective of genetic polymorphisms. *Neuroscience Bulletin*, *32*(5), 469–480. https://doi.org/10.1007/s12264-016-0055-4

Su, H., Lei, C. T., & Zhang, C. (2017). Interleukin-6 signaling pathway and its role in kidney disease: An update. *Frontiers in Immunology*, *8*(APR), 1–10. https://doi.org/10.3389/fimmu.2017.00405

Suabjakyong, P., Saiki, R., Van Griensven, L. J. L. D., Higashi, K., Nishimura, K., Igarashi, K., & Toida, T. (2015). Polyphenol extract from *Phellinus igniarius* protects against acrolein toxicity in vitro and provides protection in a mouse stroke model. *PLoS ONE*,

10(3), 1–14. https://doi.org/10.1371/journal.pone.0122733

Sullivan, R., Smith, J. E., & Rowan, N. J. (2006). Medicinal mushrooms and cancer therapy: translating a traditional practice into Western medicine. *Perspectives in Biology and Medicine*, *49*(2), 159–170. https://doi.org/10.1353/pbm.2006.0034

Sułkowska, K., Agnieszka, Z., Agnieszka, S., Joanna, G., & Argasińska, G. (2018). Chemical composition and biological activity of extracts from fruiting bodies and mycelial cultures of *Fomitopsis betulina*. *Molecular Biology Reports*, *0*(0), 0. https://doi.org/10.1007/s11033-018-4420-4

Takagi, Y., Aoki, T., Takahashi, J. C., Yoshida, K., Ishii, A., Arakawa, Y., … Miyamoto, S. (2014). Differential gene expression in relation to the clinical characteristics of human brain arteriovenous malformations. *Neurologia Medico-Chirurgica*, *54*(3), 163–175. https://doi.org/10.2176/nmc.oa2012-0422

Takei, M., Kobayashi, M., Herndon, D. N., Pollard, R. B., & Suzuki, F. (2006). Glycyrrhizin inhibits the manifestations of anti-inflammatory responses that appear in association with systemic inflammatory response syndrome (SIRS)-like reactions. *Cytokine*, *35*(5–6), 295–301. https://doi.org/10.1016/j.cyto.2006.10.002

Tel, G., Ozturk, M., Duru, M. E., Turkoglu, A., Tel, G., Ozturk, M., … Turkoglu, A. (2015). Antioxidant and anticholinesterase activities of five wild mushroom species with total bioactive contents. Pharmaceutical Biology, 53(6), 824-830. https://doi.org/10.3109/13880209.2014.943245

Treede, I., Braun, A., Jeliaskova, P., Giese, T., Füllekrug, J., Griffiths, G., … Ehehalt, R. (2009). TNF-α-induced up-regulation of pro-inflammatory cytokines is reduced by phosphatidylcholine in intestinal epithelial cells. *BMC Gastroenterology*, *11*(9:53), 1–11. https://doi.org/10.1186/1471-230X-9-53

Tsuji, T., Du, W., Nishioka, T., Chen, L., Yamamoto, D., & Chen, C. Y. (2010). *Phellinus linteus* extract sensitizes advanced prostate cancer cells to apoptosis in athymic nude mice, *5*(3). https://doi.org/10.1371/journal.pone.0009885

Valgas, C., Souza, S. M. De, Smânia, E. F. A., & Jr, A. S. (2007). Screening methods to determine antibacterial activity of natural products, 369–380.

Van, Q., Nayak, B. N., Reimer, M., Jones, P. J. H., Fulcher, R. G., & Rempel, C. B. (2009). Anti-inflammatory effect of Inonotus obliquus, Polygala senega L., and Viburnum trilobum in a cell screening assay. *Journal of Ethnopharmacology*, *125*(3), 487–493. https://doi.org/10.1016/j.jep.2009.06.026

Wang, C., Liu, X., Lian, C., Ke, J., & Liu, J. (2019). Triterpenes and Aromatic

Meroterpenoids with Antioxidant Activity and Neuroprotective Effects from Ganoderma lucidum. *Molecules*, *24*, 1–11.

Wang, F. F., Shi, C., Yang, Y., Fang, Y., Sheng, L., & Li, N. (2018). Medicinal mushroom Phellinus igniarius induced cell apoptosis in gastric cancer SGC-7901 through a mitochondria-dependent pathway. *Biomedicine and Pharmacotherapy*, *102*(December 2017), 18–25. https://doi.org/10.1016/j.biopha.2018.03.038

Wen, C. L., Chang, C. C., Huang, S. S., Kuo, C. L., Hsu, S. L., Deng, J. S., & Huang, G. J. (2011). Anti-inflammatory effects of methanol extract of Antrodia cinnamomea mycelia both in vitro and in vivo. *Journal of Ethnopharmacology*, *137*(1), 575–584.

Westin, K., Buchhave, P., Nielsen, H., Minthon, L., Janciauskiene, S., & Hansson, O. (2012). CCL2 is associated with a faster rate of cognitive decline during early stages of Alzheimer's disease. *PLoS ONE*, *7*(1), 1–6. https://doi.org/10.1371/journal.pone.0030525

Wu, D. mei, Duan, W. qiang, Liu, Y., & Cen, Y. (2010). Anti-inflammatory effect of the polysaccharides of Golden needle mushroom in burned rats. *International Journal of Biological Macromolecules*, *46*(1), 100–103. https://doi.org/10.1016/j.ijbiomac.2009.10.013

Wu, H., Lu, F., Su, Y., Ou, H., Hung, H., Wu, J., … Chang, C. (2014). In Vivo and In Vitro Anti-Tumor Effects of Fungal Extracts, 2546–2556. https://doi.org/10.3390/molecules19022546

Wu, S., Liaw, C., Pan, S., Yang, H., & Ng, L. (2013). Phellinus linteus pol ysacc har ides and their imm unomodula tory pr operties in human monoc ytic cells, *5*, 1–10. https://doi.org/10.1016/j.jff.2013.01.011

Xie, F., Xiao, P., Chen, D., Xu, L., & Zhang, B. (2012). miRDeepFinder: A miRNA analysis tool for deep sequencing of plant small RNAs. *Plant Molecular Biology*, *80*(1), 75–84. https://doi.org/10.1007/s11103-012-9885-2

Xue, Q., Sun, J., Zhao, M., & Anti-tumor, I. Á. (2011). Immunostimulatory and anti-tumor activity of a water-soluble polysaccharide from Phellinus baumii mycelia. *World J Microbiol Biotechnol*, *27*, 1017–1023. https://doi.org/10.1007/s11274-010-0545-x

Xu, Z., Yan, S., Bi, K., Han, J., Chen, Y., Wu, Z., & Liu, H. (2013). Isolation and identification of a new anti-inflammatory cyathane diterpenoid from the medicinal fungus Cyathus hookeri Berk. *Fitoterapia*, *86*(1), 159–162. https://doi.org/10.1016/j.fitote.2013.03.002

Yan, J. K., Pei, J. J., Ma, H. Le, Wang, Z. Bin, & Liu, Y. S. (2017). Advances in antitumor polysaccharides from phellinus sensu lato: roduction, isolation, structure, antitumor activity, and mechanisms. *Critical Reviews in Food Science and Nutrition*, *57*(6), 1256–1269. https://doi.org/10.1080/10408398.2014.984802

Yayeh, T., Oh, W. J., Park, S. C., Kim, T. H., Cho, J. Y., Park, H. J., … Rhee, M. H. (2012). *Phellinus baumii* ethyl acetate extract inhibits lipopolysaccharide-induced iNOS, COX-2, and proinflammatory cytokine expression in RAW264.7 cells. *Journal of Natural Medicines*, *66*(1), 49–54. https://doi.org/10.1007/s11418-011-0552-8

Ye, J., Coulouris, G., Zaretskaya, I., Cutcutache, I., Rozen, S., & Madden, T. L. (2012). Primer-bLAST: a tool to design target-specific primers for polymerase chain reaction. *BMC Bioinformatics*, *13*, 134. https://doi.org/10.1186/1471-2105-13-134

Yuan, B., Zhao, L., Rakariyatham, K., Han, Y., Gao, Z., Muinde Kimatu, B., … Xiao, H. (2017). Isolation of a novel bioactive protein from an edible mushroom *Pleurotus eryngii* and its anti-inflammatory potential. *Food and Function*, *8*(6), 2175–2183. https://doi.org/10.1039/c7fo00244k

Zhao, C., Sun, H., Tong, X., & Qi, Y. (2003). An antitumour lectin from the edible mushroom Agrocybe aegerita. *The Biochemical Journal*, *374*(Pt 2), 321–327. https://doi.org/10.1042/BJ20030300

Zhang, J. J., Li, Y., Zhou, T., Xu, D. P., Zhang, P., Li, S., & Li, H. Bin. (2016). Bioactivities and health benefits of mushrooms mainly from China. *Molecules*, *21*(7), 1–16. https://doi.org/10.3390/molecules21070938

Appendices

Appendix A

Information of using mushroom from local people

The regions that collect mushroom and interviews the people comprise of Nakhon Ratchasima, Maha Sarakham, Mukdahan, Sakon Nakhon, Yasothon, Roi Et, Chaiyaphum, Khon Kaen and Amnat Charoen.

Summary of interviews

 From the interviews, it was found that of the people being interviewed had received no formal education; they had a good knowledge regarding their health and the plants including mushrooms that they were using. Mushrooms sometimes have no use for treatment of diseases experienced, but this is justified by the fact that the people are more aware of their illnesses. For example the people in Phu Pha Khood told that they used mushroom for illness by boiling in the water with one type of mushroom or mixture of mushroom and drinking the water. Some will use by soaking mushroom in the rice whisky and leave it for a period of time and drink it in small amount everyday. Some areas will ground as a powder and put small amount when cooking. Some finely grate and mould the material into a bolus and eat it like a tablet.
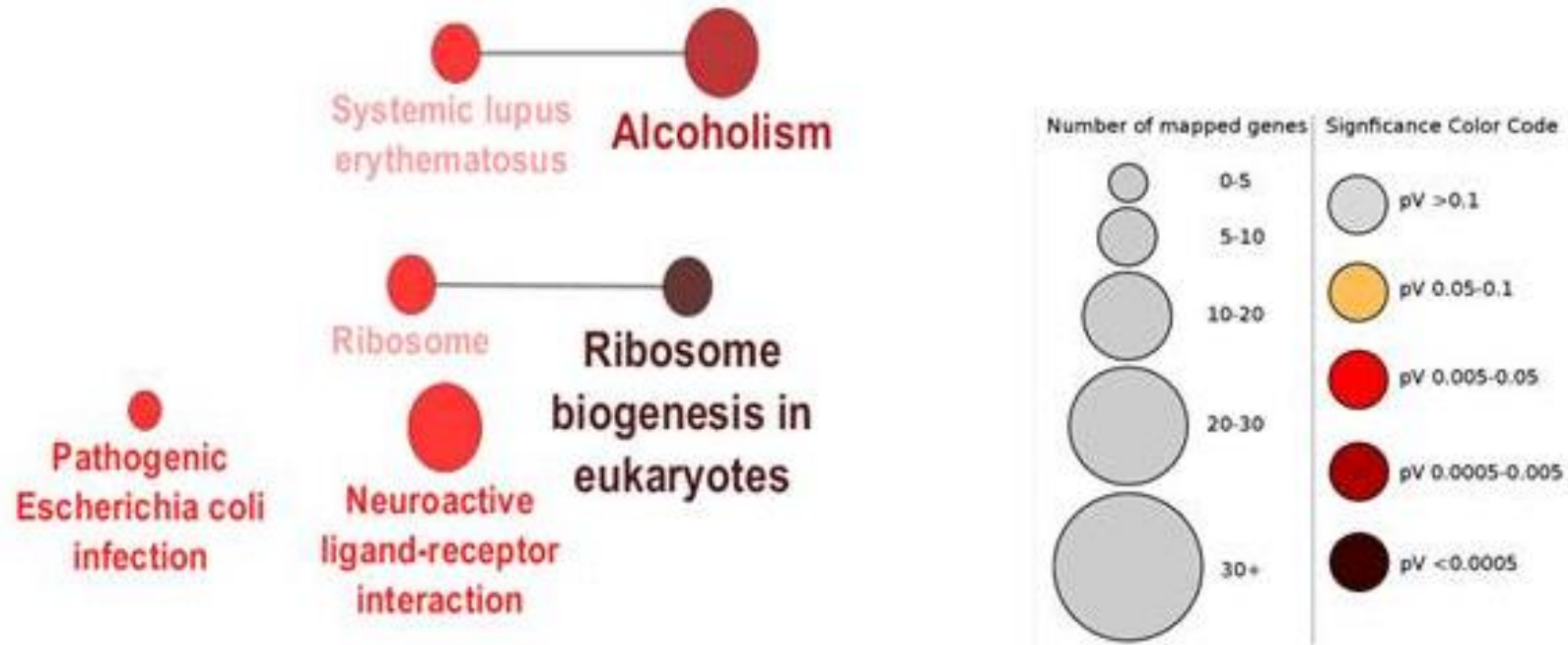
Figure 1B: Cytoscape ClueGO cluster results using the differentially expressed genes from the RNA-seq data of the THP-1 cells treated with P 30 µg/ml vs THP-1 cell control. ClueGO legend (shown on the right of the figure) – circle size represents the number of genes, colours represent the significantly enriched KEGG pathways associated with all genes up-regulated genes by more than 2-fold.
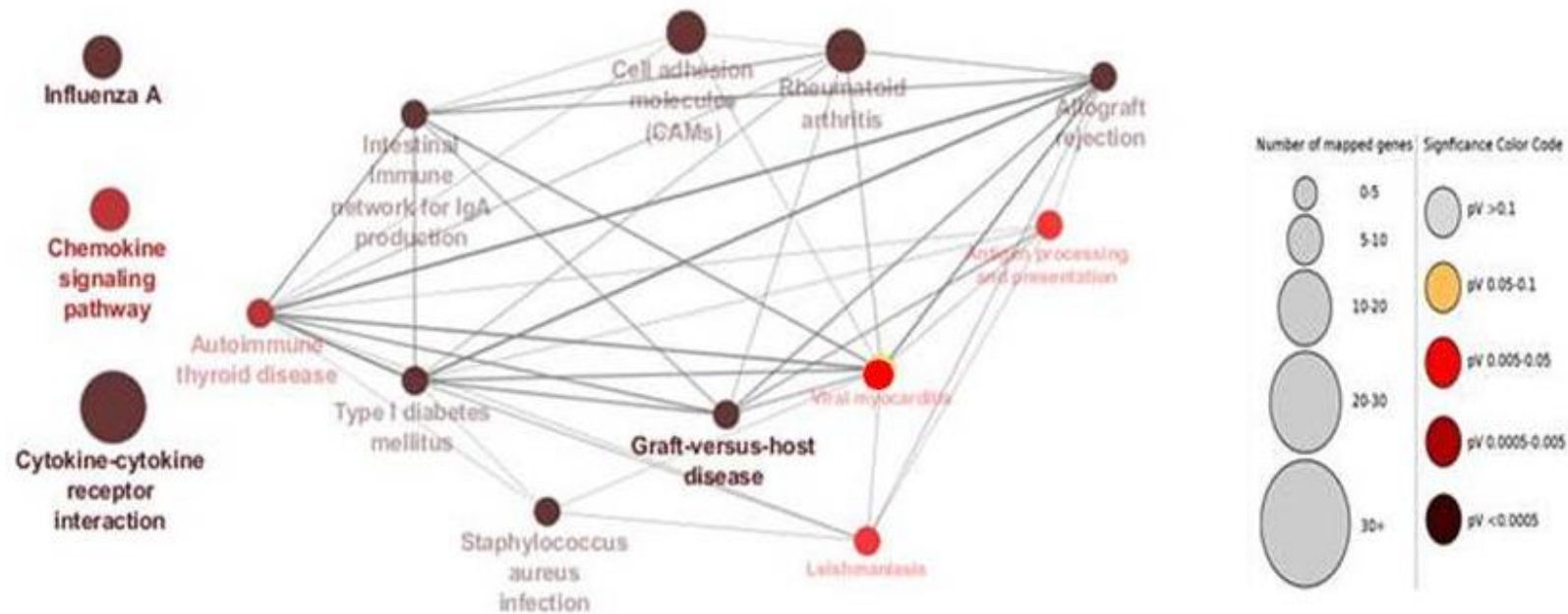
Figure 2B: Cytoscape ClueGO cluster results using the differentially expressed genes from the RNA-seq data of the THP-1 cells treated with P 30 μg/ml vs THP-1 cell control. ClueGO legend (shown on the right of the figure) – circle size represents the number of genes, colours represent the significantly enriched KEGG pathways associated with all genes down-regulated by more than 2-fold.

Figure 3B: **Cytoscape ClueGO cluster results using the differentially expressed genes from the RNA-seq data of the THP-1 cells treated with the E 30 μg/ vs THP-1 cell control.** ClueGO legend (shown on the right of the figure) – circle size represents the number of genes, colours represent the significantly enriched KEGG pathways associated with all genes up-regulated by more than 2-fold.

Figure 4B: **Cytoscape ClueGO cluster results using the differentially expressed genes from the RNA-seq data of the THP-1 cells treated with E 30 μg/ml vs THP-1 cell control.** ClueGO legend (shown on the right of the figure) – circle size represents the number of genes, colours represent the significantly enriched KEGG pathways associated with all genes down regulated by more than 2-fold.
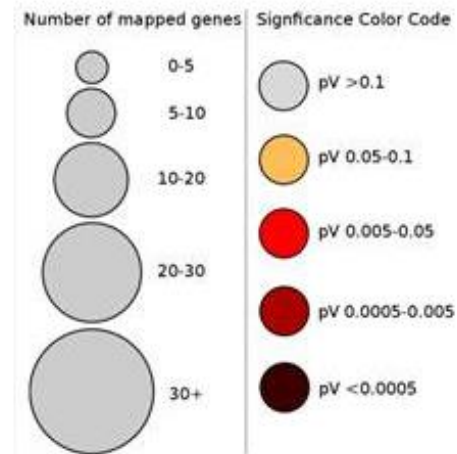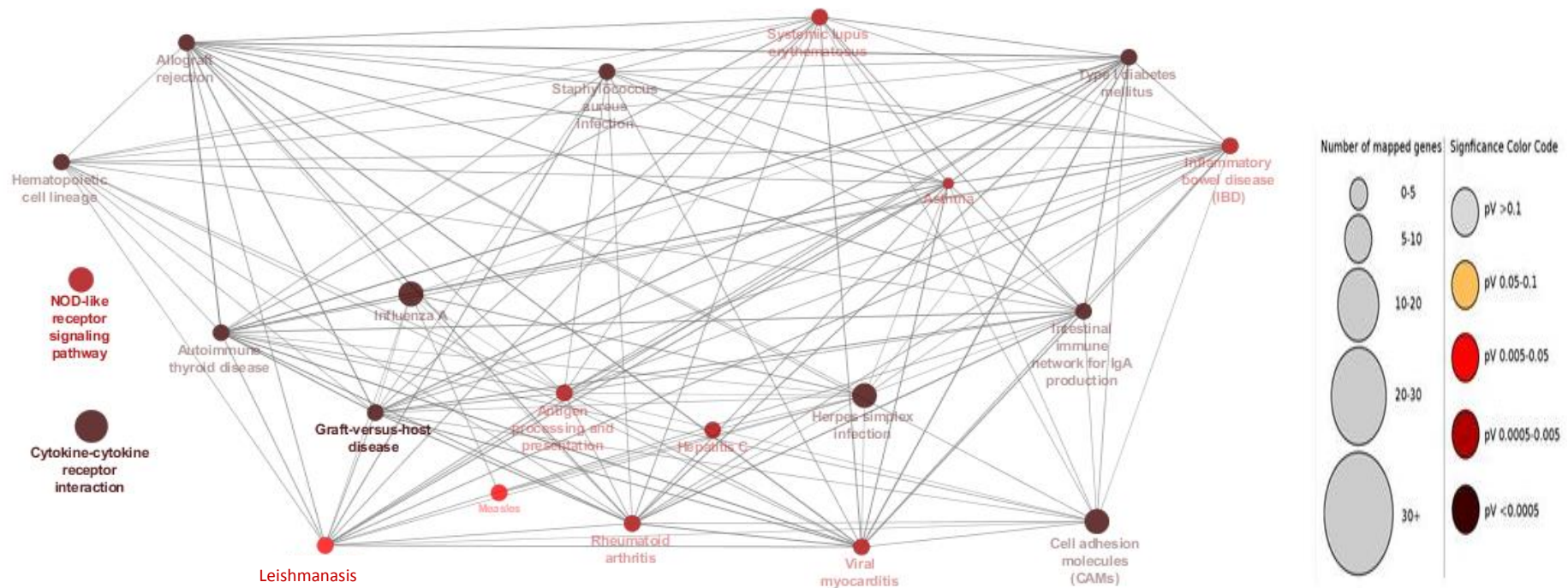
Figure 5B: Cytoscape ClueGO cluster results using the differentially expressed genes from the RNA-seq data of the THP-1 cells treated with E 10 µg/ml vs THP-1 cell control. ClueGO legend (shown on the right of the figure) – circle size represents the number of genes, colours represent the significantly enriched KEGG pathways associated with all genes down regulated by more than 2-fold.
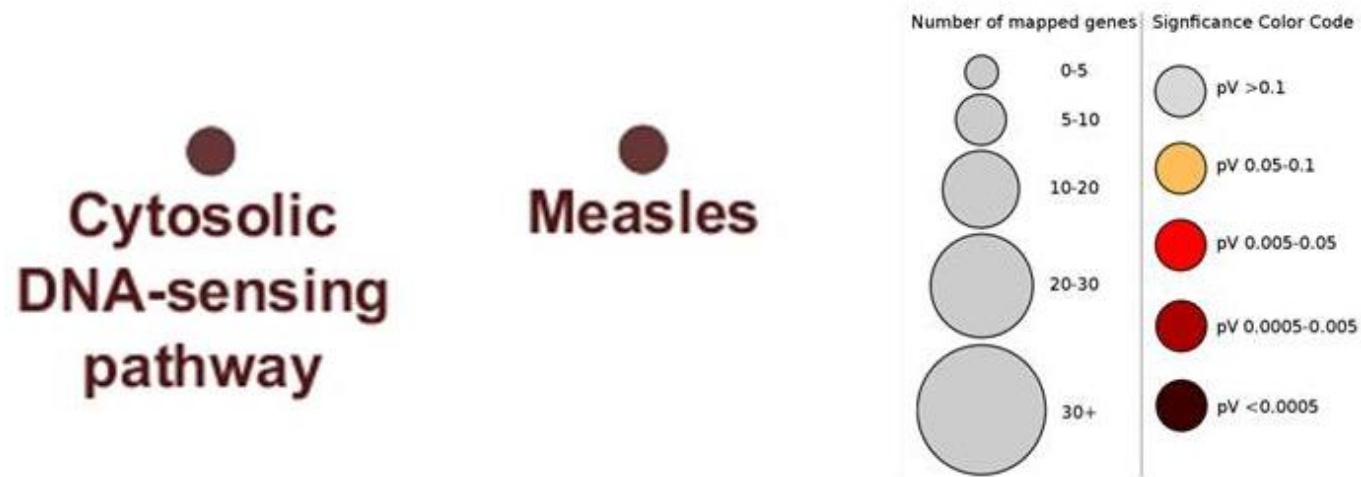
Table 1B The list of significant associated GO terms and genes with altered expressions identified using ClueGO KEGG pathway enrichment analysis when comparing RNA-Seq data of the THP-1 cells treated with P 30 µg/ml vs THP-1 cell control.

GO Term	Associated Genes Found
Cytokine-cytokine receptor interaction	*Ackr3, Amhr2, Ccl1, Ccl13, Ccl17, Ccl2, Ccl21, Ccl22, Ccl7, Ccl8, Ccr1, Ccr10, Ccr4, Ccr5, Cd40, Crlf2,Cx3cl1, Cx3cr1, Cxcl10, Cxcl11, Cxcl12, Cxcl13,Cxcl14,Cxcl16, Cxcl5, Cxcl6, Cxcl9, Cxcr5, Cxcr6, Fas, Flt1, Gdf5, Ifnk, Ifnl1, Il12a, Il12rb1, Il15ra, Il17c, Il17re, Il19, Il2rg, Il3ra, Il6, Il7, Il7r, Inhba, Inhbe, Ltb, Ngfr, Pdgfrb, Pf4v1, Tgfb3, Tnfrsf11b, Tnfrsf18, Tnfrsf6b, Tnfsf10, Tnfsf12, Tnfsf13B, Tnfsf15, Tnfsf18, Tnfsf4, Tnfsf8, Tnfsf9, Xcl2*
Neuroactive ligand-receptor interaction	*Adora3, Adra1b, Adra1d, Adra2a, Avpr1a, Avpr2, Bdkrb2, C3ar1, Cckbr, Ch17-360d5.1, Chrm2, Chrm4, Chrna1, Chrna10, Chrna3, Chrna6, Chrna7, Chrna9, Chrnb4, Cysltr2, Ednra, F2r, F2rl3, Fpr1, Gabra1, Gabra4, Gabrb2, Gabrq, Galr1, Glra2, Glrb, Gpr35, Gpr83, Grik5, Grm1, Grm2, Hrh3, Hrh4, Htr1d, Htr2b, Htr4, Lpar4, Lpar6, Mas1, Mchr2, Npbwr1, P2rx2, P2rx3, P2rx7, P2ry6, Ptafr, Rxfp1, Rxfp4, S1pr1, S1pr4, Vipr1*
Olfactory transduction	*Ncald, Or11a1, Or2a1, Or2a4, Or2a42, Or2ae1, Or2c1, Or4c6, Or4d1, Or52n4, Or5b2, Or7d4, Or7e24, Or8a1, Prkg2, Rgs2, Slc8a1, Slc8a3*

Table 1B The list of significant associated GO terms and genes with altered expressions identified using ClueGO KEGG pathway enrichment analysis when comparing RNA-Seq data of the THP-1 cells treated with P 30 μg/ml vs THP-1 cell control (continue).

GO Term	Associated Genes Found
MicroRNAs in cancer	*Bcl2l11, E2f2, Fgfr3, Irs2, Mir106b, Mir221, Myc, Notch4, Pdgfrb, Prkcg, Thbs1, Tnc, Tnxb, Trim71*
Cell adhesion molecules (CAMs)	*Cd226, Cd274, Cd28, Cd40, Cd80, Cd86, Cdh4, Cldn1, Cldn14, Cldn2, Cldn23, Cldn4, Cldn5, Cldn6, Cldn7, Hla-Dmb, Hla-Doa, Hla-Dpa1, Hla-Dpb1, Hla-Dqa1, Hla-Dqa2, Hla-Dra, Icos, Itgb8, Lrrc4c, Madcam1, Nectin1, Nrxn1, Nrxn2, Ntng1, Pdcd1,Pdcd1lg2, Ptprc, Ptprm, Sell, Siglec1, Vcam1*
Intestinal immune network for IgA production	*Ccr10, Cd28, Cd40, Cd80, Cd86, Cxcl12, Hla-Dmb, Hla-Doa, Hla-Dpa1, Hla-Dpb1, Hla-Dqa1, Hla-Dqa2, Hla-Dra, Icos, Il15ra, Il6, Madcam1, Tnfsf13b*
Type I diabetes mellitus	*Cd28, Cd80, Cd86, Fas, Gad1, Gzmb, Hla-Dmb, Hla-Doa, Hla-Dpa1, Hla-Dpb1, Hla-Dqa1, Hla-Dqa2, Hla-Dra, Il12a*

Table 1B The list of significant associated GO terms and genes with altered expressions identified using ClueGO KEGG pathway enrichment analysis when comparing RNA-Seq data of the THP-1 cells treated with P 30 µg/ml vs THP-1 cell control (continue).

GO Term	Associated Genes Found
S. aureus infection	*C1r, C1s, C3ar1, Cfb, Cfh, Fcgr3b, Fpr1, Hla-Dmb, Hla-Doa, Hla-Dpa1, Hla-Dpb1, Hla-Dqa1, Hla-Dqa2, Hla-Dra, Mbl2, Ptafr*
Rheumatoid arthritis	*Angpt1, Atp6v0d2, Ccl2, Cd28, Cd80, Cd86, Cxcl12, Cxcl5, Cxcl6, Flt1, Hla-Dmb, Hla-Doa, Hla-Dpa1, Hla-Dpb1, Hla-Dqa1, Hla-Dqa2, Hla-Dra, Il6, Ltb, Tek, Tgfb3, Tnfsf13b*
Allograft rejection	*Cd28, Cd40, Cd80, Cd86, Fas, Gzmb, Hla-Dmb, Hla-Doa, Hla-Dpa1, Hla-Dpb1, Hla-Dqa1, Hla-Dqa2, Hla-Dra, Il12a*
Graft-versus-host disease	*Cd28, Cd80, Cd86, Fas, Gzmb, Hla-Dmb, Hla-Doa, Hla-Dpa1, Hla-Dpb1, Hla-Dqa1, Hla-Dqa2, Hla-Dra, Il6, Kir2dl1, Kir2dl5a, Kir3dl2, Klrc1*

Table 2B The list of significant associated GO terms and genes with altered expressions identified by using ClueGO KEGG pathway enrichment analysis when comparing RNA-Seq data of the THP-1 cells treated with P 30 µg/ml vs THP-1 cell control.

GO Term	Associated Genes Found
Neuroactive ligand-receptor interaction	*Adra1b, Adra1d, Adra2a, Avpr1a, Bdkrb2, Cckbr, Chrm2, Chrm4, Chrna10, Chrna7, Chrnb4, Gabrq, Glra2, Glrb, Gpr83, Grik5, Grm1, Grm2, Hrh3, Htr1d, Mchr2, Npbwr1, P2rx3, Rxfp4, S1pr1, S1pr4*
Pathogenic *E. coli* infection	*Tlr5, Tuba3c, Tuba3d, Tuba3e, Tubb2a, Tubb3, Tubb4a, Tubb4b, Tubb8*
Ribosome biogenesis in eukaryotes	*Nxf1, Rmrp, Rna5s1, Rna5s10, Rna5s11, Rna5s12, Rna5s13, Rna5s14, Rna5s15, Rna5s16, Rna5s17, Rna5s2, Rna5s3, Rna5s4, Rna5s5, Rna5s6, Rna5s7, Rna5s8, Rna5s9*
Ribosome	*Rna5s1, Rna5s10, Rna5s11, Rna5s12, Rna5s13, Rna5s14, Rna5s15, Rna5s16, Rna5s17, Rna5s2, Rna5s3, Rna5s4, Rna5s5, Rna5s6, Rna5s7, Rna5s8, Rna5s9, Rpl3l*
Alcoholism	*Creb3l1, Gnao1, Gnb3, Gng2, Gng3, H2afb1, H2afx, H3f3c, Hist1h2ae, Hist1h2ag, Hist1h2al, Hist1h2am, Hist1h2be, Hist1h2bf, Hist1h2bg, Hist1h3a, Hist1h3j, Hist1h4b, Hist2h2ab, Hist2h3a, Hist2h3c, Hist4h4*

Table 2B The list of significant associated GO terms and genes with altered expressions identified by using ClueGO KEGG pathway enrichment analysis when comparing RNA-Seq data of the THP-1 cells treated with P 30 µg/ml vs THP-1 cell control (continues).

GO Term	Associated Genes Found
Systemic lupus erythematosus	*H2afb1, H2afx, H3f3c, Hist1h2ae, Hist1h2ag, Hist1h2al, Hist1h2am, Hist1h2be, Hist1h2bf, Hist1h2bg, Hist1h3a, Hist1h3j, Hist1h4b, Hist2h2ab, Hist2h3a, Hist2h3c, Hist4h4*

Table 3B The list of significant associated GO terms and genes with altered expressions identified by using ClueGO KEGG pathway enrichment analysis when comparing RNA-seq data of the THP-1 cells treated with P 30 µg/ml vs THP-1 cell control.

GO Term	Associated Genes Found
Cytokine-cytokine receptor interaction	*Ackr3, Amhr2, Ccl1, Ccl13, Ccl17, Ccl2, Ccl22, Ccl7, Ccl8, Ccr1, Ccr4, Ccr5, Cd40, Crlf2, Cx3cl1, Cx3cr1, Cxcl10, Cxcl11, Cxcl12, Cxcl13, Cxcl16, Cxcl5, Cxcl6, Cxcl9, Cxcr5, Fas, Flt1, Gdf5, Ifnk, Ifnl1, Il12a, Il12rb1, Il15ra, Il17re, Il2rg, Il3ra, Il6, Il7r, Inhba, Inhbe, Ltb, Pdgfrb, Pf4v1, Tgfb3, Tnfrsf11b, Tnfrsf18, Tnfsf10, Tnfsf13B, Tnfsf15, Tnfsf18, Tnfsf4, Xcl2*
Chemokine signalling pathway	*Adcy4, Adcy7, Ccl1, Ccl13, Ccl17, Ccl2, Ccl22, Ccl7, Ccl8, Ccr1, Ccr4, Ccr5, Cx3cl1, Cx3cr1, Cxcl10, Cxcl11, Cxcl12, Cxcl13, Cxcl16, Cxcl5, Cxcl6, Cxcl9, Cxcr5, Itk, Ncf1, Pf4v1, Stat2*
Influenza A	*Casp1, Ccl2, Cxcl10, Ddx58, Eif2ak2, Fas, Hla-Dmb, Hla-Doa, Hla-Dpa1, Hla-Dpb1, Hla-Dqa1, Hla-Dqa2, Hla-Dra, Hspa6, Ifih1, Il12a, Il33, Il6, Map2k6, Mx1, Myd88, Oas1, Oas2, Oas3, Rsad2, Stat2, Tlr3, Tmprs13, Tnfsf10*

Table 3B The list of significant associated GO terms and genes with altered expressions identified by using ClueGO KEGG pathway enrichment analysis when comparing RNA-seq data of the THP-1 cells treated with P 30 µg/ml vs THP-1 cell control (continued).

GO Term	Associated Genes Found
CAMs	*Cd226, Cd274, Cd28, Cd40, Cd80, Cd86, Cldn1, Cldn2, Cldn23, Cldn4, Cldn5, Cldn7, Hla-Dmb, Hla-Doa, Hla-Dpa1, Hla-Dpb1, Hla-Dqa1, Hla-Dqa2, Hla-Dra, Itgb8, Lrrc4c, Madcam1, Ntng1, Pdcd1, Pdcd1lg2, Ptprc, Sell, Siglec1, Vcam1*
Antigen processing and presentation	*Hla-Dmb, Hla-Doa, Hla-Dpa1, Hla-Dpb1, Hla-Dqa1, Hla-Dqa2, Hla-Dra, Hspa6, Kir2dl1, Kir2dl4, Kir2dl5a, Kir2ds2, Kir3dl2, Klrc1*
Intestinal immune network for IgA production	*Cd28, Cd40, Cd80, Cd86, Cxcl12, Hla-Dmb, Hla-Doa, Hla-Dpa1, Hla-Dpb1, Hla-Dqa1, Hla-Dqa2, Hla-Dra, Il15ra, Il6, Madcam1, Tnfsf13b*
Type I diabetes mellitus	*Cd28, Cd80, Cd86, Fas, Gzmb, Hla-Dmb, Hla-Doa, Hla-Dpa1, Hla-Dpb1, Hla-Dqa1, Hla-Dqa2, Hla-Dra, Il12a*
Leishmaniasis	*Fcgr3b, Hla-Dmb, Hla-Doa, Hla-Dpa1, Hla-Dpb1, Hla-Dqa1, Hla-Dqa2, Hla-Dra, Il12a, Myd88, Ncf1, Ncf2, Ptpn6, Tgfb3*

Table 3B The list of significant associated GO terms and genes with altered expressions identified by using ClueGO KEGG pathway enrichment analysis when comparing RNA-seq data of the THP-1 cells treated with P 30 µg/ml vs THP-1 cell control (continued).

GO Term	Associated Genes Found
S. aureus infection	*C1r, C1s, C3ar1, Cfb, Cfh, Fcgr3b, Fpr1, Hla-Dmb, Hla-Doa, Hla-Dpa1, Hla-Dpb1, Hla-Dqa1, Hla-Dqa2, Hla-Dra, Mbl2, Ptafr*
Autoimmune thyroid disease	*Cd28, Cd40, Cd80, Cd86, Fas, Gzmb, Hla-Dmb, Hla-Doa, Hla-Dpa1, Hla-Dpb1, Hla-Dqa1, Hla-Dqa2, Hla-Dra*
Rheumatoid arthritis	*Atp6v0d2, Ccl2, Cd28, Cd80, Cd86, Cxcl12, Cxcl5, Cxcl6, Flt1, Hla-Dmb, Hla-Doa, Hla-Dpa1, Hla-Dpb1, Hla-Dqa1, Hla-Dqa2, Hla-Dra, Il6, Ltb, Tek, Tgfb3, Tnfsf13b*
Allograft rejection	*Cd28, Cd40, Cd80, Cd86, Fas, Gzmb, Hla-Dmb, Hla-Doa, Hla-Dpa1, Hla-Dpb1, Hla-Dqa1, Hla-Dqa2, Hla-Dra, Il12a*
Graft-versus-host disease	*Cd28, Cd80, Cd86, Fas, Gzmb, Hla-Dmb, Hla-Doa, Hla-Dpa1, Hla-Dpb1, Hla-Dqa1, Hla-Dqa2, Hla-Dra, Il6, Kir2dl1, Kir2dl5a, Kir3dl2, Klrc1*

Table 3B The list of significant associated GO terms and genes with altered expressions identified by using ClueGO KEGG pathway enrichment analysis when comparing RNA-seq data of the THP-1 cells treated with P 30 µg/ml vs THP-1 cell control (continued).

GO Term	Associated Genes Found
Viral myocarditis	*Cav1, Cd28, Cd40, Cd80, Cd86, Hla-Dmb, Hla-Doa, Hla-Dpa1, Hla-Dpb1, Hla-Dqa1, Hla-Dqa2, Hla-Dra*

Table 4B The list of significant associated GO terms and genes with altered expressions identified by using ClueGO KEGG pathway enrichment analysis when comparing RNA-seq data of the THP-1 cells treated with E 30 μg/ml vs THP-1 cell control.

GO Term	Associated Genes Found
Cytokine-cytokine receptor interaction	*Amhr2, Ccl15, Ccl17, Ccl2, Ccl21, Ccl25, Ccl7, Ccl8, Ccr3, Ccr4, Cntfr, Crlf2, Ctf1, Cxcl10, Cxcl11, Cxcl13, Cxcl14, Cxcl9, Cxcr6, Fas, Gdf5, Ifnb1, Ifnk, Ifnl1, Il10ra, Il15ra, Il17b, Il17d, Il18r1, Il19, Il22ra1, Il23r, Il24, Il6, Il7r, Tnfrsf10c, Tnfrsf18, Tnfrsf4, Tnfsf10, Tnfsf13b, Tnfsf18, Tnfsf9, Xcl1, Xcl2*
Influenza A	*Casp1, Ccl2, Cxcl10, Ddx58, Eif2ak2, Fas, Hla-Dmb, Hla-Doa, Hla-Dob, Hla-Dpa1, Hla-Dpb1, Hla-Dqa1, Hla-Dqa2, Hla-Dra, Hspa6, Ifih1, Ifnb1, Il33, Il6, Map2k6, Nxf5, Oas1, Oas2, Oas3, Plg, Rsad2, Stat1, Stat2, Tlr3, Tnfrsf10c, Tnfsf10*
CAMs	*Cd274, Cd28, Cd80, Cd86, Cdh5, Cldn10, Cldn14, Cldn2, Cldn20, Cldn23, Cldn6, Hla-Dmb, Hla-Doa, Hla-Dob, Hla-Dpa1, Hla-Dpb1, Hla-Dqa1, Hla-Dqa2, Hla-Dra, Itga9, Lrrc4c, Ntng1, Pdcd1, Pdcd1lg2, Sell, Siglec1*

Table 4B The list of significant associated GO terms and genes with altered expressions identified by using ClueGO KEGG pathway enrichment analysis when comparing RNA-seq data of the THP-1 cells treated with E 30 µg/ml vs THP-1 cell control (continued).

GO Term	Associated Genes Found
Hematopoietic cell lineage	*Cd1a, Cd1s, Cd1e, Cd38, Cd3d, Cd5, Cd7, Fcer2, Gp1bb, Hla-Dmb, Hla-Doa, Hla-Dob, Hla-Dpa1, Hla-Dpb1, Hla-Dqa1, Hla-Dqa2, Hla-Dra, Il6, Il7r, Itga2b*
Intestinal immune network for IgA production	*Ccl25, Cd28, Cd80, Cd86, Hla-Dmb, Hla-Doa, Hla-Dob, Hla-Dpa1, Hla-Dpb1, Hla-Dqa1, Hla-Dqa2, Hla-Dra, Il15ra, Il6, Tnfsf13b*
Type I diabetes mellitus	*Cd28, Cd80, Cd86, Fas, Hla-Dmb, Hla-Doa, Hla-Dob, Hla-Dpa1, Hla-Dpb1, Hla-Dqa1, Hla-Dqa2, Hla-Dra*
S. aureus infection	*C1qb, C3ar1, C4a, Cfb, Cfh, Fcgr2a, Fcgr2c, Fcgr3a, Fcgr3b, Fpr1, Hla-Dmb, Hla-Doa, Hla-Dob, Hla-Dpa1, Hla-Dpb1, Hla-Dqa1, Hla-Dqa2, Hla-Dra, Plg*
Autoimmune thyroid disease	*Cd28, Cd80, Cd86, Fas, Hla-Dmb, Hla-Doa, Hla-Dob, Hla-Dpa1, Hla-Dpb1, Hla-Dqa1, Hla-Dqa2, Hla-Dra*

Table 4B The list of significant associated GO terms and genes with altered expressions identified by using ClueGO KEGG pathway enrichment analysis when comparing RNA-seq data of the THP-1 cells treated with E 30 µg/ml vs THP-1 cell control (continue).

GO Term	Associated Genes Found
IBD	*Hla-Dmb, Hla-Doa, Hla-Dob, Hla-Dpa1, Hla-Dpb1, Hla-Dqa1, Hla-Dqa2, Hla-Dra, Il18r1, Il23r, Il6, Nod2, Stat1*
Systemic lupus erythematosus	*C1qb, C4a, Cd28, Cd80, Cd86, Fcgr2a, Fcge3a, Fcgr3b, H2afb1, H2afb3, H3f3c, Hist1h2ae, Hist1h2ah, Hist1h2al, Hist1h2bb, Hist1h2be, Hist1h2bh, Hist1h2bi, Hist1h2bn, Hist1h3a, Hla-Dmb, Hla-Doa, Hla-Dob, Hla-Dpa1, Hla-Dpb1, Hla-Dqa1, Hla-Dqa2, Hla-Dra*
Allograft rejection	*Cd28, Cd80, Cd86, Fas, Hla-Dmb, Hla-Doa, Hla-Dob, Hla-Dpa1, Hla-Dpb1, Hla-Dqa1, Hla-Dqa2, Hla-Dra*
Graft-versus-host disease	*Cd28, Cd80, Cd86, Fas, Hla-Dmb, Hla-Doa, Hla-Dob, Hla-Dpa1, Hla-Dpb1, Hla-Dqa1, Hla-Dqa2, Hla-Dra, Il6, Kir2dl2, Kir3dl1, Klrc1*

Table 5B The list of significant associated GO terms and genes with altered expressions identified by using ClueGO KEGG pathway enrichment analysis when comparing RNA-seq data of the THP-1 cells treated with E 30 μg/ml vs THP-1 cell control.

GO Term	Associated Genes Found
Systemic lupus erythematosus	*C1qb, C4a, Fcgr3a, H2afb1, H3f3c, Hist1h2ae, Hist1h2ah, Hist1h2al, Hist1h2bb, Hist1h2be, Hist1h3a*

Table 6B The list of significant associated GO terms and genes with altered expressions identified by using ClueGO KEGG pathway enrichment analysis when comparing RNA-seq data of the THP-1 cells treated with E 30 µg/ml vs THP-1 cell control.

GO Term	Associated Genes Found
Cytokine-cytokine receptor interaction	*Amhr2, Ccl15, Ccl17, Ccl2, Ccl7, Ccl8, Ccr4, Crlf2, Ctf1, Cxcl10, Cxcl11, CXCL13, Cxcl9, Fas, Gdf5, Ifnb1, Ifnk, Ifnl1, Il10ra, Il15ra, Il17d, Il18r1, Il24, Il6, Il7r, Tnfrsf18, Tnfsf10, Tnfsf13b, Tnfsf18, Xcl2*
NOD-like receptor signaling pathway	*Aim2, Camp, Card16, Casp1, Casp5, Ccl2, Gbp1, Gbp2, Gbp3, Gbp4, Gbp7, Ifi16, Ifnb1, Il6, Nod2, Oas1, Oas2, Oas3, Stat1, Stat2*
CAMs	*Cd274, Cd28, Cd80, Cd86, Cldn2, Cldn20, Cldn23, Cldn6, Hla-Dmb, Hla-Doa, Hla-Dob, Hla-Dpa1, Hla-Dpb1, Hla-Dqa1, Hla-Dqa2, Hla-Dra, Itga9, Lrrc4c, Ntng1, Pdcd1, Pdcd1lg2, Sell, Siglec1*
Antigen processing and presentation	*Hla-Dmb, Hla-Doa, Hla-Dob, Hla-Dpa1, Hla-Dpb1, Hla-Dqa1, Hla-Dqa2, Hla-Dra, Hspa6, Kir2dl2, Kir2ds4, Klrc1*

Table 6B The list of significant associated GO terms and genes with altered expressions identified by using ClueGO KEGG pathway enrichment analysis when comparing RNA-seq data of the THP-1 cells treated with E 30 μg/ml vs THP-1 cell control (continued).

GO Term	Associated Genes Found
Hematopoietic cell lineage	*Cd1a, Cd1d, Cd1e, Cd38, Cd5, Cd7, Fcer2, Hla-Dmb, Hla-Doa, Hla-Dob, Hla-Dpa1, Hla-Dpb1, Hla-Dqa1, Hla-Dqa2, Hla-Dra, Il6, Il7r*
Intestinal immune network for IgA production	*Cd28, Cd80, Cd86, Hla-Dmb, Hla-Doa, Hla-Dob, Hla-Dpa1, Hla-Dpb1, Hla-Dqa1, Hla-Dqa2, Hla-Dra, Il15ra, Il6, Tnfsf13b*
Type I diabetes mellitus	*Cd28, Cd80, Cd86, Fas, Hla-Dmb, Hla-Doa, Hla-Dob, Hla-Dpa1, Hla-Dpb1, Hla-Dqa1, Hla-Dqa2, Hla-Dra*
Leishmaniasis	*Fcgr2a, Fcgr3b, Hla-Dmb, Hla-Doa, Hla-Dob, Hla-Dpa1, Hla-Dpb1, Hla-Dqa1, Hla-Dqa2, Hla-Dra, Stat1*
S. aureus infection	*C3ar1, Cfb, Cfh, Fcgr2a, Fcgr3b, Fpr1, Hla-Dmb, Hla-Doa, Hla-Dob, Hla-Dpa1, Hla-Dpb1, Hla-Dqa1, Hla-Dqa2, Hla-Dra*

Table 6B The list of significant associated GO terms and genes with altered expressions identified by using ClueGO KEGG pathway enrichment analysis when comparing RNA-seq data of the THP-1 cells treated with E 30 μg/ml vs THP-1 cell control (continued).

GO Term	Associated Genes Found
Hepatitis C	*Cldn2, Cldn20, Cldn23, Cldn6, Ddx58, Eif2ak2, Ifit1, Ifit1b, Ifnb1, Oas1, Oas2, Oas3, Ppp2r2b, Ppp2r2c, Stat1, Stat2, Tlr3*
Measles	*Cd28, Csnk2a3, Ddx58, Eif2ak2, Fas, Hspa6, Ifih1, Ifnb1, Il6, Oas1, Oas2, Oas3, Stat1, Stat2, Tnfsf10*
Influenza A	*Casp1, Ccl2, Cxcl10, Ddx58, Eif2ak2, Fas, Hla-Dmb, Hla-Doa, Hla-Dob, Hla-Dpa1, Hla-Dpb1, Hla-Dqa1, Hla-Dqa2, Hla-Dra, Hspa6, Ifih1, Ifnb1, Il33, Il6, Map2k6, Oas1, Oas2, Oas3, Rsad2, Stat1, Stat2, Tlr3, Tnfsf10*
Herpes simplex infection	*Ccl2, Csnk2a3, Ddx58, Eif2ak2, Fas, Hla-Dmb, Hla-Doa, Hla-Dob, Hla-Dpa1, Hla-Dpb1, Hla-Dqa1, Hla-Dqa2, Hla-Dra, Ifih1, Ifit1, Ifit1b, Ifnb1, Il6, Oas1, Oas2, Oas3, Stat1, Stat2, Tlr3*
Asthma	*Hla-Dmb, Hla-Doa, Hla-Dob, Hla-Dpa1, Hla-Dpb1, Hla-Dqa1, Hla-Dqa2, Hla-Dra*

Table 6B The list of significant associated GO terms and genes with altered expressions identified by using ClueGO KEGG pathway enrichment analysis when comparing RNA-seq data of the THP-1 cells treated with E 30 μg/ml vs THP-1 cell control (continued).

GO Term	Associated Genes Found
Autoimmune thyroid disease	*Cd28, Cd80, Cd86, Fas, Hla-Dmb, Hla-Doa, Hla-Dob, Hla-Dpa1, Hla-Dpb1, Hla-Dqa1, Hla-Dqa2, Hla-Dra*
IBD	*Hla-Dmb, Hla-Doa, Hla-Dob, Hla-Dpa1, Hla-Dpb1, Hla-Dqa1, Hla-Dqa2, Hla-Dra, Il18r1, Il6, Nod2, Stat1*
Systemic lupus erythematosus	*Cd28, Cd80, Cd86, Fcgr2a, Fcgr3b, H2afb3, Hist1h2bh, Hist1h2bi, Hist1h2bn, Hla-Dmb, Hla-Doa, Hla-Dob, Hla-Dpa1, Hla-Dpb1, Hla-Dqa1, Hla-Dqa2, Hla-Dra*
Rheumatoid arthritis	*Ccl2, Cd28, Cd80, Cd86, Hla-Dmb, Hla-Doa, Hla-Dob, Hla-Dpa1, Hla-Dpb1, Hla-Dqa1, Hla-Dqa2, Hla-Dra, Il6, Tnfsf13b*
Allograft rejection	*Cd28, Cd80, Cd86, Fas, Hla-Dmb, Hla-Doa, Hla-Dob, Hla-Dpa1, Hla-Dpb1, Hla-Dqa1, Hla-Dqa2, Hla-Dra*

Table 6B The list of significant associated GO terms and genes with altered expressions identified by using ClueGO KEGG pathway enrichment analysis when comparing RNA-seq data of the THP-1 cells treated with E 30 µg/ml vs THP-1 cell control (continued).

GO Term	Associated Genes Found
Graft-versus-host disease	*Cd28, Cd80, Cd86, Fas, Hla-Dmb, Hla-Doa, Hla-Dob, Hla-Dpa1, Hla-Dpb1, Hla-Dqa1, Hla-Dqa2, Hla-Dra, Il6, Kir2dl2, Klrc1*
Viral myocarditis	*Cd28, Cd80, Cd86, Hla-Dmb, Hla-Doa, Hla-Dob, Hla-Dpa1, Hla-Dpb1, Hla-Dqa1, Hla-Dqa2, Hla-Dra*

Table 7B The list of significant associated GO terms and genes with altered expressions identified by using ClueGO KEGG pathway enrichment analysis when comparing RNA-seq data of the THP-1 cells treated with E 10 μg/ml vs THP-1 cell control.

GO Term	Associated Genes Found
Cytosolic DNA-sensing pathway	*Aim2, Cxcl10, Il6*

Table 8B The list of significant associated GO terms and genes with altered expressions identified by using ClueGO KEGG pathway enrichment analysis when comparing RNA-seq data of the THP-1 cells treated with E 10 μg/ml vs THP-1 cell control.

GO Term	Associated Genes Found
Cytosolic DNA-sensing pathway	*Aim22, Cxcl10, Il6*
Measles	*Csnk2a3, Fas, Il6, Tnfsf10*